Functional analysis of the ependymal marker protein Wdr16

Funktionelle Analyse des Ependymzell-*Marker*-Proteins Wdr16

Dissertation

der Mathematisch-Naturwissenschaftlichen Fakultät

der Eberhard Karls Universität Tübingen

zur Erlangung des Grades eines

Doktors der Naturwissenschaften

(Dr. rer. nat.)

vorgelegt von

Dipl. Biol. Andreas Bubis

aus Mannheim

Tübingen

2012

Tag der mündlichen Qualifikation:	29.04.2013
Dekan:	Prof. Dr. Wolfgang Rosenstiel
1. Berichterstatter:	Prof. Dr. Thilo Stehle
2. Berichterstatter:	Prof. Dr. Bernd Hamprecht

Acknowledgements

Above all, I would like to express my sincere thanks and appreciation to my doctoral supervisor, PD Dr. Stephan Verleysdonk, for the opportunity to do scientific work in his research group and for his guidance, ideas, and criticism.

I am very grateful to Prof. Bernd Hamprecht for his valuable advice, guidance, for sharing his wide knowledge, and especially for the support in the final phase of my doctoral thesis, in particular for critically reading my thesis manuscript.

My thanks are also due to Prof. Thilo Stehle for guiding me through the promotion procedure after Dr. S. Verleysdonk had left this university. I should also like to thank him for providing necessary reagents (e.g. restriction enzymes) in the final stage of my experimental work and for granting me access to his CD spectrometer.

My special and sincere thanks go to my colleague Franklin Christopher Vincent for his help and discussions and especially for preparing primary cultures for my research several times.

I am thankful to Nicolas Binder, Barbara Birk and Steffi Hoppe for excellent technical support during my PhD thesis. My special thanks go to Nicolas Binder for doing an excellent job in providing the research group with freshly prepared fibronectin for the ependymal primary cultures. I would also like to extend my thanks to other biological-technical assistants with whom I had the opportunity of working, particularly Ruth Schmidt and Ulrike Thiess.

I should like to thank Dr. Bhavani Kowtharapu and Dr. Wolfgang Hirschner for laying the scientific groundwork, in their respective doctoral theses, which this dissertation is based on.

I should like to express my sincere thanks to PD Dr. Frank Essmann for providing reagents (e.g. antibodies and the Flag M2 affinity gel), for granting me access to the fluorescence microscope, and also for sharing his knowledge about deconvolution microscopy.

I wish to thank Mathias Hillenbrand for introducing me to insect cells culture and for providing his advice and for sharing his experience in the production of baculoviruses.

I wish to thank Dr. Mirna Rapp for the provision of thrombin, an indispensable reagent for the generation of ependymal primary cultures.

I wish to thank Prof. Gabriele Dodt, Dr. Brigitte Pfeiffer-Guglielmi and Dr. Daniela Scheible for providing valuable antibodies, and Dr. Roland Vogel and Dr. Ralf Schäfer for providing cell lines for the present doctoral thesis.

I should like to thank Dr. Arie Geerlof for providing me with his self-constructed plasmids for the generation of baculoviruses.

I should like to express my gratitude to the Section of Neuropharmacology of the University of Tübingen (research group of Prof. Werner Schmidt) for carrying out the microinjections and for providing Sprague-Dawley rats. Special thanks are due to Ferdinand Kluge for performing the stereotactic microinjections and to Ulrich Ruess for showing me how to perform the perfusion fixations of the rats and cryosectioning of frozen tissues.

I am grateful to Martin Thunemann and Dr. Susanne Feil for their valuable advice on the culture of embryonic stem cells and feeder cells.

I am grateful to to Prof. Ralf-Peter Jansen for giving me access to his cryostat, to Prof. Michael Duszenko for allowing me to use his UV spectrophotometer, Prof. Doron Rappaport for sharing his cold room and storing space and to Prof. Hans-Georg Rammensee and the Department of Immunology for granting me access to their gamma cell irradiator.

Finally, I should like to thank the entire staff of the Interfacultary Institute of Biochemistry of the University of Tuebingen for their support and nice collaboration, in particular Dr. Klaus Möschel, Ursula Schaal, Hermann Liggesmeyer and many others that I had the pleasure to know during my doctoral thesis.

Gewidmet
in Gedenken an
Angela Bubis

Abbreviations

AcNPV	*Autographa californica* nuclear polyhedrosis virus
AEBSF	4-(2-aminoethyl)benzenesulfonyl fluoride hydrochloride
Ak7	adenylate kinase 7
AP	alkaline phosphatase
APS	ammonium persulfate
Approx.	approximate(ly)
ATCC	American Type Culture Collection
bla	beta-lactamase
BLAST	Basic Local Alignment Search Tool
BUG	basal body proteins with up-regulated genes
BV	budded virus
CD	circular dichroism
CIAP	calf intestine alkaline phosphatase
CMV	cytomegalovirus
Co-IP	co-immunoprecipitation
CSF	cerebrospinal fluid
Cy3	carbocyanin 3
d	days
DAPI	4’,6-diamidino-2-phenylindole
ddH_2O	double distilled water
DIV	day(s) in vitro
DMEM	Dulbecco’s Modified Eagle´s Medium
DNA	deoxyribonucleic acid
dNTP	deoxyribonucleoside triphosphate
ECL	enhanced chemiluminescence
EF1	elongation factor 1
EGFP	enhanced green fluorescent protein
EPC	ependymal primary culture
ES cell	embryonic stem cell
FCS	fetal calf serum
Fig.	Figure
Flag	antigenic polypeptide; protein tag (sequence

	DYKDDDDK)
FOXJ1	forkhead box J1 transcription factor
GFP	green fluorescent protein
GOI	gene of interest
GP-BB	glycogen phosphorylase isoenzyme BB
GST	glutathione S-transferase
h	hour(s)
HBS	HEPES-buffered saline
HEK	human embryonic kidney cell line
HeLa	Henrietta Lacks cervical cancer cell line
HEPES	N-2-hydroxyethylpiperazine-N'-2-ethanesulfonic acid
HIV-1	human immunodeficiency virus type 1
IFT	intraflagellar transport
IMAC	immobilized metal affinity chromatography
IP	immunoprecipitation
IPTG	isopropyl β-D-1-thiogalactopyranoside
LB	lysogeny broth
LTR	long terminal repeat
LV	lentiviral vector
MCS	multiple cloning site
MEM_c	Minimal Essential Medium, complete
MEM_{ct}	Minimal Essential Medium, complete, with thrombin
MEM_{wash}	Minimal Essential Medium, for washing steps
min	minutes
MOI	multiplicity of infection
neo	neomycin
NPV	nucleopolyhedrovirus
OD	optical density (absorbance)
ODA	outer dynein arm
ODV	occlusion-derived virions, virions released from occlusion bodies in the insect midgut
ORF	open reading frame
PBS	phosphate-buffered saline
PCP	planar cell polarity

PCR	polymerase chain reaction
PFA	paraformaldehyde
Pfu	plaque forming units
p.i.	post infection
PS	penicillin/streptomycin
RISC	RNA-induced silencing complex
RNA	ribonucleic acid
RNAi	RNA interference
rpm	revolutions per minute
RT	1. reverse transcriptase 2. reverse transcription 3. room temperature
s	seconds
SDS	sodium dodecyl sulfate
SDS-PAGE	sodium dodecyl sulfate polyacrylamide gel electrophoresis
Sf9	*Spodoptera frugiperda* insect cell line
siRNA	short interfering RNA
SOC	superoptimal broth with catabolite repression
Spag6	sperm-associated antigen 6
SV40	simian virus 40
TBS-T	Tris-Buffered Saline with Tween 20
TEMED	N,N,N’,N’-tetramethylethylenediamine
TK	thymidine kinase
Tris	tris(hydroxymethyl)aminomethane
VSV-G	vesicular stomatitis virus G protein
Wdr16	WD-repeat protein 16
X-Gal	5-bromo-4-chloro-indolyl-β-D-galactopyranoside

1 Introduction

1.1 The ventricular system and cerebrospinal fluid

The ventricular system consists of four fluid-filled intra-cerebral cavities. The ventricles originate from the lumen of the embryonic neural tube. There are two lateral ventricles (one within each of the cerebral hemispheres) that each empty into the third ventricle through the so-called foramina of Monro. The lateral ventricles are the largest fluid-filled spaces of the brain, and their volume is known to increase even further with age. The third ventricle is embedded in the midbrain between the halves of the thalamus. It is connected to the fourth ventricle through the aqueduct of Sylvius. The fourth ventricle is delineated by the cerebellum and the brain stem. It narrows caudally to connect to the central canal of the spinal cord. All ventricles are filled with cerebrospinal fluid (CSF), which is mainly produced by special structures consisting of capillary convolutes covered with an ependymal (see below) epithelium (choroid plexus), which are found in each ventricle (Nicholson, 1999). The CSF circulates in the ventricular system; it flows into the subarachnoid space where it is absorbed by arachnoid villi, returning to the venous circulation. In the human, the total CSF volume is ca. 165 ml (Kohn et al., 1991). The CSF is a clear fluid consisting of 99% (v/v) water. The most abundant ions in the CSF are Na^+ (151 mM), Cl^- (133 mM) and HCO_3^- (25.8 mM) (Davson et al., 1987). The CSF is secreted by the epithelial cells of the choroid plexus by a process involving the active transport of ions from the blood into the ventricular system. The protein content of the CSF is twenty times lower than in serum (Fishman, 1992) and the glucose concentration is also significantly lower. The maximum concentration for CSF glucose is 300 mg/dl (16.7 mM; Seehusen et al., 2003). The CSF is a route of transportation for messenger compounds such as thyroid hormones (Hagen and Elliott, 1973) and prolactin (Assies et al., 1978) and the choroid plexus produces a compound named transthyretin that might regulate hormone transport from blood to brain (Nilsson et al., 1992). The directional beating of

ependymal kinocilia may play a role in the circulation of the CSF (Sawamoto et al., 2006), particularly in the narrow regions of the ventricular system such as the aqueduct of Sylvius. In many cases, primary ciliary diskinesia or immotile cilia syndrome results in hydrocephalus as evidenced in mice, rats, dogs and other small animals (Badano et al., 2006; Reichler et al., 2001).

1.2 The ependyma and its functions

The ependyma is the mostly single-layered epithelium lining the ventricles of the brain and the canal of the spinal cord. The epithelium is isoprismatic to columnar and mostly kinocilia-bearing. The term 'ependyma' was coined by Virchow (1858). The ependymocytes are cells with special structural and functional properties. They are ontogenetically derived from radial glia (Spassky et al., 2005) and form the interface between CSF and brain parenchyma on the walls of the cerebral ventricles. The ependyma is composed of several different cell types. They can be distinguished by their location, the types of their cell-cell junction complexes and the presence or absence of kinocilia on their apical surfaces (Siegel and Sapru, 2006). Generally, the ependymocytes of the ventricular epithelia are kinocilia-bearing, whereas the so-called tanycytes in the floor of the third ventricle lack those motile cell appendages (Flament-Durand and Brion, 1985; Rodríguez et al., 2005). Most ciliated and non-ciliated ependymocytes lack functional tight junctions. Only in the ependymal layer of the circumventricular organs, which the choroid plexus and the subcommissural organ belong to, truly functional tight junctions are found that are a diffusion barrier between the tissue and the CSF. Otherwise, the CSF is continuous with the brain interstitial fluid (Petrov et al., 1994). The role of the ependyma in normal brain function is not fully understood even after almost two centuries of research. Ependymal cells play an essential role for the maintenance of the flow through the ventricular system and their malfunction causes hydrocephalus (Ibanez-Tallon et al., 2004). The ciliary beating of the ependyma appears to control the direction of CSF flow and in doing so also influences the distribution of signal molecules in the ventricular system. Johansson et al. (1999) have provided several lines of evidence that the multi-ciliated ependymal cells lining

the lateral ventricles act as slowly proliferating neural stem cells. After several other groups failed to produce multipotent stem cells from purified ependymal cells, Johansson's hypothesis was rejected by the scientific community. In 2009, another research group led by Jonas Frisén could demonstrate that ependymal cells do not fulfill criteria for stem cells but serve as a reservoir of olfactory bulb neurons that is activated and recruited by injury, e.g. in response to stroke (Carlén et al., 2009).

1.3 Ependymal primary cultures

Ependymal primary cultures are highly enriched in multi-ciliated ependymal cells and represent a powerful tool for studying ependymal cells. EPCs were developed by Marc Weibel and colleagues at the University of Strasbourg (Weibel et al., 1986). EPCs are being generated from mechanically dissociated brains of neonatal Wistar rats. In order to accomplish a high percentage of ependymal cells, several items must be observed: the freshly dissociated cells must be seeded on a fibronectin substratum; ii) the cells must be cultured for at least 14 days in a serum-free minimal medium (Minimal Essential Medium Eagle, MEM) supplemented with insulin, transferrin, fatty acid-free bovine serum albumin and, above all, thrombin. The addition of thrombin is crucial to obtain cultures with a high percentage (> 75%) of kinociliated ependymal cells. The molecular mechanism underlying the thrombin dependence of EPCs has been elucidated by Tritschler et al. (2007). These authors demonstrated that the serine protease thrombin enhances the proliferation of ependymal precursor cells *in vitro* and causes a significant reduction of programmed cell death (apoptosis) of this specific cell type. It was also demonstrated that the effect of thrombin requires the protease activity, the downstream action of the protease-activated receptor 1 (PAR1) and, to a lesser extent, the protease-activated receptor 2 (PAR2; Tritschler et al., 2007). Over the last decades, EPCs have been used to facilitate many studies about the development, molecular biology and biochemistry of ependymal cells. For instance, the glycogen metabolism of ependymal cells and its regulation by the neurotransmitter serotonin was studied in detail using EPCs (Prothmann et al., 2001; Verleysdonk et al., 2005).

More recent studies have also demonstrated the usefulness of EPCs for the molecular analysis of ciliated ependymal cells. Using a subtractive cDNA library technique, S. Verleysdonk and his colleagues (Hirschner et al., 2007) discovered several novel ependymal marker proteins (e.g. Wdr16 and AK7). They also established lentiviral gene transfer in EPCs (Kowtharapu et al., 2009), a method they subsequently utilized for the analysis of ependymal cell-specific gene expression (Kowtharapu et al., 2009).

1.4 Cilia

Two types of true cilia can be found on eukaryotic cells, primary cilia and kinocilia. The so-called "stereocilia" of the inner ear hair cells are in fact modified microvilli and do not fall into this category. The central component and at the same time the functional apparatus of cilia is the axoneme, which is an extension of a basal body. The axoneme consists of 9 doublets of a complete (A) and an incomplete microtubule (B) arranged in a circle around a central microtubule doublet. The outer doublets are numbered 1-9; the central microtubules are termed C1 and C2, respectively. The A tubule consists of 13, the B tubule of 10 or 11 protofilaments (Lodish et al., 2000). At least one of the protofilaments of the A tubule is not composed of tubulin; it has been proposed that it may be composed of tektins (Nojima et al., 1995). Besides tubulin, around 250 other proteins are thought to be part of the kinocilia proteome (Ostrowski et al., 2002), more than 50% of which are still uncharacterized. The most important axonemal proteins beside the tubulins are the constituent parts of the inner and outer dynein arms, radial spokes, nexin links and the proteins of the central apparatus. Ciliary motility is caused by the relative sliding of the nine outer axonemal doublets along each other. They operate as two sets; the doublets 1-4 produce the effective stroke (principal bend) and doublets 6-9 produce the recovery stroke (reverse bend) (Sleigh, 1989). This motion is powered by ATP hydrolysis via the heavy chains of the dynein arms. The inner (IDA) and outer dynein arms (ODA) are large axonemal protein complexes that contain the microtubule-dependent ATPases which generate the force for the ciliary movement (Lodish et al, 2000). There are three classes of inner dynein

arms and they are sufficient and necessary to generate the axonemal motion (Bowman and Goldstein, 2001). IDA and ODA function together, but the ODAs mainly regulate ciliary beat frequency and IDAs control the beat form (Satir and Christensen, 2008).

Non-motile primary cilia feature a 9+0 type axoneme that lacks a central microtubule doublet, dynein arms and radial spokes. They are present on many differentiated cells, e.g. fibroblasts and neurons and are thought to be involved in environmental sensing. For instance, the renal cell primary cilium on the epithelial cells of the distal tubule functions as a urine flow sensor (Praetorius and Spring, 2003). Primary cilia are also involved in olfactory signaling. Cilia-less olfactory neurons lack odorant sensation (Alaiwi et al., 2009).

Kinocilia are motile and possess an axoneme of the 9+2 type. Motile cilia are found on cells of the fallopian tube of the female reproductive system which are involved in oocyte transport (Yoder, 2008). The function of kinocilia in the airway epithelia of the lung is to propel both water and mucus (Shields, 2009). In the brain kinocilia are only found on the ependymal cells lining the brain ventricles. The kinocilia at the apical pole of ependymal cells are approximately 8 µm long and their most important role may be enhancement of the flow of CSF through the cerebral aqueduct (Yamadori and Nara, 1979). Ciliary defects are associated with numerous human diseases, e.g. primary ciliary dyskinesia, hydrocephalus, polycystic liver and kidney disease and retinal degeneration. Nowadays, even more ciliopathies with mutations in ciliary proteins are known, such as nephronophthisis, Bardet-Biedl syndrome, Alstrom syndrome, and Meckel-Gruber syndrome (Badano et al., 2006). Bardet-Biedl Syndrome (BBS) is defined by a range of symptoms, but the syndrome's hallmark is retinal degeneration (Waters and Beales, 2011). Fourteen genes are known to be associated with BBS and all BBS gene products are believed to be involved in intraflagellar transport (IFT; Pagon et al., 2003). The evolutionary relationship between flagella, motile cilia and primary cilia and their origin was controversial and unclear for more than thirty years. One hypothesis claimed that cilia were the remnants of symbiotic spirochaete-like prokaryotes. Another hypothesis assumed that they originated from a simpler cytoplasmic microtubule-based

intracellular transport system. Overwhelming evidence nowadays supports the latter hypothesis and it is assumed that the last common eukaryotic ancestor possessed a motile 9+2 sensory organelle. In primary cilia or sensory cilia, the motile function has been discarded in the course of time and with it the dyneins, radial spokes, the central pair complex, and other proteins needed for ciliary motility but not the proteins necessary for IFT (Mitchell, 2006).

1.5 Wdr16

WD-repeat proteins belong to a large conservative protein family with extremely diversified functions. They are defined by at least four repeating units with a conserved core of 40 amino acids that usually ends with tryptophan-aspartic acid (WD). WD-repeat proteins are thought to form a circularized propeller structure composed of β-sheets. The three-dimensional structure was first demonstrated by the crystal structure of the G protein β subunit (Li and Roberts, 2001). WD-repeat proteins are important for many biological functions, such as signal transduction, transcriptional regulation, developmental processes and apoptosis (Li and Roberts, 2001). They are also associated with many human diseases, e.g. autoinflammatory disease (WDR1; Kile et al., 2007). The common function of all WD-repeat family members appears to be the coordination of multiprotein complex assemblies. Their WD-repeats are believed to function as a scaffold for multiple simultaneous protein interactions. The specificity of the protein interactions is most probably determined by sequences outside the repeats themselves (Li and Roberts, 2001). WD-repeat proteins form multi-bladed β-propeller structures with nearly all of them containing seven blades. The blades in the β-propeller are formed by small anti-parallel β-sheets consisting of four β-strands. These four β-stands ar labeled A, B, C, and D, beginning with the strand that is closest to the center of the propeller. One single WD sequence repeat comprises the D strand of one blade and strands A, B and C of the next blade (Voegtli et al., 2003).

In search for marker proteins defining the differentiation state of ependymal cells or of kinocilia-bearing cells in general, a subtractive cDNA library of ependyma minus total brain was generated and screened by several coworkers

of the research group of Stephan Verleysdonk at the University of Tuebingen (Hirschner et al., 2007; Verleysdonk, 2006). A significant number of clones contained the ORF of an mRNA of a novel unknown protein that was very likely to be ependyma-specific: Wdr16. The full-length cDNA (accession number: DQ445463) of wdr16 translates into a protein of 620 amino acid residues (molecular mass = 68 kDa) and 11 WD40 repeats were predicted by the bioinformatic SMART tool (Simple Modular Architecture Research Tool; Schultz et al., 1998; Letunic et al., 2009). The human gene for wdr16 is located on chromosome 17 (17p12-17p13) and consists of 15 exons (Hirschner et al., 2007). There are three splice variants; the standard splice form uses exons 1–14 and has been designated ‘transcript variant 2’ (Verleysdonk, 2006). The membership of Wdr16 to the family of WD40 repeat proteins suggests its involvement in protein-protein interactions (Li and Roberts, 2001). According to bioinformatic tertiary structure prediction by “threading”, the structure of the Wd16 protein resembles the two covalently linked 7-bladed β-propellers of actin-interacting protein 1 (Aip1, Wdr1; Hirschner et al., 2007). Wdr16 mRNA is strongly detected in ependymal primary cultures (EPC) and testis by RT-PCR, and a weak expression is observed in lung and other organs (Hirschner et al., 2007). Immunoblotting detects the wdr16 translation product in EPC and testis only. The failure to detect the Wdr16 protein in lung as an organ in possession of kinocilia by this method was probably due to insufficient antibody sensitivity. In EPC, the expression of the Wdr16 protein starts at the time of ependymal differentiation and kinocilia formation, approximately from day 7 onward in culture (Hirschner et al., 2007). A Wdr16 antibody produced by means of an antigenic peptide specifically labels the cytosol of kinocilia-bearing cells of the ependymal layer (Hirschner et al., 2007). In the embryonic brain, the cells of the ventricular wall do not yet bear kinocilia and there is also no Wdr16 immunoreactivity observed in them. Real-time PCR experiments have demonstrated that in EPC and testis, Wdr16 mRNA levels rise concomitantly with the messages for sperm-associated antigen 6 (Spag6), an axonemal protein and kinocilia marker, and for hydin, another protein of the 9+2 axoneme central apparatus (Hirschner et al., 2007). In contrast, the transcription kinetics of polaris, a component of the IFT apparatus present in all types of cilia, non-motile primary cilia and motile 9 + 2 kinocilia, is markedly distinct from the ones

of wdr16, Spag6 and hydin. This difference links wdr16 to kinocilia and differentiation of kinocilia-bearing cells rather than to cilia in general. Morpholino-induced knockdown of wdr16 in developing zebrafish resulted in severe hydrocephalus (Hirschner et al., 2007). In situ hybridization experiments identified Wdr16 mRNA in the zebrafish neural tube, otic and olfactory placode, pronephric duct as well as in the SCO and the regions between the midbrain and hindbrain ventricles. All these are regions in which kinocilia are found (Hirschner et al., 2007). Experiments using high-speed videography demonstrated that hydrocephalus in zebrafish resulting from wdr16 knockdown is without general disorganization of the ependymal layer or impaired motility of the ependymal cilia. It is therefore possible that hydrocephalus in wdr16 knockdown morphants is caused by a disturbance in brain water homeostasis and osmoregulation (Hirschner et al., 2007). Another possibility is that Wdr16 plays a role in basal body function in ciliated cells. Both in the green algae *Chlamydomonas* and in trypanosomes, the respective orthologues localize at the basal bodies and, to a lesser extent, in the flagellum (Keller et al., 2005, 2009; Hodges et al., 2010).

1.6 RNA interference

RNA interference (RNAi) is a sequence-specific method for gene silencing induced by double-stranded RNA. RNAi has been induced in many different organisms ranging from worms to vertebrates (Fire et al., 1998). Prior to the discovery of RNAi, several other methods for gene silencing were known (e.g. methods using ribozymes and oligodeoxynucleotides) but RNAi led to an explosion of interest in gene silencing among scientists because of its specifity, efficiency and cost-effectiveness. The first step in the RNAi pathway is the fragmentation of long dsRNAs (e.g. of viral origin) by the RNase III-type enzyme Dicer (Bernstein et al., 2001). The cleavage results in double-stranded, 21 to 23 nt long so-called short interfering RNAs (siRNAs) containing 2 nt overhangs at their 3’ ends and 5’ phosphate groups (Zamore et al., 2000; Elbashir et al., 2001). The strands of the siRNA duplex are subsequently separated and the antisense strand (guide strand) is assembled into the RNA-induced silencing complex (RISC; Hammond et al., 2000). The other strand of the siRNA duplex

(the passenger strand) is removed by the enzyme Argonaute 2 (Ago2) which directly binds to the siRNA duplex and cleaves the passenger strand the same way as it cleaves mRNA substrates (Maiti et al., 2007; Matranga et al., 2005). The activated RISC nuclease complex now targets and cleaves any mRNA that is fully complementary to its siRNA. Initial RNAi attempts proved disappointing because introduction of dsRNA larger than 30 bp triggered the interferon response (Provost et al., 2002), resulting in global protein shutdown and dramatic changes of cellular metabolism. Elbashir and colleagues were the first to chemically synthesize small RNAs mimicking the Dicer products and thus avoiding such problems (Elbashir et al., 2001). Today it is clear that plants and animals use RNAi as an effective anti-viral mechanism that protects their cells from viral replication. Many different approaches have been tested and used to introduce siRNAs into cells and whole organisms: electroporation, soaking in siRNAs, feeding C. elegans with bacteria containing siRNAs, transfection with commercial reagents, and vector-based strategies. The latter are now widely used due to their therapeutic potential (Devroe and Silver, 2004), high transfection efficiency and sensitivity.

1.7 HIV-1-derived lentiviral vectors

In lentiviral vectors (LVs) the normal viral genome is partially replaced by cassettes needed for the expression of a gene of interest or the synthesis of RNA. The viral vectors do not carry all the genetic elements required for the production of all essential viral components such as viral structural proteins or enzymes. Hence, they cannot replicate. For their production, the missing elements have to be provided *in trans*, e.g. by helper plasmids and packaging cell lines. The tropism of viral vectors, i.e. the range of different cells they are able to infect, can be easily modified by equipping them with heterologous envelope proteins of choice via corresponding envelope helper plasmids. For the silencing of wdr16 in kinocilia-bearing cells of ependymal primary cultures, lentiviral HIV-1-based vectors pseudotyped with the envelope protein G of the vesicular stomatitis virus (VSV-G) were used (Khowtharapu et al., 2009). Lentiviral particles are spherical and surrounded by a lipid membrane bilayer.

The shape of the nucleocapsid varies from virus species to virus species. The lentiviruses have cylindrical or conical nucleocapsid cores. All retroviruses carry three major genes for viral replication and assembly, gag, pol and env. Lentiviruses are complex retroviruses; they contain accessory genes which are important for viral replication, persistence and pathogenicity. Lentiviral vectors are the only gene-transfer systems which afford stable gene delivery because they can persist in dividing cells by integration of the gene of interest into the genome where it is copied along with the chromosomal DNA. A unique feature of LVs is their ability to integrate in the genome of non-dividing cells in contrast to other non-viral or viral vectors (e.g. adenoviruses) or retroviruses (e.g. murine leukemia viruses, MuLV) which can only integrate upon cell division. Other reasons for the use of LVs are high transfection efficiencies and low toxicity to most types of cell lines and primary cells. The human immunodeficiency virus (HIV) is the etiological agent of the acquired immunodeficiency syndrome (AIDS), a progressive disease characterized by immunologic dysfunction with reduced numbers of $CD4^+$ T-Helper cells. It first appeared in the United States and Europe in the early 1980s (Chermann and Barré-Sinoussi, 1987). The only known lentiviruses until then were the Maedi/Visna virus of sheep, the caprine arthritis encephalitis virus of goats and the equine infectious anemia virus (EIAV) of horses (Narayan and Clements, 1989). For the generation of replication-defective lentiviral particles (LVs), the sequences coding for viral components and for the transgene are carried *in trans* by different plasmids. E.g., the packaging plasmid carries the genes for essential viral structural proteins and enzymes, while the transfer vector bears the coding sequence for the gene of interest (GOI). The envelope plasmid carries the genetic information for the viral coat protein. Most lentiviral vectors are pseudotyped with VSV-G, which confers pantropism and high virion stability. The transfer plasmid for the generation of HIV-1-derived lentiviral vectors includes the viral LTRs, the primer binding site, the packaging signal, the Rev responsive element and a transcriptional unit containing a promoter linked to the GOI. Importantly, the GOI is the only coding sequence that is transferred to the target cells. Some virus-producing systems have additionally modified transfer vectors. The system developed by Prof. Didier Trono and coworkers, used for the experimental work of this PhD thesis, has two such elements. The central polypurine tract (cPPT)

codes for the so-called central DNA flap, which improves the import of the HIV-1 preintegration complex into the nucleus and thus the gene transfer efficiency (VandenDrissche et al., 2002). The woodchuck hepatitis virus post-transcriptional regulatory element (WPRE) improves transgene expression by supporting mRNA 3' end processing and polyadenylation (Zufferey et al., 1999). The first generation of HIV-1-based vector packaging systems already comprised three plasmids, but only two of nine native HIV-1 genes were deleted, vpu and env (Buchschacher, 2003). The second geration packaging systems only utilize HIV-1 gag, env, pol, rev and tat genes, because all other genes are not necessary for the efficient production of lentiviral particles (Buchschacher, 2003). The third generation packaging systems that are currently used, e.g. the one from Trono and coworkers, have some additional safety measures (Wiznerowicz and Trono, 2003; Zufferey et al., 1998). The most important modification is that the vectors are self-inactivating (SIN). Self-inactivation relies on the deletion of a part of the U3 region of the 3' long terminal repeat (LTR) in the DNA used for virus production (Zufferey et al., 1998). This region is used as template for the U3 regions of both LTRs in the produced provirus. Additionally, in the third generation systems the U3 promoter of the 5'LTR is replaced with the CMV promoter and the tat gene is deleted. Thus third generation systems are safer and have a reduced potential for the generation of replication-competent viruses. When using viral vectors for gene delivery, the choice of the promoter for transgene expression and the choice of reporter genes are not always easy. The use of highly active viral or cellular promoters, like CMV or EF1 promoters, may have deleterious effects in some target cells. Another problem is possible promoter attenuation in target cells and consequent silencing of the transgene. The CMV promoter is known to undergo transcriptional inactivation in several tissues, e.g. airway epithelial cells (Goldmann et al., 1997). Kowtharapu and colleagues (2009) have demonstrated that EPCs cannot be transfected with plasmid-based methods, and treatment with lentiviral vectors encoding green fluorescent protein (GFP) under the control of the ubiquitously recognized EF1 promoter also does not cause transgene expression. Only lentiviral vectors with transgenes placed under the control of a cell-type-specific promoter lead to transgene expression.

1.8 Baculovirus expression system

Insect viruses are classified into 12 families of which the family Baculoviridae is the most ubiquitous and most intensely studied one. The baculoviruses have rod-shaped and enveloped nucleocapsids. They contain a large circular, double-stranded DNA genome. There are two genera of the Baculoviridae, nucleopolyhedrovirus (NPV) and granulovirus (GV); usually only the former is used as a baculovirus expression vector. The baculoviruses produce two types of progeny, the budded virus (BV) and the occluded virus (OV) (Miller, 1997). The OVs of the NPV are named polyhedron. The polyhedron contains multiple virions and one NPV can even contain multiple nucleocapsids (M morphotype) (Inceoglu et al., 2006). The BVs are produced during an early stage of infection when the nucleocapsid buds through the plasma membrane. The BVs are responsible for the systemic cell-to-cell spread of the virus within an infected animal (Fleming and Hunt, 2000; O'Reilly et al., 1994). OVs are produced during the late stage of infection when the progeny nucleocapsids are deposited in the baculovirus polyhedra. The OVs are responsible for the horizontal or larva-to-larva spread of the virus. When an insect larva ingests the OVs, the progeny virus is liberated because the OVs are sensitive to the alkaline insect gut fluid and the enzymes contained in it that break down the crystalline protein matrix of the OV. The baculovirus life cycle begins when a susceptible insect host ingests a polyhedron (e.g., one from a dead larva) resulting in the release of hundreds of occlusion-derived virions (ODVs) into their gut. The released ODVs enter the midgut cells where the nucleocapsids are released and uncoated; viral replication is then initiated. The infection spreads in the host because of the BVs. About one week following the ingestions of NPVs, the infected host finally succumbs to the virus and dies. Recombinant baculoviruses (e.g. *Autographa californica* nuclear polyhedrosis virus, AcNPV) are widely used to express transgenes in cultured insect cells or larvae (Luckow and Summers, 1988). This technique has great advantages. It guarantees high levels of heterologous gene expression since the GOI is placed under the control of the very strong polyhedron promoter. Secondly, the recombinant proteins are mostly processed, modified and targeted to the appropriate cellular compartment. Most recombinant proteins are soluble and can easily be

recovered. Finally, the work is very safe because the virus host range is limited to specific invertebrate species. AcNPV infects cell lines derived from the fall armyworm *Spodoptera frugiperda* which grow in suspension, permitting easy large-scale protein expression. Since the baculovirus has a large circular double-stranded DNA genome (>100 kb) with many restriction sites, recombinant baculoviruses must be constructed in two steps using homologous recombination *in vivo*. The GOI is cloned into a donor plasmid downstream of the promoter that is flanked by non-essential baculovirus DNA, usually the polyhedron gene. The donor plasmid is then co-transfected with circular wild-type viral DNA into insect cells. Normally, only up to 1% of the viral progeny is recombinant and carries the transgene under the control of the strong polyhedron promoter. Another disadvantage of this method is the need for sequential plaque assays to purify the recombinant virus away from the parental wild-type virus. Nowadays, there exist faster and more efficient ways of producing recombinant baculoviruses. By far, the most widely used is the Bacmid-to-Baculovirus (Bac-to-Bac) procedure developed by researchers at Monsanto (Luckow et al., 1993). An expression cassette carrying the GOI is integrated into a “bacmid“ coding for the baculovirus genome by site-specific transposition in bacteria. The recombinant “bacmid” is then used for the transfection of insect cells.

1.9 Knockout mice

A knockout mouse is a genetically modified mouse in which an existing gene was removed or disrupted. Knockout mice allow researchers to study the function of genes and this information can be used to understand the role of these genes in human disease because humans share many genes with mice. A routine method for modifying the mouse genome at a specific locus is homologous recombination in embryonic stem cells. The DNA construct to be introduced (the targeting vector) into the genome of the ES cells should contain several kilobases of DNA that are homologous to the mouse genome flanking the gene of interest. The vector also must contain some parts of the gene itself (the deletion cassette, e.g. the two first exons) flanked by loxP sites as well as

genes conferring drug resistance or sensitivity so researchers can select the rare recombination events from a large population of ES cells. The first knockout mouse was engineered by Mario Capecchi and coworkers in 1990 using this gene targeting method. These mice which were homozygous for the loss of the int-1 proto-oncogene developed severe abnormalities in the midbrain and cerebellum (Thomas and Capecchi, 1990). Capecchi was awarded the Nobel Prize for Medicine in 2007 for this work together with Oliver Smithies and Martin Evans for their discoveries of the principles for introducing specific gene modifications in mice by the use of embryonic stem cells. Since then some variations of this technique have been developed, e.g. knock-in and knock-down mice where the expression of a specific gene is altered but not necessarily completely shut down. The benefits of knockout mice are obvious; they permit the complete inactivation of a gene and the identification of the molecular function of many genes and their role in important diseases. But there are also limitations because more than 10 % of all knockout mice are developmentally lethal and the genetically modified embryos cannot grow into adult mice. This problem can be circumvented by the use of conditional mutations. Another drawback of knockout mice is their difficult generation which comprises many steps and is quite expensive.

1.10 Aim of the thesis

Wdr16 is a protein that is abundantly expressed in kinocilia-bearing tissues such as ependyma and testis and that was linked to ciliary function and hydrocephalus (Hirschner et al., 2007). The aim of the present PhD thesis was a molecular biological approach to contribute to the understanding of the molecular function and spatial structure of this protein. In order to achieve this goal, it was highly desirable to perform experiments by which the expression of the Wdr16 protein could be abolished or reduced in kinocilia-bearing cells and tissues. One method that was used for this purpose is the “knockdown” of wdr16 gene expression in EPCs using lentiviral gene transfer (Stewart et al., 2003). Another method employed is the generation of a transgenic Wdr16 “knockout” mice strain (Walinski, 2004). To achieve such an ambitious

objective, it is important to establish basic techniques, e.g the cloning of a targeting vector, ES cell culture and the procedures for electroporation, and screening of the ES cells. A further objective of this PhD thesis was to study the cellular and subcellular location of Wdr16. This can be carried out by using immunohistochemical stainings as well as by expressing GFP- or Flag-tagged fusions of Wdr16 in EPCs or cell lines. Finally, another aim of this PhD thesis was the expression of Wdr16 in insect cells as a prerequisite for the purification of the protein by affinity chromoatography. The purified protein then has to be subjected to CD analysis in order to determine its secondary structure. The availability of a purified protein would also facilitate, among other things, the determination of the crystal structure of Wdr16, production of a new polyclonal antibody, and the search for protein interaction partners using “pull down” assays. The search for binding partners of Wdr16 (using Co-IP) was also a topic of this thesis since the identification of a binding partner can instantly provide valuable information about the molecular function of a gene product.

2 Results

2.1 Gene knockdown of wdr16 in EPC by RNA interference (RNAi)

Wdr16 knockdown in zebrafish by antisense morpholinos resulted in severe hydrocephalus without visibly affecting ciliary beat (Hirschner et al., 2007). RNAi-based gene knockdown experiments in EPCs open up the possibility to identify the function of the wdr16 gene at molecular and cellular level. In order to suppress wdr16 expression in EPCs, a lentivirus encoding anti-wdr16 siRNA and GFP as reporter (HIV1 / VSV-G / Ef1p-GFP / H1p-wdr16 siRNA), and a control virus expressing a random siRNA (HIV1 / VSV-G / Ef1p-GFP / H1p-control siRNA) were produced. The lentiviruses were produced by transient transfection of HEK293T cells with a second generation packaging system (developed by Prof. Didier Trono and coworkers). They were pseudotyped with the surface protein of the vesicular stomatitis virus (VSV-G). The siRNA cassettes were under the control of the H1 promoter, the GFP reporter cassettes under the control of the EF1 promoter. The H1 promoter is the region of DNA which normally initiates the transcription of the Histone H1 gene and which is constitutively active in most mammalian cell types. The EF1 promoter normally acts as a regulator for the level of Elongation factor 1-α gene expression. HIV1 / VSV-G / Ef1p-GFP / H1p-wdr16 siRNA failed to specifically downregulate wdr16 expression in EPC. The reason behind this was most likely a cytotoxic and anti-differentiation effect elicited by early GFP expression under the control of the ubiquitously recognized EF1 promoter, as described by Kowtharapu et al. (2009). For this reason, the EF1 promoter in front of the GFP cassette was replaced by the kinocilia-specific wdr16 promoter, and new lentiviral vectors were produced. These viruses were used to infect EPCs, and the respective levels of Wdr16, adenylate kinase 7 and glycogen phosphorylase isoform BB in the cultures synthesizing anti-wdr16 siRNA and control-siRNA were compared by Western blotting. The brain isoform of glycogen phosphorylase was used as a control because this enzyme is almost exclusively located in ependymal cells (and astrocytes) of rat brain (Pfeiffer et al., 2003) and it is always expressed in the ependymal cells of EPCs

(Prothmann et al., 2001; Verleysdonk et al., 2005). Adenylate kinase 7 is a differentiation marker for kinocilia-bearing ependymal cells; it participates in the synthesis of adenosine triphosphate and thus helps providing energy for the beating of the cilia (Scheible et al., 2007; Milara et al., 2010).

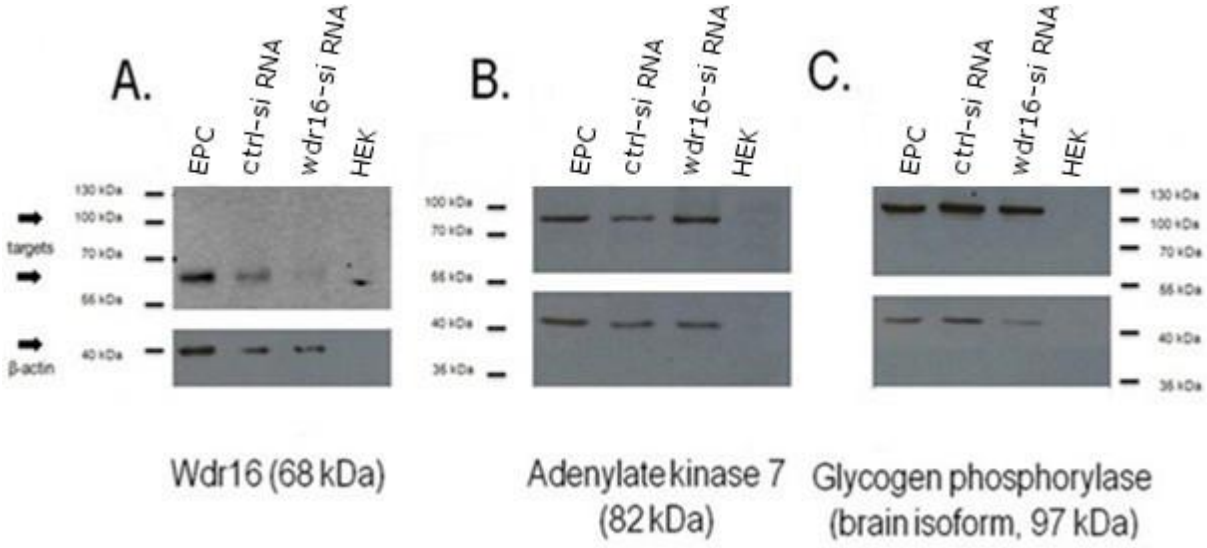

Fig. 1. A: Wdr16 expression is specifically suppressed in EPCs infected with lentivirus encoding a siRNA targeting Wdr16 mRNA as compared to EPCs mock-infected with culture medium (EPC) or with a control siRNA virus (Ctrl-siRNA). The HIV-1 lentiviral particles were produced in HEK293T cells and are pseudotyped with the surface protein of vesicular stomatitis virus (VSV-G). EPCs were prepared as described in Methods and infected on day in vitro 1 (DIV1) with the indicated viruses. Each lane of polyacrylamide Tris-glycine gels was loaded with 40 µg protein (homogenate) of an EPC. After electrophoresis, the gels were subjected to Western blotting and the membranes stained for Wdr16 protein. All membranes were thoroughly washed with TBS-T and then reprobed with anti-rat β-actin antibody to control for equal loading. **B, C:** Control blots using antibodies against adenylate kinase 7 and glycogen phosphorylase (brain isoform), respectively.

Only the target protein Wdr16 was knocked down by the wdr16 siRNA construct, confirming the specificity of the RNAi approach (Fig. 1). The loss of Wdr16 in EPCs treated with anti-wdr16 siRNA was not caused by unspecific toxicity of the lentiviral particles. This was shown in Western blots for the marker proteins for kinocilia-bearing cells, adenylate kinase 7 and glycogen phosphorylase BB (Scheible et al., 2007; Verleysdonk et al., 2005) which were performed with protein homogenates (40 µg/lane) from EPCs infected with anti-wdr16 siRNA and control-siRNA viruses, respectively. The expression levels of

both marker proteins are not reduced by anti-wdr16 siRNA virus.The RNAi experiment and Western blotting were carried out three times with comparable results.

In particular, the decrease in wdr16 expression was not due to unspecific loss of the highly damageable (Kowtharapu et al., 2009) kinocilia-bearing ependymal cells of the EPCs. In these experiments the Wdr16 band was still visible but the expression was reduced by 50 - 80 % compared to cultures infected with control-siRNA virus as determined by densitometry. Successful knockdown of wdr16 was further confirmed by immunocytochemistry.

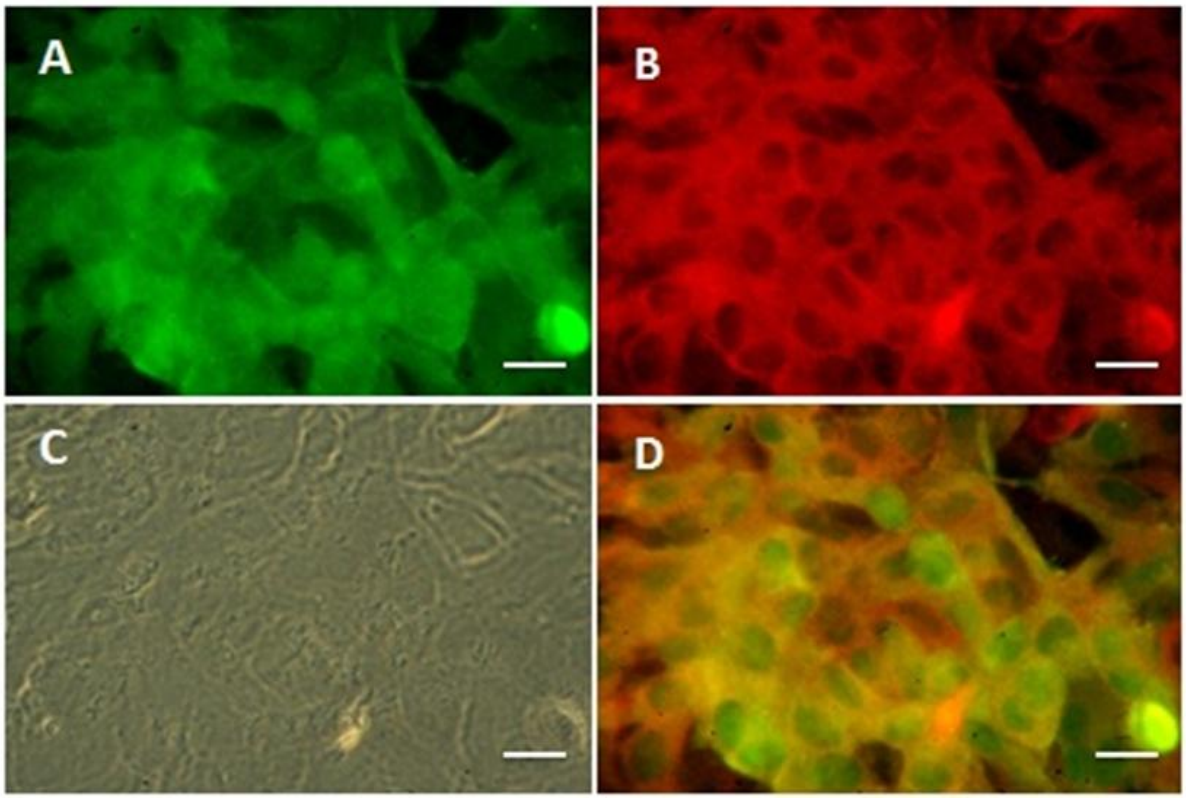

Fig. 2. (part 1) Immunofluorescent staining for Wdr16 protein is specifically reduced in ependymal cells that were infected by a lentivirus encoding an anti-wdr16 siRNA (infection indicated by GFP reporter gene expression). These images show the cells which were infected with viruses expressing control-siRNA (**A-D**). On DIV 12 the cells were fixed with paraformaldehyde and stained with anti-GFP (**A**, green) and anti-Wdr16 antibody (**B**, red). **C**: Phase contrast view. **D**: Merged images of A and B. The bars in A-D correspond to 50 µm.

The cultures were not only stained against Wdr16 protein but also against the GFP reporter protein expressed by the virus in order to facilitate the identification of infected cells. Wdr16 immunoreactivity in cells infected with the anti-wdr16-siRNA virus was greatly reduced compared to cells infected with the control-siRNA virus (Fig. 2). The expression level of the brain isoform of glycogen phosphorylase was not affected in cells hit by the virus bearing the RNAi construct (Fig. 3).

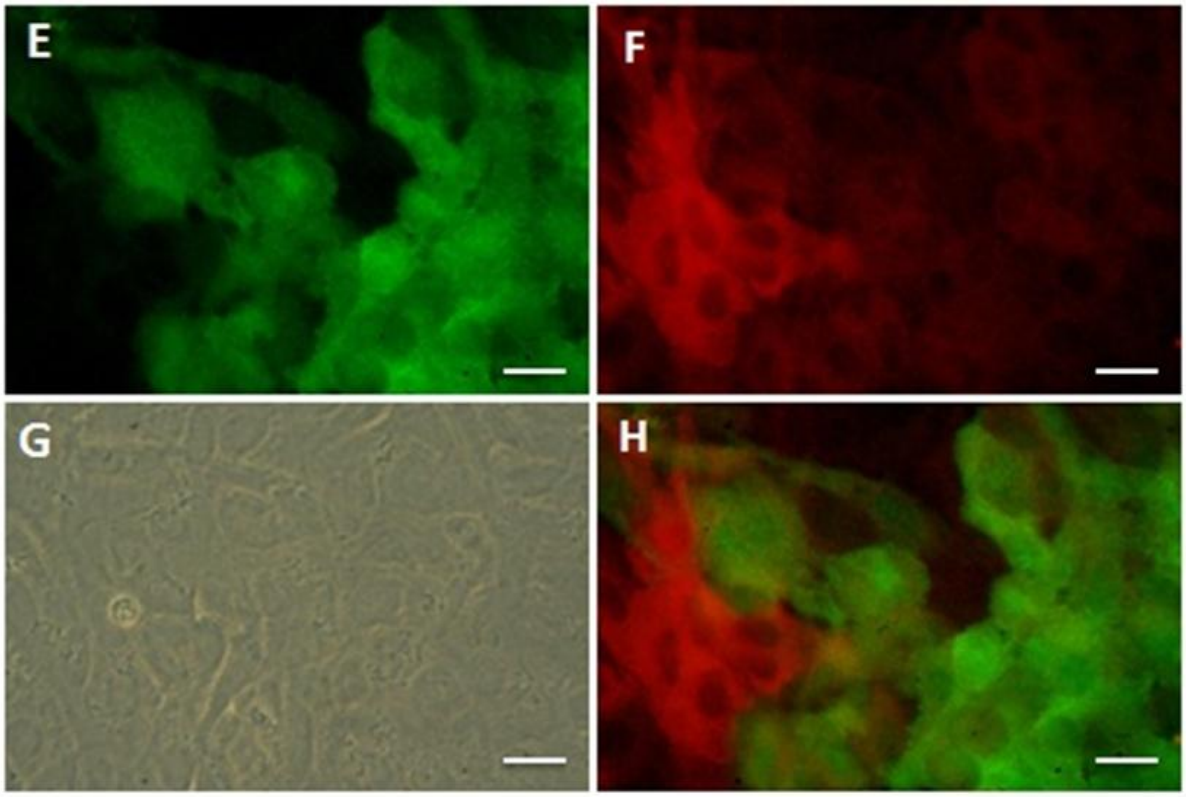

Fig. 2. (part 2) Immunofluorescent staining for Wdr16 protein is specifically reduced in ependymal cells that were infected by a lentivirus encoding an anti-wdr16 siRNA (infection indicated by GFP reporter gene expression). These images show the cells which were infected with viruses expressing wdr16 antisense siRNA (**E-H**). On DIV 12 the cells were fixed with paraformaldehyde and stained with anti-GFP (**E**, green) and anti-Wdr16 antibody (**F**, red). **G**: Phase contrast view. **H**: Merged images of E and F. The bars in E-H correspond to 50 µm.

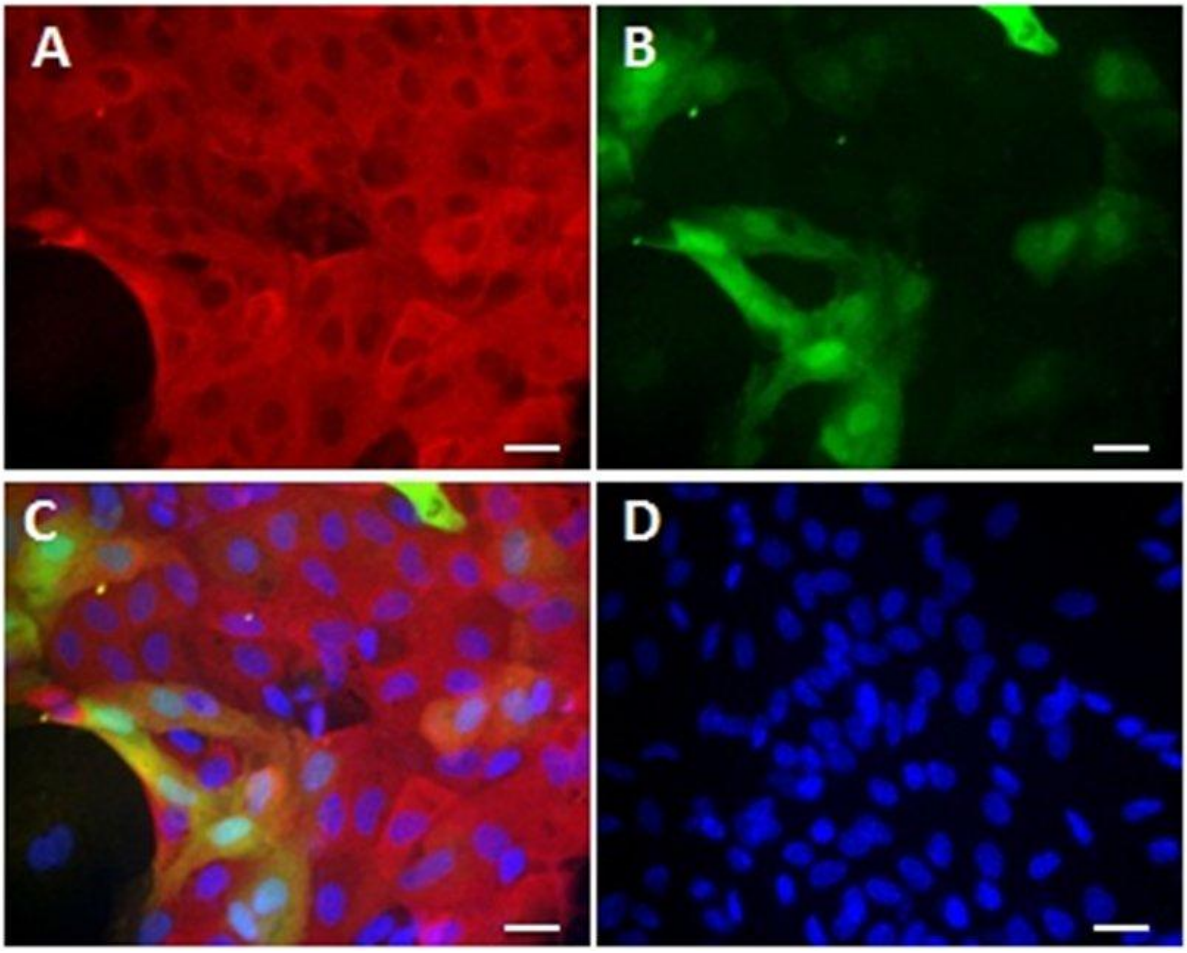

Fig. 3. (part 1) Downregulation of wdr16 expression is not a result of unspecific loss and destruction of ependymal cells. Co-immunostaining of EPCs (DIV 12) against the ependymal cell marker brain isoform of glycogen phosphorylase (GP-BB), and GFP. These images show the cultures infected on DIV1 with lentiviruses expressing anti-wdr16 siRNA (**A** - **D**). The cultures were fixed with 4% paraformaldehyde on DIV 12. **A**: GP-BB (red); **B**: GFP (green);); **C**: Overlay of green, red and blue channels. **D**: Nuclei were counterstained with 4',6-diamidino-2-phenylindole (DAPI). The bars in A-D correspond to 50 µm.

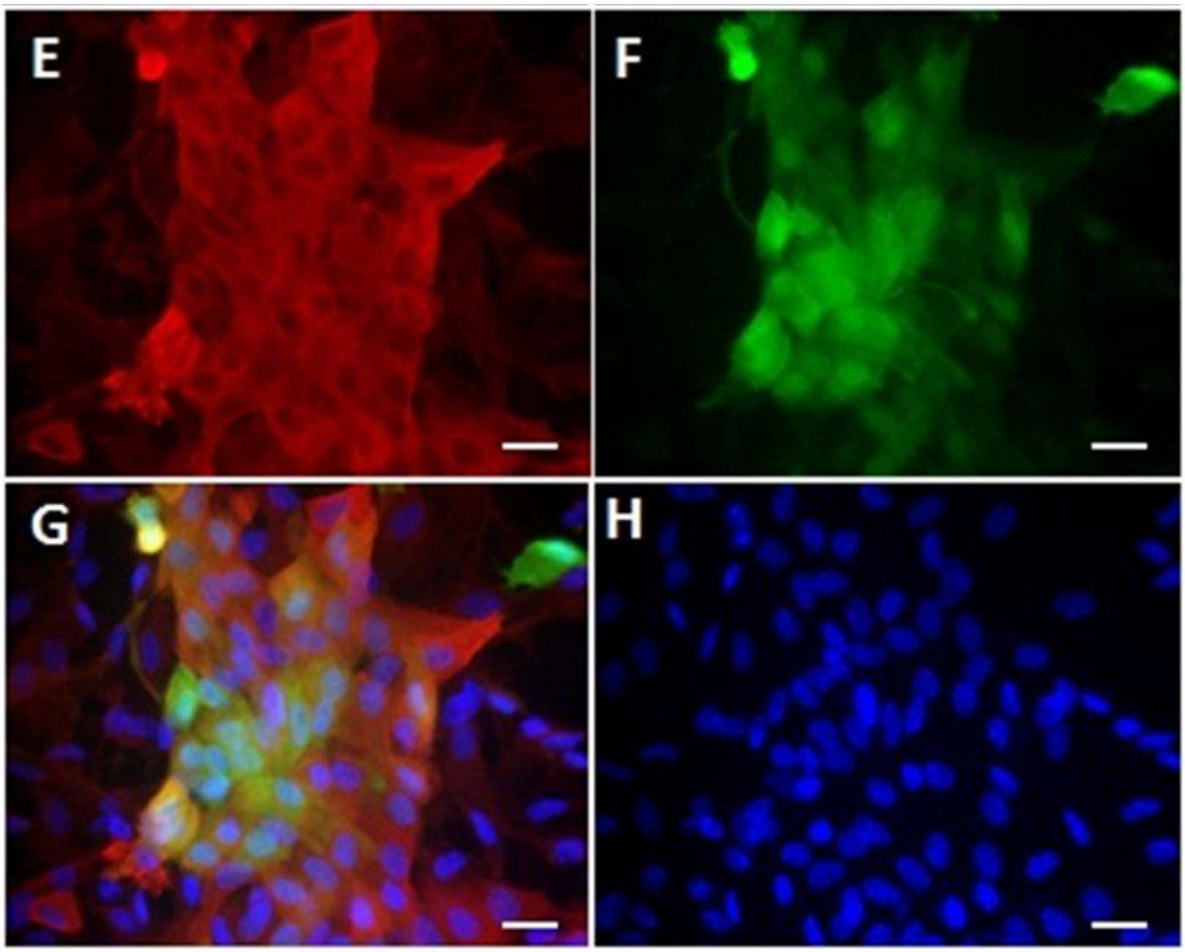

Fig. 3. (part 2) Downregulation of wdr16 expression is not a result of unspecific loss and destruction of ependymal cells. Co-immunostaining of EPCs (DIV 12) against the ependymal cell marker brain isoform of adenylate kinase 7 and GFP. These images show the cultures infected on DIV1 with lentiviruses expressing control siRNA (**E** - **H**). The cultures were fixed with 4% paraformaldehyde on DIV 12. **E**: Ak7 (red); **F**: GFP (green); **G**: Overlay of green, red and blue channels. **H**: Nuclei were counterstained with 4',6-diamidino-2-phenylindole (DAPI); The bars in E-H correspond to 50 µm

2.2 Effect of wdr16 knockdown on ependymal cells

The morphology and appearance of ependymal cells in EPC after wdr16 knockdown was indistinguishable from that of normal ependymal cells. Following immunostaining using an anti-acetylated α-tubulin antibody the EPCs appeared to feature normal-looking kinocilia bundles (Fig. 4) and the number of ependymal cells bearing kinocilia bundles was only slightly, but insignificantly, reduced in EPC treated with the anti-wdr16 siRNA virus (approx. 5 %) compared to the cells infected with the control siRNA virus (Fig. 5). For

obtaining this result the infected GFP-positive ciliated and non-ciliated cells were counted under the fluorescence microscope following immunostaining. The number of GFP-positive ependymal cells on coverslips treated with anti-Wdr16 siRNAs *with* (n^k) and *without* kinocilia bundles (n^0) were counted. At least 5 coverslips with at least 100 GFP-positive cells were analyzed and the percentage of ciliated cells was calculated using the ratio of n^k and n^0 for each coverslip. The same procedure was performed using 5 coverslips treated with control siRNAs. The hypothesis that the mean percentage of ciliated cells of both groups is significantly different was checked using a Student's t-test for independent samples against the null hypothesis (no significant difference). The p-value was calculated using the PRISM 6 software (GraphPad) and was not considered to be statistically significant ($p > 0.5$). Hence, there is only a random chance that the treatment of the EPCs with anti-Wdr16 siRNAs had caused a reduction in ciliated cells in this experiment as compared to the treatment with control siRNAs.

Ciliary beating was still present following wr16 RNAi interference and it was indistinguishable from that in EPCs infected with lentiviral vectors expressing sense siRNAs when observed under the phase contrast microscope.

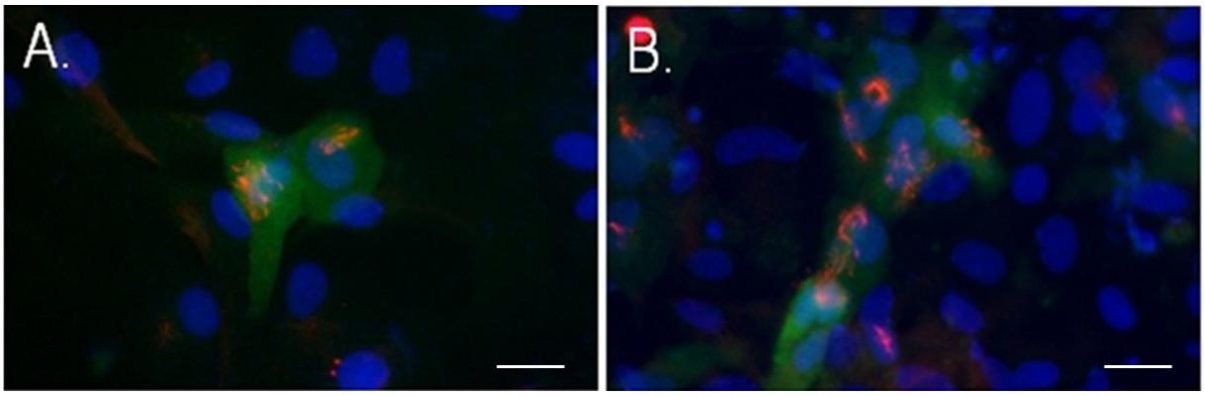

Fig. 4. Analysis of kinocilia and morphology of ependymal cells following wdr16 knockdown by RNAi. On DIV1, EPCs were infected with lentiviruses bearing an anti-wdr16-siRNA cassette (**A**) or a cassette with control siRNA (**B**). Both viruses also encoded GFP under the control of the wdr16 promoter. On DIV 12, the cultures were fixed, the kinocilia were stained with anti-α-tubulin antibody (1:100; red) and the GFP fluorescence was enhanced with an anti-GFP antibody (1:100; green). Nuclei were counterstained with 4',6-diamidino-2-phenylindole (DAPI, blue). For both images, the red, green and blue fluorescence channels were merged. The bars in A and B correspond to 30 µm.

A central question is how wdr16 downregulation affects the kinocilia-bearing ependymal cells and how this disturbance could result in hydrocephalus formation as seen in the zebrafish model (Hirschner et al., 2007). One hypothetical mechanism is impairment of cell polarity. Mice of the hyh (hydrocephalus with hop gait) strain develop congenital hydrocephalus (Bronson and Lane, 1990) and carry a missense mutation in the gene encoding α-SNAP, a protein essential for trafficking of proteins to the apical membrane (Chae et al., 2004).

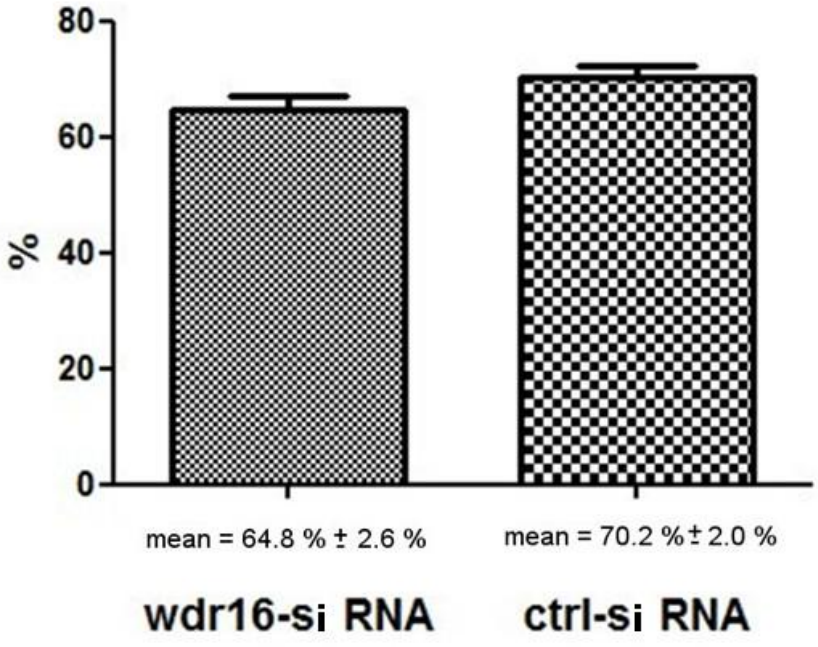

Fig. 5. Comparison of the percentage of kinocilia-bearing cells in EPC after transfection with either anti-wdr16 siRNA (left) or control siRNA (right). EPCs seeded on coverslips were infected with the siRNA lentiviruses on DIV1. The cells were fixed on DIV 12 and stained for GFP, α-tubulin and DAPI. The coverslips were photographed with a Canon EOS 350D digital camera mounted on a Zeiss IM35 fluorescence microscope. After image processing and merging (Photoshop software), the ciliated and non-ciliated GFP-positive cells were counted by hand.

Ezrin, a membrane cytoskeleton linker, was used as a tentative marker for cell polarity. The protein normally localizes just beneath the plasma membrane of epithelial cells (Berryman et al., 1993; Cao et al., 2005). In frozen sections of rat brain, the available anti-ezrin antibody stained the apical side of the ependymal layer just as in EPCs (Fig. 7).

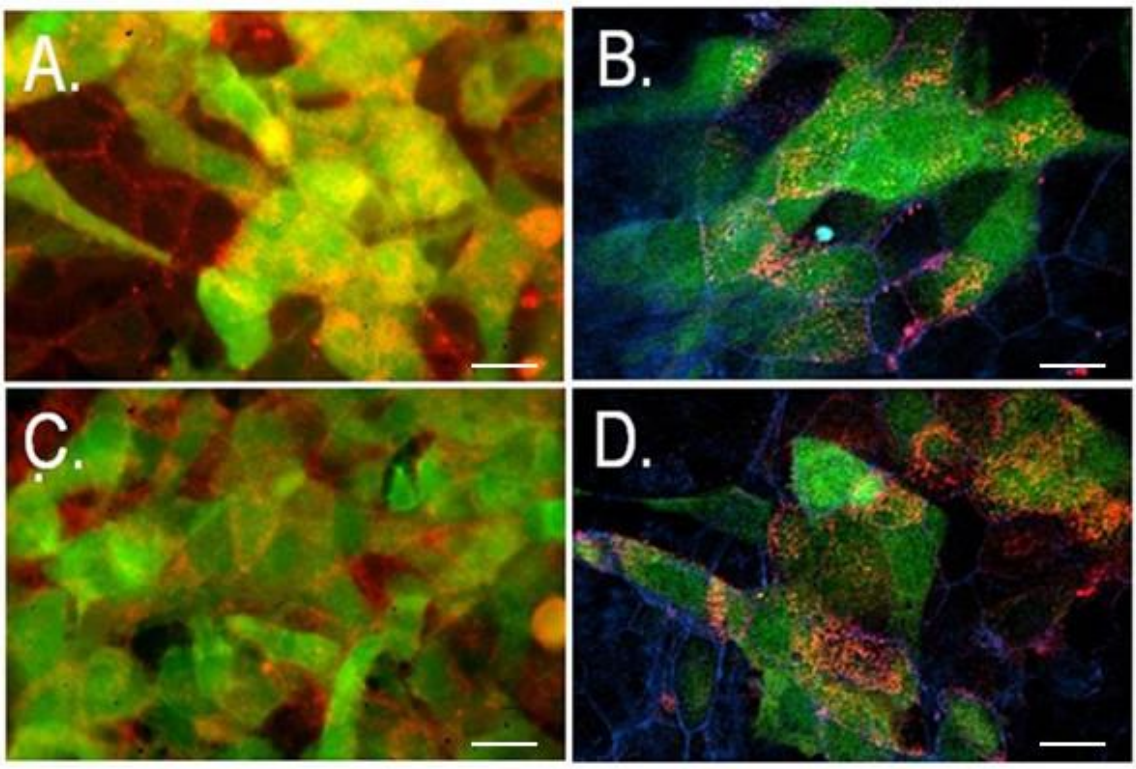

Fig. 6. The 87 kDa actin-associated protein ezrin is localized beneath the apical plasma membrane of cultured ependymal cells and was used as a marker for normal cell polarity. Both EPCs infected with control siRNA lentivirus (**A**, **B**) and with anti-wdr16 siRNA virus (**C**, **D**), showed the expected distribution of ezrin (red) which is associated with microvilli and the cell borders on the apical side. Only cells infected with the corresponding virus and therefore expressing GFP (green) were analyzed. To analyze the presence of ezrin on the apical cell surface with more precision, deconvolution analysis (see chapter 4.2.23) was applied to the images (**B** and **D**). The bars in A-D correspond to 30 µm.

This antibody was subsequently employed to study the distribution of ezrin in EPCs with and without RNAi-mediated knockdown of wdr16 (Fig. 6). EPCs infected with anti-wdr16 siRNA and control siRNA virus showed the same standard distribution of ezrin at microvilli and cell borders on the apical side. In order to analyze the presence of ezrin on the apical cell surface with more precision, deconvolution analysis was applied to the images. This is a computational method for reducing out-of-focus fluorescence. The deconvoluted fluorescence images confirmed the normal ezrin distribution and thus apical-basal cell polarity in ependymal cells infected with the anti-wdr16 siRNA virus.

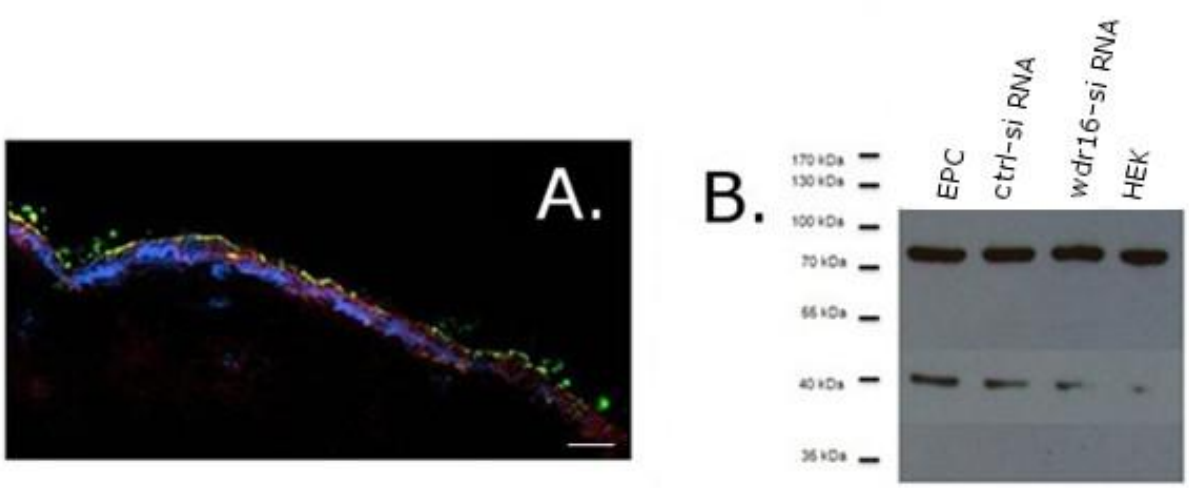

Fig. 7. (**A**) The ezrin antibody used for this analysis stains the apical side (green) of the ependymal layer (counter-stained against Wdr16, red) in frozen sections of rat brain, confirming its specificity. Cell nuclei were stained with DAPI (blue). The bar corresponds to 100 µm. (**B**) Protein homogenates from control and "knockdown" cultures were subjected to SDS-PAGE electrophoresis and Western blotting. The blotting membrane was probed with an antibody against ezrin. An anti-rat β-actin antibody was used for the loading control (band at 42 kDa). The amount of ezrin protein is not changed following wdr16 “knockdown”.

2.3 Injection of anti-wdr16 siRNA lentivirus in the rat brain ventricles

The lentiviral vectors expressing anti-wdr16-siRNA and control-siRNA were injected into the cerebral ventricles of adult Sprague-Dawley rats in order to examine the effect of wdr16 knockdown on the ependymal cells *in vivo*. The viral solutions were stereotactically microinjected in both lateral ventricles of the rats. Additionally, one rat was mock-infected with vehicle instead of virus solution. After 6 weeks, the rats looked still healthy and showed no unusual behavior. Afterwards, the rats were sacrificed and frozen sections of the brains were produced. First, the ependymal layer was successfully labeled using the Wdr16 antibody. Afterwards, the frozen sections were stained for GFP. No expression of the reporter gene indicating virus-infected cells could be detected while other immunofluorescent stainings worked well on the frozen sections, e.g. against α-tubulin, GFAP or γ-tubulin (photomicrographs not shown).

2.4 Expression of Flag-tagged Wdr16 in HEK cells and EPC

In order to analyze the location of Wdr16 in EPCs and different cell lines and to facilitate immunoprecipitation experiments with Wdr16 protein, lentiviral vectors expressing Flag-tagged Wdr16 protein were produced. This had deemed necessary due to the likelihood that the available anti-Wdr16 peptide antibody would not recognize its target in protein complexes, its recognition site of only 15 amino acyl residues length (Hirschner et al., 2007) perhaps being blocked by interaction partners. For infection of cell lines, e.g. HEK293T and HeLa, the wdr16-Flag expression cassette was put under the control of the constitutively active EF1 promoter (HIV / VSV-G / Ef1p-wdr16-Flag). For the infection of EPCs, the Wdr16-Flag expression was driven by the kinocilia-specific wdr16 promoter (HIV / VSV-G / wdr16p-Wdr16-Flag). The 766 nucleotides of the sequence between the rat genes stx8 and wdr16 were used as the wdr16 promoter (as described by Kowtharapu et al., 2009), due to the fact that the core wdr16 promoter is still unknown. HEK293T cells were infected with the HIV / VSV-G / Ef1p-Wdr16-Flag lentivirus and analyzed for transgene expression by Western blotting 48 h after the infection. Immunoblots of the lysates developed with anti-Wdr16 and anti-Flag confirmed the expression of Wdr16-Flag in the HEK293T cells (Fig. 8). The additional small bands present in both lanes of the anti-Flag Western blot were most likely caused by unspecific binding of the first or the secondary antibody to unknown proteins. This unwanted “background” is most likely caused by the incubation at too high a concentration of first or secondary antibody or is due to insufficent addition of milk powder, BSA or other blocking reagents.

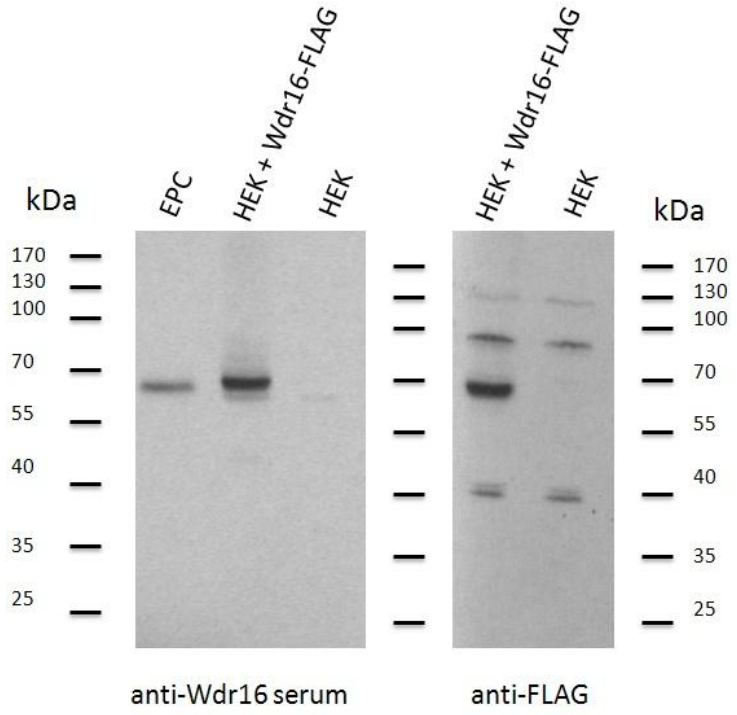

Fig. 8. Western blot analysis of the expression of Flag-tagged Wdr16 in HEK293T cells transfected with an appropriate expression plasmid. Cells were collected 48 h after transfection. As a negative control, a lysate of non-transfected HEK293T cells was prepared. A lysate of 12 d old EPCs served as the positive control. Each lane was loaded with 40 µg of protein. After blotting, the membrane was probed with guinea pig anti-Wdr16 antiserum (left) or rabbit anti-Flag polyclonal antibody diluted 1: 10,000 (right). The secondary antibodies were donkey anti-guinea pig IgG-peroxidase conjugate and anti-rabbit goat IgG-peroxidase conjugate. Detection was performed with the enhanced chemiluminescence (ECL) system from Pierce.

2.5 HEK cell line expressing Wdr16-Flag

The ability of the lentiviruses to integrate into the genome of a host cell was exploited to produce a stable HEK293T cell line expressing Flag-tagged Wdr16 protein. For this purpose, the HEKT293T cells were stably transfected with the respective lentivirus and the cells were seeded in a 96-well plate following trypsination and dilution to a final concentration of approximately one cell per well. The single colonies were analyzed, by fluorescence microscopy, for Wdr16-Flag expression by using anti-Wdr16 and anti-Flag antibodies. The single colonies expressing the protein of interest were further propagated and a final assessment of Wdr16-Flag protein expression was made using antibody staining and fluorescence microscopy (Fig. 9).

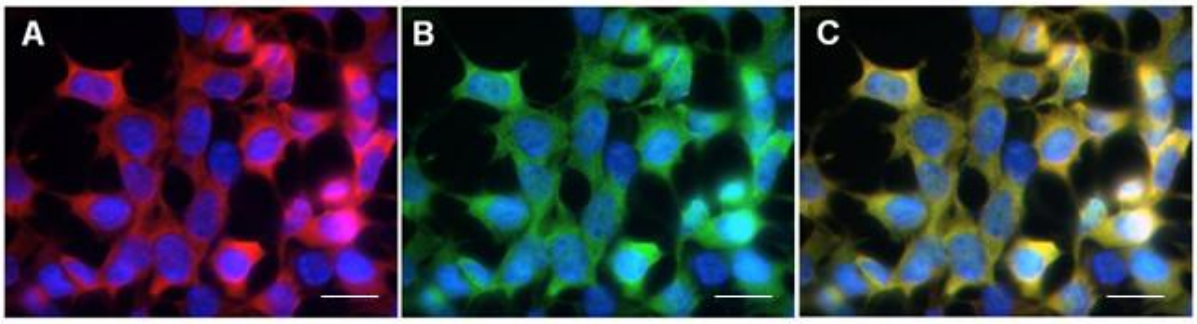

Fig. 9. Immunofluorescent images of the stable HEK-Wdr16-Flag cell line. The pictures demonstrate the cytoplasmic location of the Flag-tagged Wdr16 protein. HEK293T cells were infected with HIV/VSV-G/Ef1-Wdr16-Flag lentiviral particles, and fluorescence-positive cells were cloned to yield the cell line permanently expressing Wdr16-Flag protein. **A.** Immunostaining against Wdr16 with the established (Hirschner et al., 2007) anti-Wdr16 peptide antibodies (red) **B.** Immunostaining of the stable cell line with a monoclonal antibody (M2) against the Flag epitope (green). **C.** Overlay of the images A and B. Overlapping cellular domains of wdr16 and Flag-tag expression appear yellow, in this case the cytosol. Nuclei were counterstained with 4',6-diamidino-2-phenylindole (DAPI). The bars in A-C correspond to 20 µm.

2.6 Immunoprecipitation of Wdr16

WD-repeat proteins are known to form a scaffold for protein interactions and the assembly of protein complexes. The identification of protein interaction partners of Wdr16 would certainly shed some light on its molecular function. In the past, Yeast-2-Hybrid experiments and immunoprecipitation of Wdr16 using an established (Hirschner et al., 2007) anti-Wdr16 peptide antibody failed to identify protein interaction partners (S. Verleysdonk, personal communication). Silva et al. (2005) demonstrated that Wdr16 associates with HSP70, proteins of the chaperonin-containing TCP-1 (CCT1) complex and with BRCA2 in HepG2 cells. However, the relevance of these protein-protein interactions for the physiological function of Wdr16 remains to be demonstrated. TCP1α is not expressed in EPC. The TCP1α complex is a ciliary and flagellar component in protozoa and mammals, possibly related to cilia biogenesis and axonemal protein dynamics (Stephans and Lemieux, 1999; Seixas et al., 2003). In order to identify relevant Wdr16 interaction partners, immunoprecipitation was performed using the M2 monoclonal anti-Flag antibody. The success of the immunoprecipitation was verified by an anti-Wdr16 immunoblot (Fig. 10). The Co-IP eluate from the EPC/HEK293T-Wdr16-Flag lysate did not exhibit

additional protein bands that could be attributed to potential protein interaction partners compared to the control eluate following SDS-PAGE and Coomassie Brilliant Blue or silver staining (not shown).

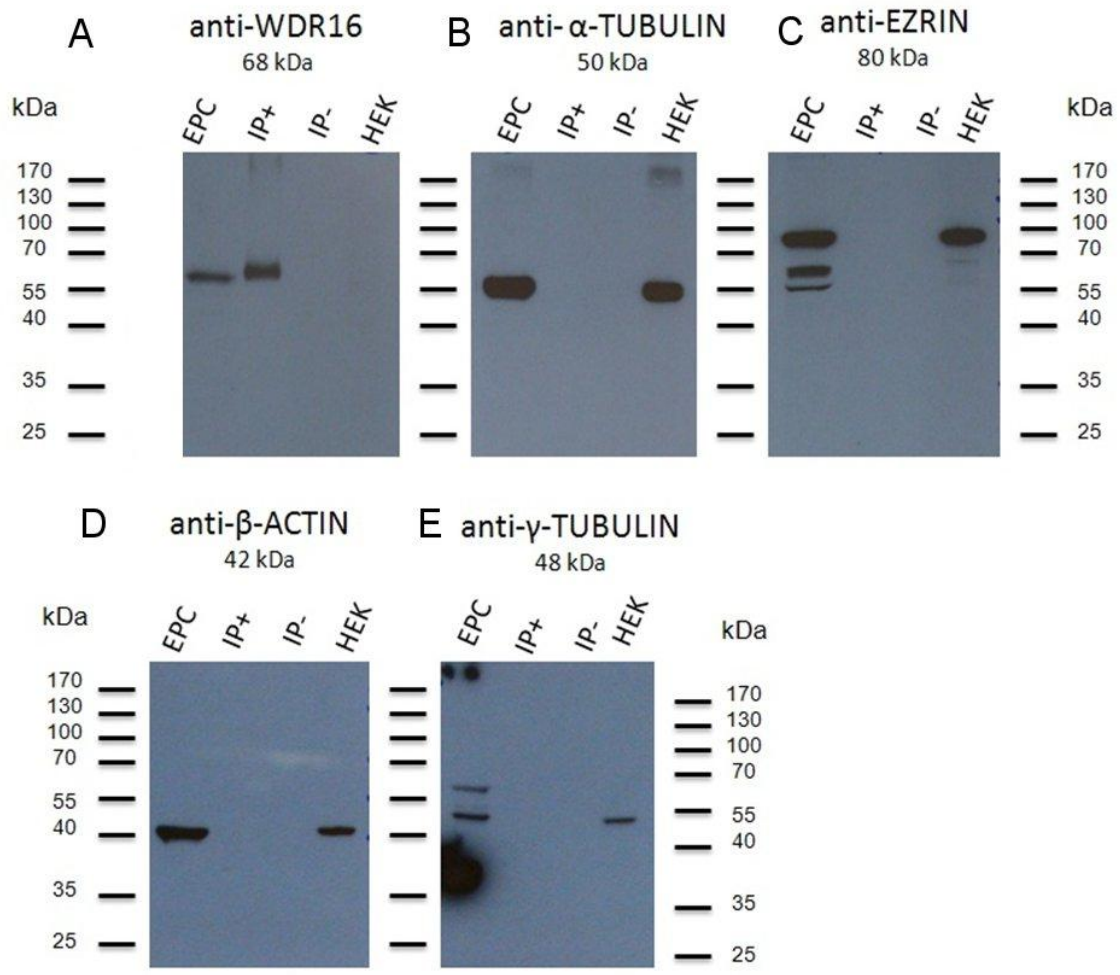

Fig. 10. Immunoprecipitation of Wdr16 protein and Western blot analysis of the Co-IP eluates for possible interactions of Wdr16 with other protein. EPCs, cultures of the HEK-Wdr16-Flag cell line and HEK293T cells were lysed with lysis buffer. The EPC lysates were mixed with equal amounts of HEK293T lysate and lysate of the HEK-Wdr16-Flag cell line. The lysates were pre-incubated overnight at 4°C to facilitate the interaction of the proteins contained in the two different lysates. Afterwards the lysates were mixed with a purified monoclonal M2 anti-Flag antibody covalently attached to agarose. The samples were incubated overnight at 4°C and thoroughly washed with lysis buffer. Afterwards, the Wdr16-Flag protein was eluted using a high concentration of Flag peptide. Afterwards, the eluates were subjected to Western blotting for detection of Wdr16 **(A)** and four other proteins: α-tubulin **(B)**, ezrin **(C)**, β-actin **(D)** and γ-tubulin **(E)**. IP+: Co-IP eluate from the EPC/HEK-Wdr16-Flag lysate. IP-: eluate from the EPC/HEK293T lysate (negative control). HEK: Co-IP eluate from HEK293T lysate (additional negative control). The dark spots in image **(E)** are originating from the application of the Western blotting substrate prior to the development of the x-ray film.

Since immunoblotting is more sensitive than such unspecific staining methods, α-tubulin, β-actin and γ-tubulin were freely chosen as interaction candidates for Wdr16 and tested accordingly by this method. While α-tubulin is a major structural protein of cilia, γ-tubulin occurs in basal bodies, and β-actin was chosen because Wdr16 bears a striking similarity with the actin-interacting protein Aip1. Fig. 10A is the positive control for the Co-IP experiment. The band in the lane labeled IP+ demonstrates that Wdr16 is present in the Co-IP eluate from the EPC/HEK293T-Wdr16-Flag lysate and shows that the Co-IP using the Flag-antibody worked. There is no such band in the negative control (IP-) which contains the Co-IP eluate from the EPC/HEK293T lysate and was treated equally. The same Co-IP eluates were also used for Western blots against α-tubulin, ezrin, β-actin and γ-tubulin. There are no additional bands corresponding to these proteins in the IP+ lanes of Figure 10B - 10E. This means, neither of these proteins was co-immunoprecipitated with the Flag-tagged Wdr16.

2.7 Localization of Flag-tagged and GFP-tagged Wdr16 in HeLa cells

The *Chlamydomonas* orthologue of Wdr16, BUG14, is a component of the basal bodies, and its expression correlates with flagellar assembly (Keller et al., 2005). The acronym "BUG" stands for "*b*asal body proteins with *u*p-regulated *g*enes". A Wdr16 orthologue is also present in the basal bodies and pro-basal bodies of trypanosomes (Hodges et al., 2010). Keller et al. demonstrated that a fusion protein of Wdr16 and GFP localizes to the centrioles after transient transfection of a corresponding construct into HeLa cells. These results are inconsistent with the ones obtained using the guinea-pig anti-Wdr16 peptide antibody available in our laboratory (Hirschner et al., 2007). This Wdr16 antibody specifically labels the ependymal layer when applied to frozen sections of rat brain, and also the kinocilia-bearing cells in EPCs. The Wdr16 immunoreactivity is always restricted to the cytoplasm and never concentrated at the basal bodies or other subcellular structures. In order to elucidate the subcellular location of Wdr16 independently from the guinea pig Wdr16 antibody, N- and C-terminal GFP fusion proteins of rat Wdr16 were expressed

in HeLa cells. In HeLa cells transfected with pEGFP plasmid, the green fluorescence of its expressed GFP part was evenly distributed in the nucleus and cytoplasm of the cells (Fig. 11 B). The N-terminal fusion structure of Wdr16 and GFP was exclusively seen in the cytoplasm of the HeLa cells (Fig. 11 D) in agreement with the results obtained with the Wdr16 antibody (Hirschner et al., 2007). For this experiment, HeLa cells were transfected with the plasmid pEGFP-N1-Wdr16. The acronym N1 stands for N-terminal and for the number 1 (there are other variants of these plasmids available with small modifications in the MCS, designated pEGFP-N2, pEGFP-C2, etc.). The plasmid PEGFP-N1-wdr16 was generated by inserting the ORF of wdr16 into the MCS of the commercially available pEGFP-N1 plasmid. The MCS in pEGFP-N1 is located between the promoter and the EGFP coding sequences. Thus, genes cloned into the MCS will be expressed as fusions to the N-terminus of EGFP if they are in the same reading frame as EGFP and there are no intervening stop codons. The C-terminal fusion structure of Wdr16 and GFP was also exclusively seen in the cytoplasm (Fig. 11 F). For this experiment, HeLa cells were transfected with pEGFP-C1-Wdr16 plasmid DNA ((the acronym C1 stands for C-terminal and for the number 1). The MCS of this plasmid is located downstream of the sequence coding for EGFP leading to the expression of fusions to the C-terminus of EGFP. HeLa cells were also infected with lentiviral vectors expressing Flag-tagged Wdr16 (HIV / VSV-G / Ef1p-Wdr16-Flag). The expression of Flag-tagged Wdr16 was confirmed using anti-Wd16 immunohistochemistry and the centrioles were labeled using an anti-γ-tubulin antibody in order to detect any co-localization of Wdr16 and the centrioles. First, the specificity of the employed anti-γ-tubulin antibody was investigated. The antibody recognizes γ-tubulin clearly located at the centrioles in metaphase cells (Fig. 12).

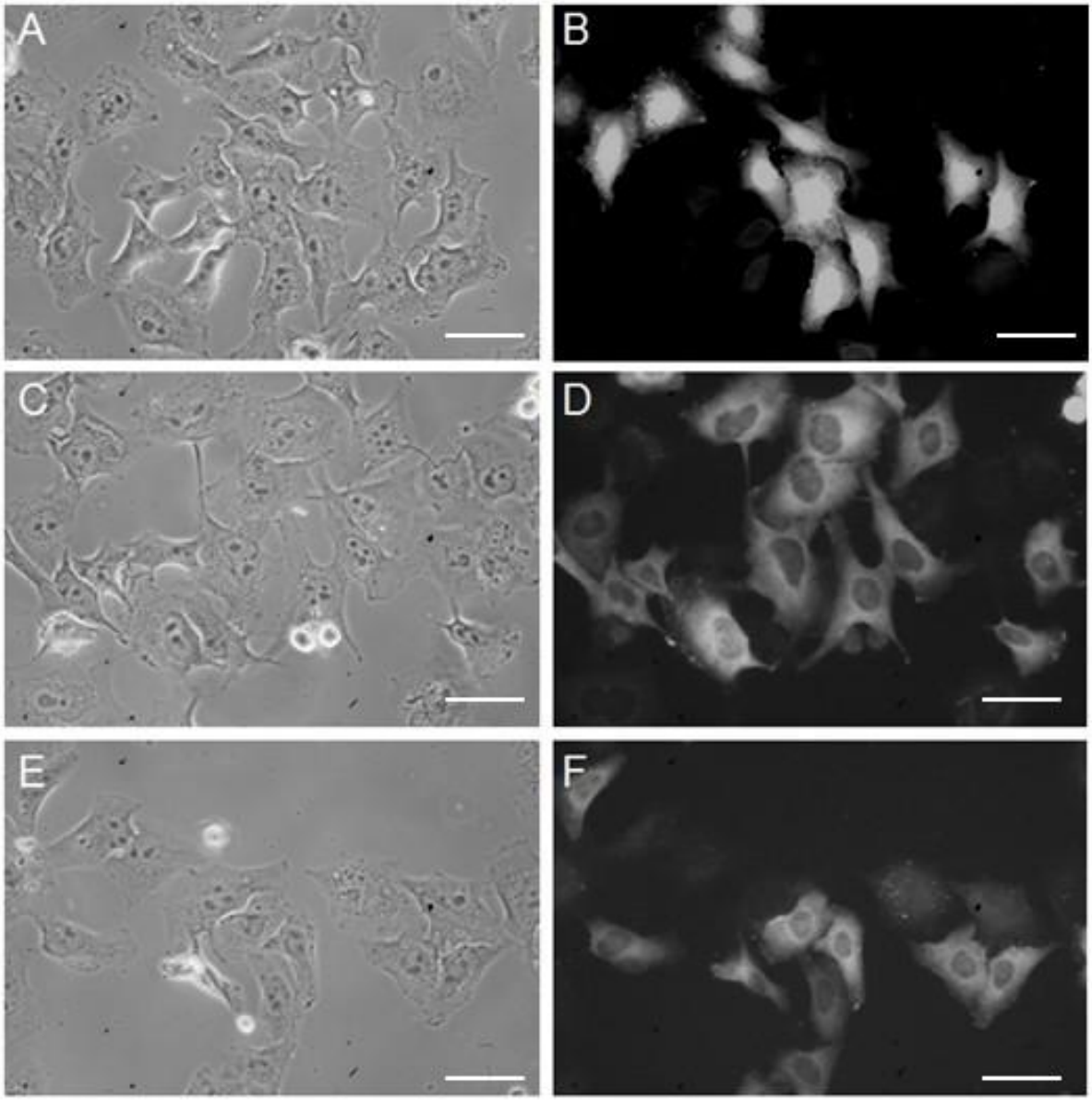

Fig. 11. N- and C-terminal GFP-fusion proteins of Wdr16 are located in the cytoplasm of transfected HeLa cells. HeLa cells were grown in Dulbecco's Modified Eagle's Medium (DMEM) with 10% fetal bovine serum (FCS) and antibiotic solution. They were incubated in a humidified atmosphere with 10% CO_2 at 37°C. One day after seeding, the cells were transfected with either pEGFP plasmid, a plasmid coding for EGFP-Wdr16 (N-term.) or a plasmid coding for Wdr16-EGFP fusion protein (C-term.) using the Jetpei™ transfection reagent. Two days after transfection the HeLa cells were fixed with PFA and they were analyzed for expression of the GFP fusion proteins using phase contrast and fluorescence microscopy. **A**: Phase contrast image of HeLa cells transfected with pEGFP plasmid DNA. **B**: Greyscale image depicting the green fluorescence signal from HeLa cells transfected with pEGFP plasmid DNA. The EGFP expressed is located in the nucleus and cytoplasm of the transfected cells. **C**: Phase contrast image of HeLa cells transfected with pEGFP-N1-Wdr16 plasmid DNA. **D**: Greyscale micrograph showing the green fluorescence signal from HeLa cells transfected with pEGFP-N1-Wdr16 plasmid DNA. The EGFP-Wdr16 fusion protein is located in the cytoplasm of transfected cells. **E**: Phase contrast image of HeLa cells transfected with pEGFP-C1-Wdr16 plasmid DNA.

F: Greyscale micrograph depicting the green fluorescence signal from HeLa cells transfected with pEGFP-C1-Wdr16 plasmid DNA. The Wdr16-EGFP fusion protein is located in the cytoplasm of transfected cells. The white bars in A-F correspond to 30 µm.

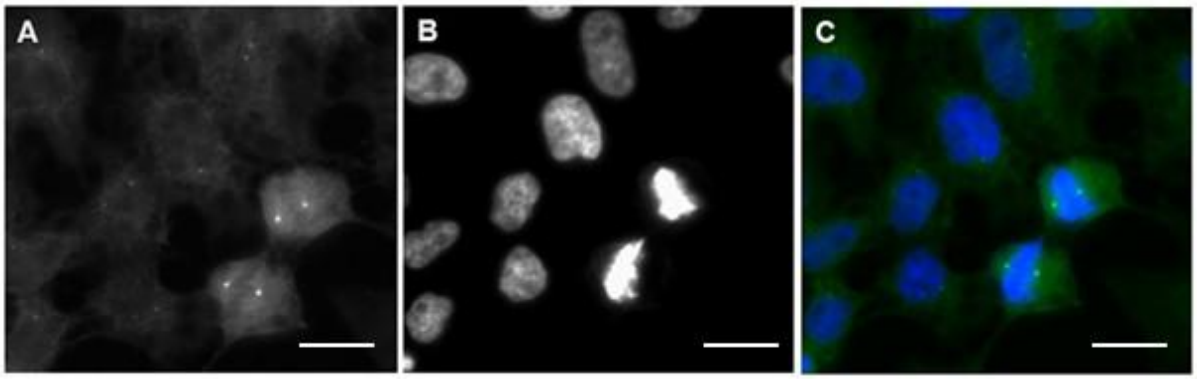

Fig. 12. Immunostaining of centrioles in Hela cells using a monoclonal anti-γ-tubulin antibody. After 3 days in culture the cells were fixed with 4% paraformaldehyde. **A.** The centrioles can best be seen in the two metaphase cells on the right side where they are enlarged and located at the opposing poles of the cells. A rabbit anti-mouse Alexa-488 conjugate (Jackson), diluted 1:500, was used as a secondary antibody. **B.** Here the nuclei were counterstained with 4',6-diamidino-2-phenylindole (DAPI). **C.** Overlay of green (γ-tubulin) and blue (cell nuclei) fluorescence channels demonstrates the specific staining of the centrioles by the anti γ-tubulin antibody. The white bars in A-C correspond to 20 µm.

Next, infected HeLa cell cultures expressing Wdr16-Flag were stained using the anti-Flag antibody. The resulting images confirm the previous results and exclude any co-localization of rat Wdr16-Flag with the centrioles in HeLa cells. The anti-Flag immunoreactivity was only detectable in the cytosol. The color overlay of the red and green fluorescence channels exhibit no co-localization of anti-Flag (red) and anti-γ-tubulin (green) immunoreactivity (Fig. 13). The samples were also subjected to a software-based deconvolution process to remove out-of-focus light from a z-series of images (Fig. 14).

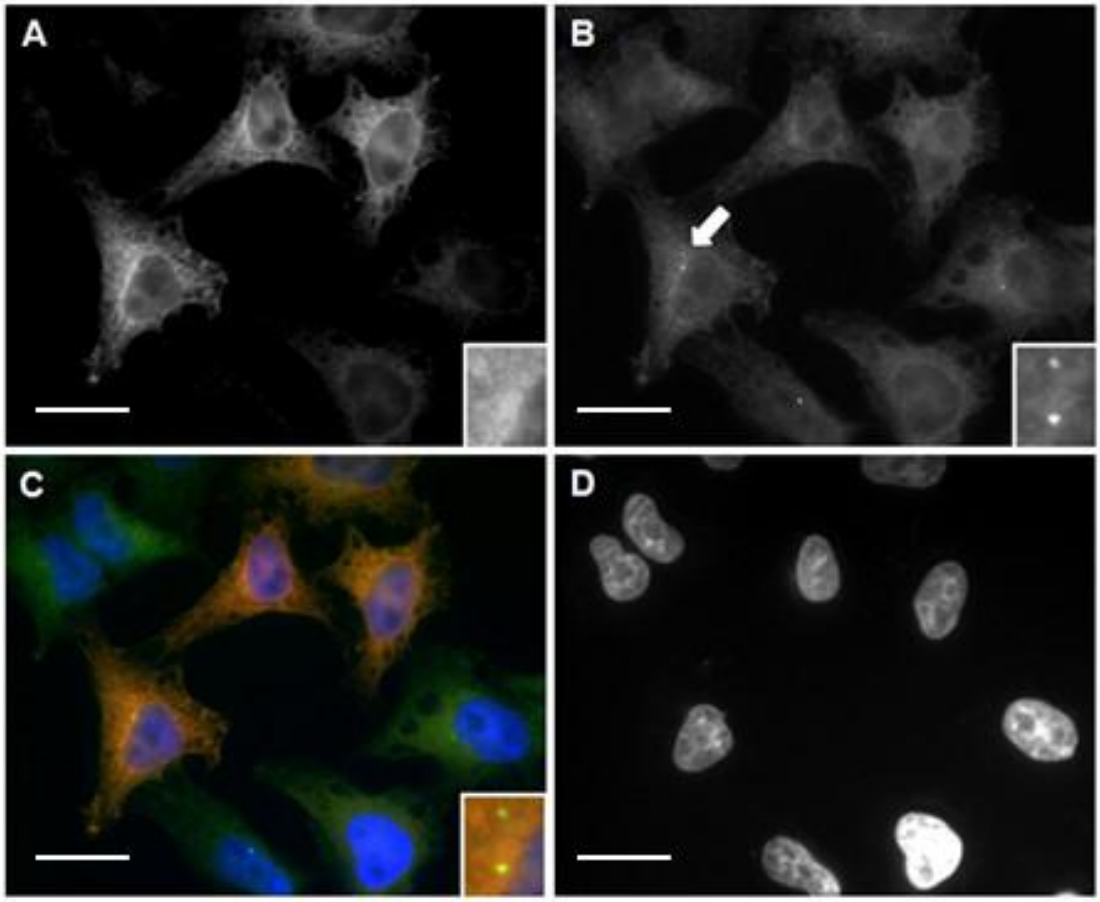

Fig. 13. Double immunostaining against Flag-tag and γ-tubulin of HeLa cells infected with HIV/VSV-G/EF1p-Wdr16-Flag lentivirus. The location of the Flag-tagged Wdr16 protein appears to be unrelated to the centrioles. The cells were fixed with 4% paraformaldehyde / PBS 48 h post infection. The small windows in the lower right corner show the enlarged images of the region containing the centrioles (arrow in **B**). **A.** Immunostaining against the Flag-tag. The rabbit anti-Flag antibody was diluted 1:200 and a goat anti-rabbit-Cy3 conjugate (diluted 1:500) was employed as secondary antibody. **B.** Immunostaining against γ-tubulin. The monoclonal anti-γ-tubulin antibody was diluted 1:2,000. A rabbit anti-mouse Alexa-488 conjugate (diluted 1:500) was used as secondary antibody.The white arrow in D indicates the single cell that was analyzed at higher magnification in Fig. 14. **C.** Overlay of γ-tubulin (B, green), Flag (A, red) and cell nuclei (C, blue) indirect immunofluorescence. **D.** Nuclei were counterstained with 4',6-diamidino-2-phenylindole (DAPI, grey-scale). The white bars in A-D correspond to 25 µm.

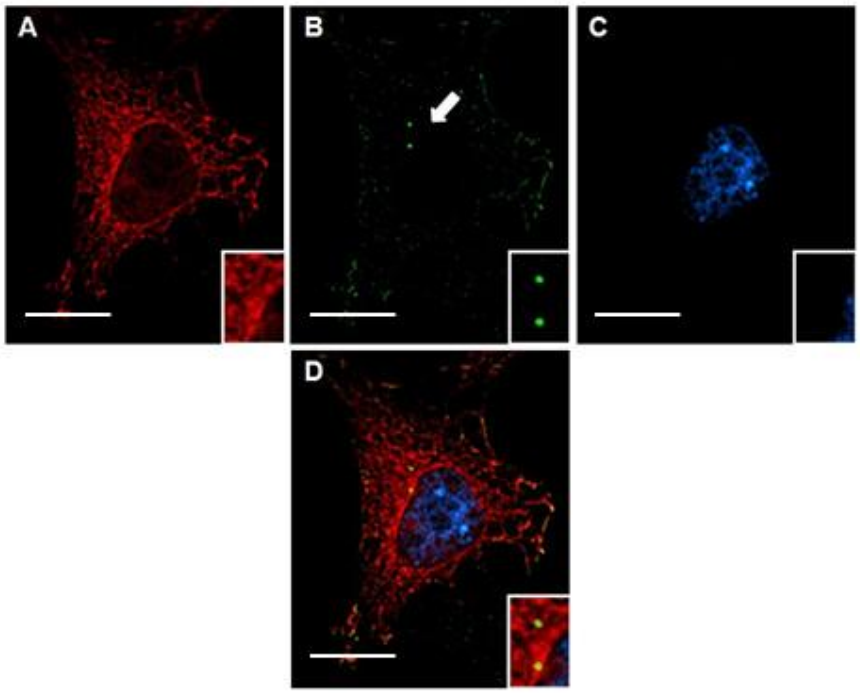

Fig. 14. Digital deconvolution analysis of HeLa cells infected with HIV/VSV-G/EF1p-Wdr16-Flag lentivirus. The location of the Wdr16-Flag fusion protein appears to be unrelated to the centrioles. The distance between the images of the z-stack used for deconvolution was 0.5 µM. The same HeLa cells as in Fig. 13 were analyzed and the cell in the lower left-hand corner of Fig. 13 is shown in this figure. **A.** Immunostaining of Flag-tag (red). **B.** Immunostaining of γ-tubulin (green). **C.** Nuclei were stained with 4',6-diamidino-2-phenylindole (DAPI, blue). **D.** Overlay of green (γ-tubulin), red (Flag-tag) and blue (nuclei) fluorescence channels. In areas devoid of Flag-tag, such as the location of organelles, no red staining can be seen. Therefore, the red staining presents itself as a net-like structure. The small windows in the bottom-right corners show enlarged images of the region containing the centrioles. The white bars in A-D correspond to 15 µm.

2.8 Baculoviral expression of Wdr16

High-level expression of a protein is the prerequisite for the purification of the protein for subsequent studies and applications, e.g. circular dichroism, x-ray crystallography, or the generation of an improved, polyclonal anti-Wdr16 antibody. Previous attempts to express Wdr16 in bacteria and yeast expression systems were unsuccessful (S. Verleysdonk, personal communication). Therefore, a baculovirus expression vector system was chosen, because in it high levels of heterologous protein expression are often achieved, particularly for soluble proteins. In most cases, the recombinant proteins are correctly processed and modified, so that they are functionally identical to their

counterparts naturally produced in their source tissues (Kost et al., 2005). Additionally, in the majority of cases, the recombinant proteins are soluble and easily recovered from the infected cells. For the generation of recombinant *Autographa californica* nuclear polyhedrosis viruses driving the expression of Wdr16, the "Bac-to-Bac"-baculovirus expression system (Invitrogen) was utilized, which offers a rapid and efficient method to generate recombinant baculoviruses. It is based on the site-specific transposition of an expression cassette from a donor plasmid into a baculovirus shuttle vector. This so-called “bacmid” is propagated in E.coli and following DNA isolation, it is used for the transfection of insect cells. In the first instance, a baculovirus expressing Wdr16 with an N-terminal polyhistidine-tag was generated. The cDNA coding for rat Wdr16 was amplified by PCR and cloned in the transfer vector pFastbac-HTB using BamHI and SalI restriction sites. The transfer plasmid was electroporated into DH10Bac™ competent bacterial cells which contain the “bacmid”-DNA with a mini-attTn7 target site and the helper plasmid. The mini-Tn7 element on the pFastBac donor plasmid can transpose to the mini-attTn7 target site on the “bacmid” in the presence of transposition proteins coded for *in trans* by the helper plasmid. Bacterial colonies containing recombinant “bacmids” were identified by their white color because of the disruption of the lacZα gene following transposition. After the transposition was completed, white candidate colonies were selected. The correct insertion of the gene of interest was confirmed by PCR using M13 standard sequencing primers which are directed at sequences on either side of the mini-attTn7 site of the “bacmid”. Due to the large size of the “bacmid” DNA (> 135 kbp), restriction endonuclease digestion would have resulted in too many or too long fragments making a convenient analysis by agarose gel electrophoresis impossible. Indeed, using the PCR approach, several bacterial colonies could be identified which contained the “bacmid” and the gene of interest (Fig. 15). The “bacmid” DNA of these colonies was used for the production of baculoviruses.

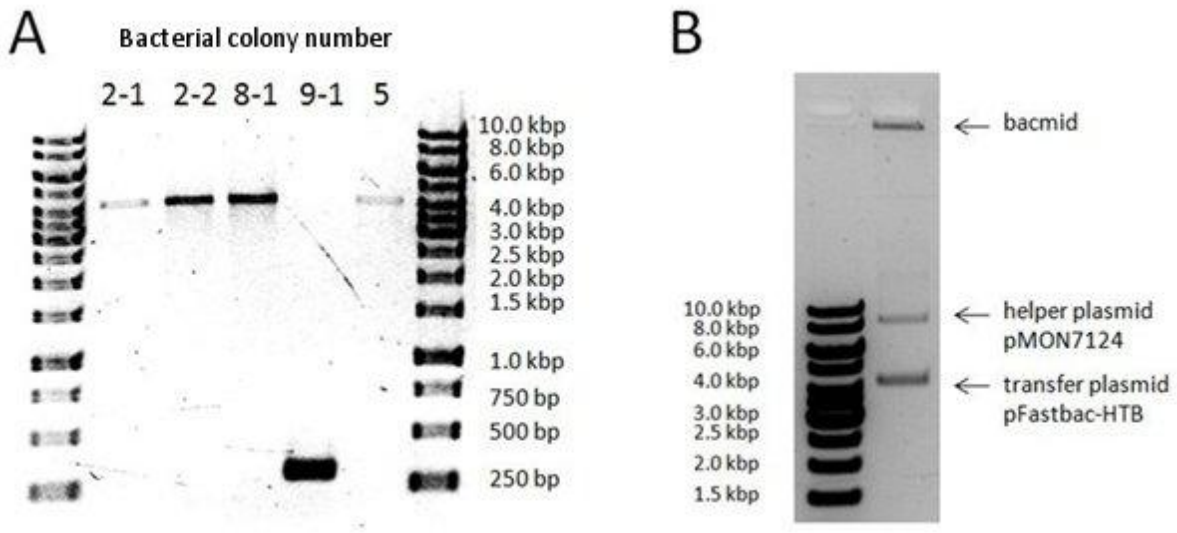

Fig. 15. **A.** Colony-PCR screening of recombinant "bacmid" colonies. White candidate colonies were restreaked on agar plates containing X-Gal, isopropyl β-D-1-thiogalactopyranoside (IPTG) and antibiotics. After incubation at 37°C for 24 h, single colonies were placed in PCR tubes using a sterile plastic pipette tip. The PCR tubes already contained the PCR reaction mixture that was prepared according to the protocol of the HotStarTaq Master Mix Kit (Qiagen). The PCR was performed with M13 forward and reverse primers following the manufacturer's instructions. The PCR product indicating successful transposition has a length of 2.3 kbp plus the size of the wdr16 cDNA (ca. 1.8 kbp). In the case of failed transposition, the PCR product (produced from the "bacmid" alone) is expected to be approximately 300 bp long. All screened colonies, except 9-1, are positive, i.e. transposition of the expression cassette has occurred. The DNA of the colonies was subjected to agarose gel electrophoresis together with a "DNA ladder" (in the first and last lanes) to estimate the size of the DNA molecules. **B.** Agarose gel electrophoresis for the analysis of the recombinant "bacmid" DNA. Aside from the "bacmid" DNA, the bands for the helper and transfer plasmid are visible. They have no influence on the production of infectious baculovirus following the transfection of insect cells. First lane: DNA ladder.

The isolated recombinant "bacmid" DNA was used for the transfection of Sf9 insect cells using the commercially available Lipofectamine transfection reagent. Five days after transfection, the insect cells that had been transfected with the recombinant "bacmid" stopped growing. More than 90% of the cells were detached from the 6-well plate and looked perforated under the phase contrast microscope. The control cells that had been mock-transfected with deionized water instead of DNA solution looked normal and the bottom oft the culture vessel was completely covered by layers of cells. For the harvest of the virus, the supernatant (ca. 2 ml) was transferred to a fresh conical tube and centrifuged in order to remove cell debris. For the amplification of the viral

stock, a monolayer culture was infected at a multiplicity of infection (MOI) of 0.1 and the viral titer was determined using the end-point-dilution assay (Darling et al., 1998). The amplified virus was then used for the infection of Sf9 suspension cultures. The successful expression of hexahistidine (6xHis)-tagged Wdr16 in these cultures was confirmed by Western blotting (Fig. 16). The band location of the 6xHis-Wdr16 protein (lane 3) is located a little bit higher on the blotting membrane than the band for the endogenous Wdr16 protein from EPCs because of the additional molecular weight of the histidine residues and of the amino acids of the linker region of the 6xHis-Wdr16.

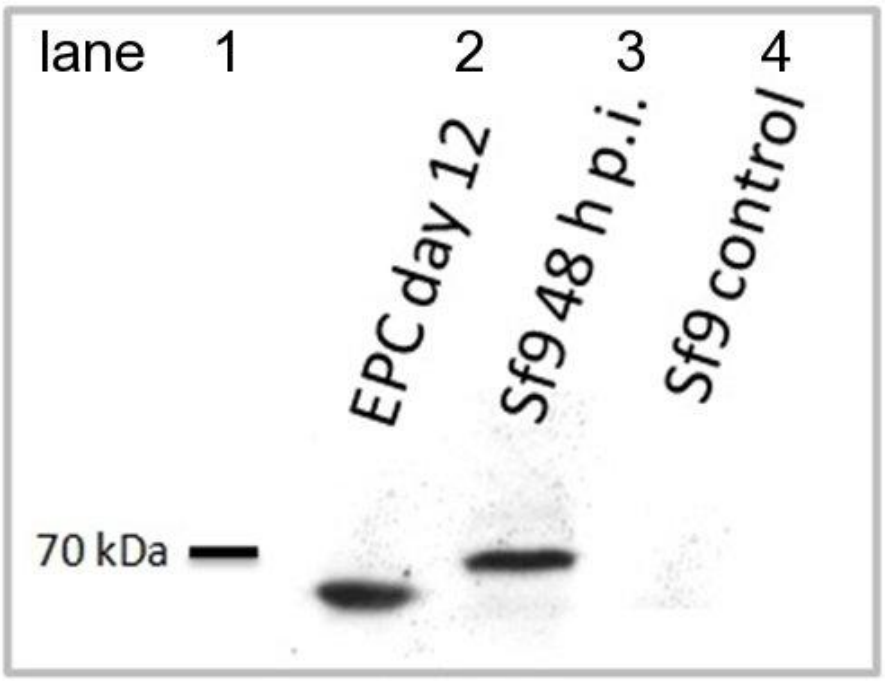

Fig. 16. 6xHis-Wdr16 expression in insect cells confirmed by Western blotting. A suspension culture of Sf9 insect cells was infected (MOI: 1) with recombinant baculovirus bearing an expression cassette for polyhistidine-tagged Wdr16. The cells were harvested by centrifugation 48 h post infection. A lane of a SDS polyacrylamide gel (10% acrylamide) was loaded with 20 µg of protein from the cleared lysate (see chapter 4.2.31) of the infected insect cells. Homogenates of EPC (positive control) and of uninfected insect cells (negative control) were loaded in the adjacent lanes (20 µg protein each). The samples were separated by SDS-PAGE and transferred to a nitrocellulose membrane by electroblotting. For the anti-Wd16 Western blot, the membrane was probed with guinea pig Wdr16 antiserum diluted 1:10,000. The secondary antibody was a donkey anti-guinea pig IgG-peroxidase conjugate diluted 1:50,000. The black bar in lane 1 marks the position of the 70 kDa band of the protein ladder. The 70 kDa protein band contained a special blue dye and was the only band of the protein ladder which could be seen on the nitrocellulose membrane after the Western blotting

procedure. The band in lane 2, which is not present in the Sf9 control (lane 4), demonstrates the success of the baculoviral expression of 6xHis-Wdr16. As expected, the location of the 6xHis-Wdr16 protein band (lane 3) is a little bit higher on the blotting membrane than the band for the endogenous Wdr16 protein in EPCs. The reason for this is the additional molecular mass of the histidine residues and of the amino acids of the linker region of the 6xHis-Wdr16.

The 6xHis-tagged Wdr16 protein was purified from the baculovirus-infected insect cells under non-denaturing conditions using Immobilized metal affinity chromatography (IMAC). IMAC purification is a robust method for purifying polyhistidine-tagged recombinant proteins (Bornhorst and Falke, 2000). This is achieved by using the natural tendency of histidine to form a complex with divalent metal ions around neutral pH. Even though blots demonstrated that Wdr16 is enriched in the IMAC eluates, the result of the purification was not satisfactory. After Coomassie staining of the gel, a multitude of bands was visible, and the one corresponding to Wdr16 could not be identified without ambiguity. Due to concerns that the native conformation of Wdr16 may physically hide the polyhistidine affinity tag, the purification was repeated under denaturing conditions (6 M guanidine hydrochloride). However, this did not lead to an improvement of the purification result. Because of the failure to purify the polyhistidine-tagged Wdr16 protein, new baculoviruses were produced in order to purify Wdr16 using different affinity tags (Fig. 17).

Baculovirus inducing the expression of Wdr16 tagged with both GST (N-terminal relative to Wdr16) and 6xHis (C-terminal relative to Wdr16), was produced using the same baculovirus expression vector system as for the polyhistidine-tagged Wdr16 protein. The baculovirus bearing an expression cassette for Wdr16 tagged with both GST and 6xHis was infectious for insect cells as evidenced by the lack of growth and the morphology of the insect cells in the late phase of infection (after 24 h): the diameter of the cells increased, the nuclei were enlarged and the cytoplasm contained vacuoles. Despite the infection there was no expression of the recombinant target protein. Only Wdr16 single-tagged by GST could be purified from insect cells infected with the respective baculovirus. The purification was performed with glutathione Sepharose-packed columns as well as in batch format. Elution was effected by

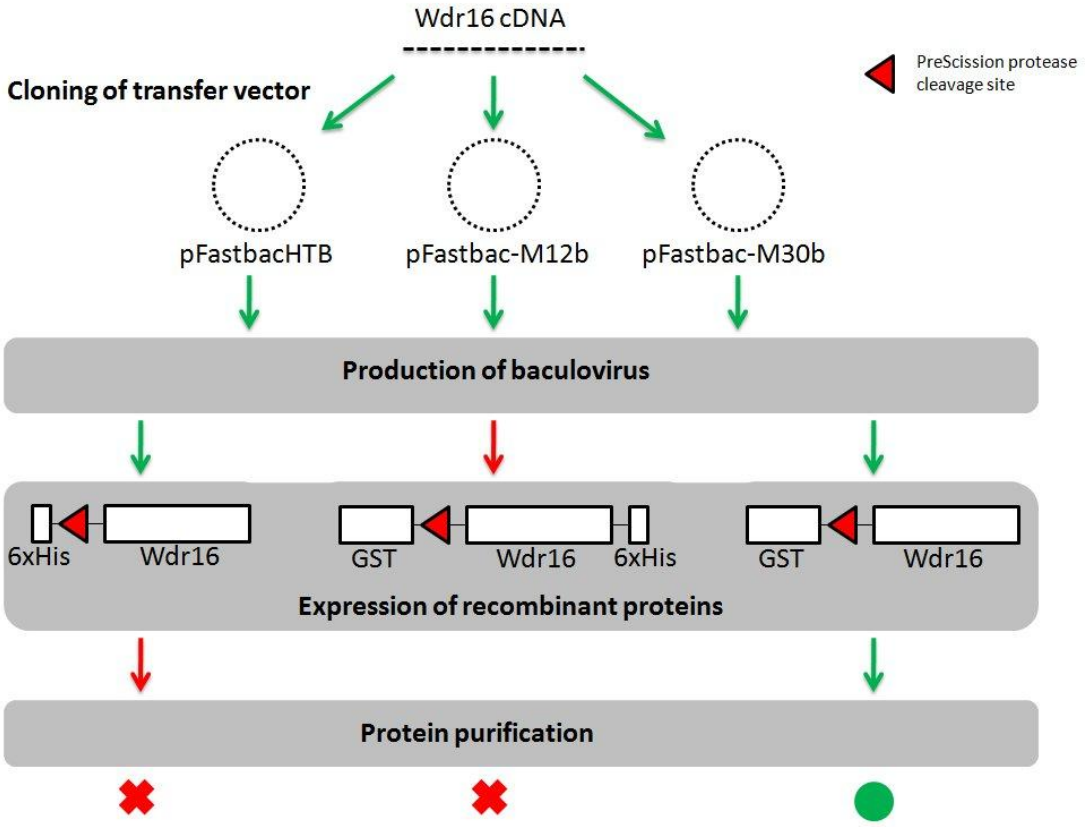

Fig. 17. Flowchart indicating the results of different strategies for the baculoviral expression of Wdr16 in and and purification from insect cells. Three recombinant baculoviruses expressing different Wdr16 fusion proteins were generated using the Bac-to-Bac^{TM} baculovirus expression vector system. The polyhistidine-tagged Wdr16 protein could not be purified sufficiently with affinity purification under non-denaturing and denaturing conditions.(red cross) The baculovirus expressing Wdr16 tagged with both glutathione-S-transferase (GST) and 6xHis was infectious for insect cells, but there was no expression of the recombinant target protein (red cross). Most probably this was caused by an error in the donor plasmid pFastbac-M12b. Finally, virus-induced expression of GST-Wdr16 and the purification of the recombinant protein were successful (green circle). The green arrows designate successful experimental steps whereas the red ones signify that the respective step could not be completed successfully.

either 15 mM reduced glutathione, resulting in GST-tagged Wdr16 (ca. 92 kDa), or by on-column cleavage with Prescission protease, resulting in untagged Wdr16 (68 kDa). Presscission protease is a fusion protein consisting of human rhinovirus 3C protease and GST, allowing simultaneous protease. The yield of purified protein was ca. 1 mg using 1 ml of gluthatione-Sepharose in batch format or ca. 500 µg of Wdr16 protein using 1 ml bed volume of gluthatione-Sepharose in columns following protease cleavage.

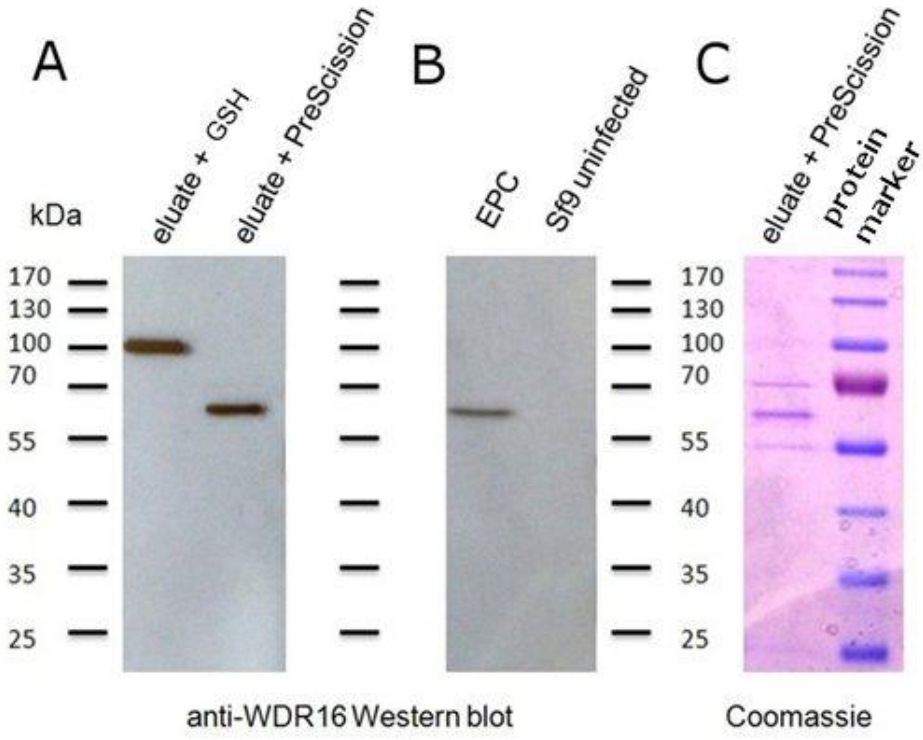

Fig. 18. Purification of GST-Wdr16 and Wdr16 protein from baculovirus-infected insect cells. Sf9 insect cells were cultured in suspension and infected at a MOI between 1 and 3 with a recombinant baculovirus bearing a GST-Wdr16 fusion protein expression cassette. The cells were harvested 48 h p.i., lysed, and the lysate was incubated overnight with glutathione-Sepharose slurry. The GST-Wdr16 fusion protein (approx. molecular mass 92 kDa) was eluted either by reduced glutathione or using on-column cleavage with "PreScission" protease. This protease specifically cleaves between the Gln and Gly residues of the recognition sequence of LeuGluValLeuPheGln/GlyPro (Cordingley et al., 1990). **A**. The eluate was analyzed by SDS-PAGE followed by Western blotting with antibodies against Wdr16. **B**. As a control for the specificity of the Western blot, EPC (positive control) and uninfected Sf9 cell (negative control) homogenates were analyzed for Wdr16 immunoreactivity on the same nitrocellulose membrane. **C**. Shows the Coomassie Blue staining of the lane for the eluate generated by application of "PreScission" protease and the lane for the molecular mass marker proteins.

immobilization and cleavage of GST. The protease cleaves in the specific sequence (Leu-Glu-Val-Leu-Phe-Gln/Gly-Pro) at the end of the GST-tag (Cordingley et al., 1990). The success of the purification was confirmed with Western blot analysis and Coomassie staining (Fig. 18).

2.9 Circular dichroism

Next, the protein folding and stability of the purified Wdr16 protein was investigated by circular dichroism (CD). Each of the three basic secondary structures of a polypeptide chain (α-helix, β-sheet, random coil) show a characteristic CD spectrum.

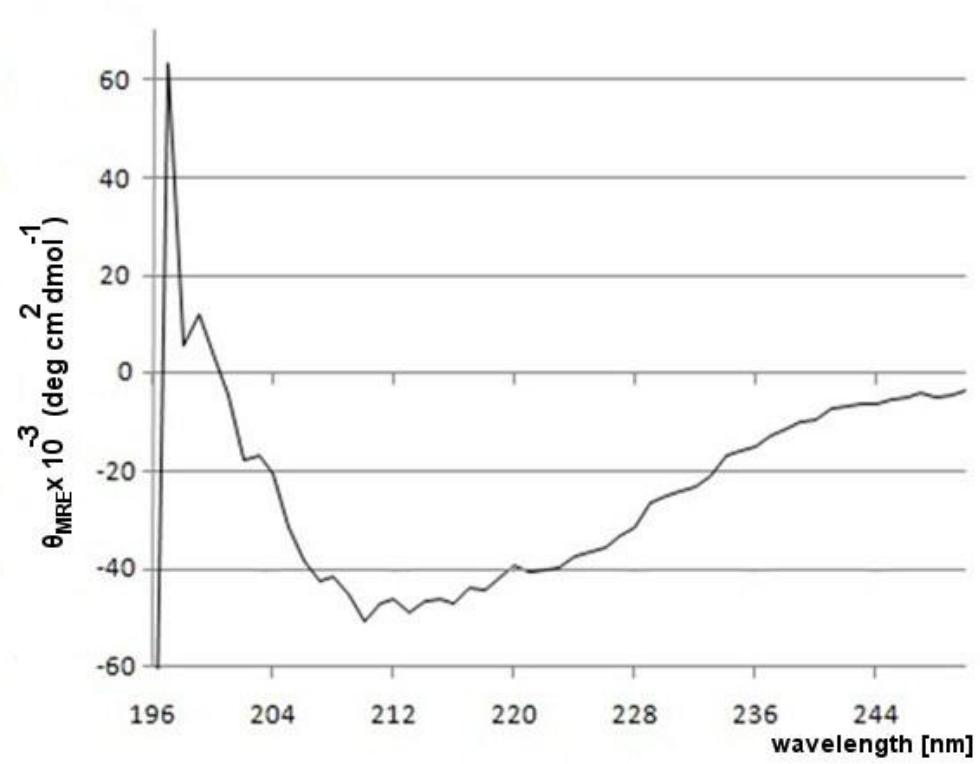

Fig. 19. Measurement of the circular dichroism (CD) and determination of the secondary structure of purified, non-tagged Wdr16 protein by CD spectrometry in the far UV spectral region. The plot shows the relationship between the mean residue ellipticity of Wdr16 (ordinate) and the wavelength of the polarized light (abscissa). The CD spectrum of Wdr16 has the characteristic shape of a protein composed of β sheets (Ma and Asher, 2010).

According to tertiary structure prediction by threading, the Wdr16 protein features two covalently linked seven-bladed β-propellers similar to the Aip1 protein (Verleysdonk, 2006; Voegtli et al., 2003). Each propeller blade consists of 4 strands of β-sheet. Consequently, Wdr16 should be exclusively composed of β-sheets without α-helical or random coil elements. The CD spectrum of purified non-tagged Wdr16 (Fig. 19) was compatible with a pure β-sheet structure (Fig. 20).

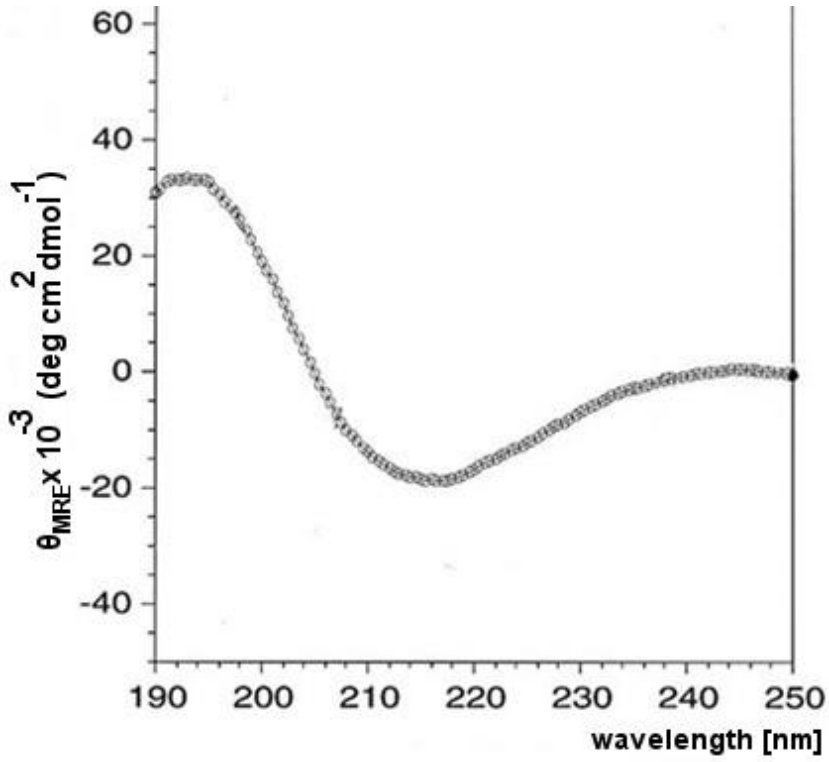

Fig. 20. CD spectrum of the β-sheet conformation of poly-L-lysine at pH 11.1 after heating for 15 min at 52°C (Fändrich and Dobson, 2002).

2.10 Cloning of a targeting vector for the generation of transgenic wdr16 knockout mice

A vector for the targeting of the wdr16 gene in ES cells and the generation of transgenic wdr16 knockout mice was designed, produced and tested. The targeting vector was designed to flank the exons 2 and 3 of wdr16 with loxP sites (“flox”) and to insert a selection cassette into the genome of the ES cells (Fig. 21). After successful homologous recombination, the wdr16 gene can be deleted by transfection of the “floxed” ES cells with a plasmid expressing the Cre recombinase enzyme of bacteriophage P1 (Sauer and Henderson, 1988). Alternatively, the mice bearing the floxed wdr16 locus can be crossbred with transgenic Cre mice. The mRNA transcribed from the mutated wdr16 gene would only contain the first exon of wdr16 because the deletion of exons 2 and 3 would result in a frame shift. This strategy guarantees the generation of an

effective wdr16 gene knockout. Following electroporation of the targeting vector into ES cells and homologous recombination, positive ES cell colonies can be

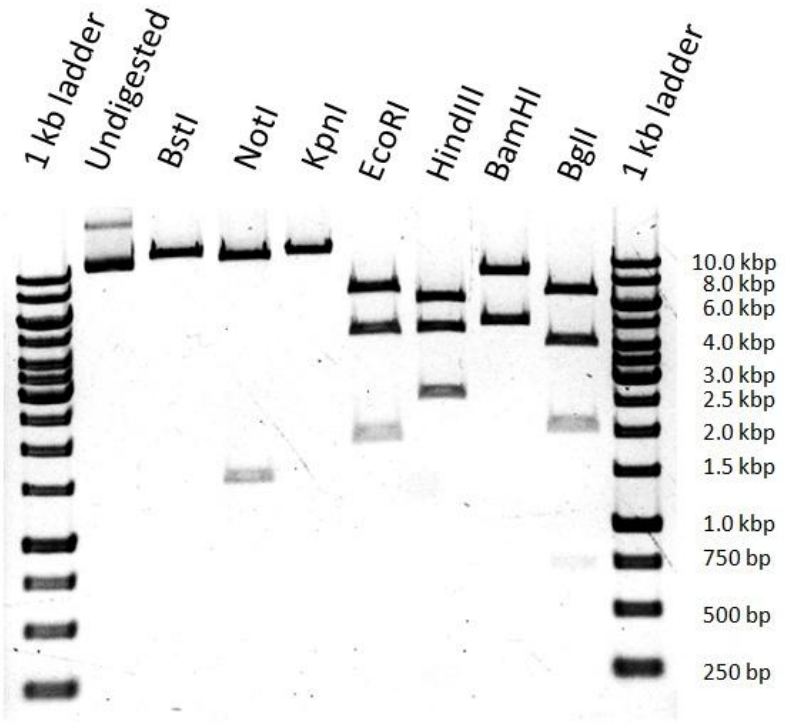

Fig. 22. Analysis of the wdr16 targeting vector by digestion with restriction endonucleases. The vector DNA was digested, in separate incubations, with 7 different enzymes in their appropriate buffers. The samples were incubated overnight at 37°C. Afterwards, they were mixed with DNA loading dye and loaded onto a 1% (w/v) agarose gel. After electrophoresis, the agarose gel was incubated in an ethidium bromide solution (1 µg/ml) for 10 min and the DNA bands were visualized on a UV transilluminator. Pictures were taken with a digital camera. The obtained pattern of DNA bands reflects the restriction sites present in the wdr16 targeting vector.

selected by addition of geneticin (G418) to the culture medium (positive selection). After the Cre recombination, the selection markers can be eliminated by gancyclovir treatment (negative selection). The generation of the wdr16 targeting vector included four separate cloning steps. First, an additional loxP site was inserted into the plasmid pBS-loxP-neoTK-loxP. Afterwards, the 1.5 kb short arm (5'-end arm) was cloned in front of the first loxP site. Next, the deletion cassette with exons 2 and 3 of wdr16 was put between the first two loxP sites, and finally the 2.7 kb long arm (3'-end arm) was inserted behind the

selection cassette and the third loxP site. After each cloning step, the inserted DNA fragment was verified by DNA sequencing. Finally, the wdr16 targeting vector was obtained and checked by restriction digestion analysis. The correct pattern of DNA fragments could be observed following visualization using agarose gel electrophoresis (Fig. 22). In addition to the DNA sequencing and restriction digestion analysis, the presence and correct location of the loxP sites was examined. For this, commercially available bacteria expressing Cre recombinase were transformed with the wdr16 targeting vector DNA and the length of the isolated DNA fragments was analyzed by agarose gel electrophoresis following linearization using BamHI digestion. The resulting band on the agarose gel is equivalent to the size of the wdr16 targeting vector DNA without the deletion and selection cassettes that are lying between the two outer loxP sites (approx. 7.7 kbp; Fig. 23). Hence, it appears that the construction of a functional wdr16 targeting vector has been completed successfully.

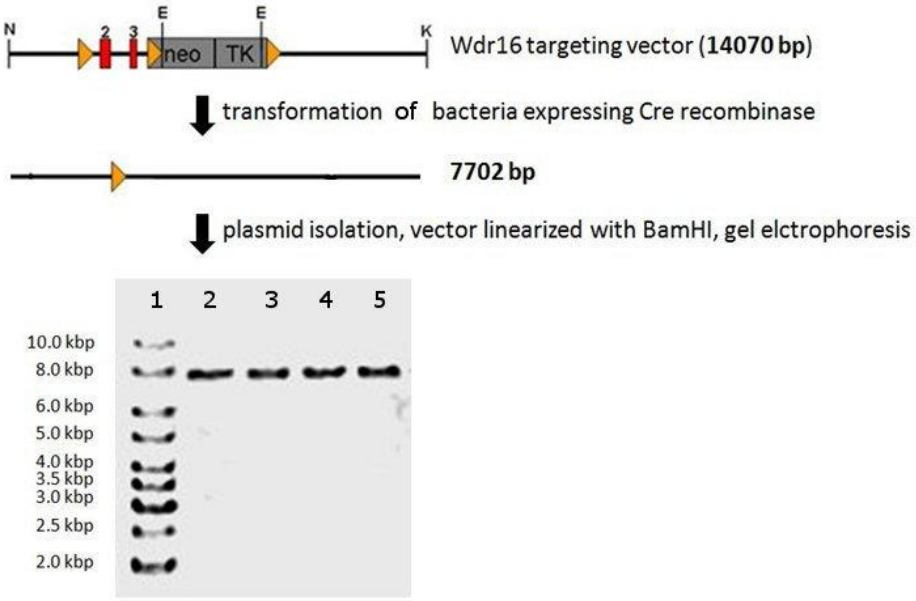

Fig. 23. Testing of Cre/loxP recombination. A competent bacterial cell line (Stratagene) engineered to transiently express the Cre recombinase of bacteriophage P1 was transformed with the wdr16 targeting vector DNA. Following transformation, the bacteria were streaked onto agar plates containing the antibiotic carbenicillin. The plates were incubated overnight at 37°C, and four of the ensuing colonies were each used to inoculate 5 ml of lysogeny broth (LB) containing carbenicillin. On the next day, the plasmid DNA was isolated from the grown bacteria via the alkaline lysis procedure ("mini-prep", see chapter 4.2.13) and linearized by digestion with BamHI. After successful Cre/loxP recombination, the targeting vector was expected to show a band of less than 8 kb after agarose gel electrophoresis. Without Cre/loxP

recombination, the unmodified targeting vector has a length of more than 14 kb (not shown). Restriction sites for the analysis of ES cell colonies by in-situ hybridization: N (NotI), E (EcoRV), K (KpnI). neo: neomycin resistance gene (for positive selection of ES cell colonies). TK: thymidine kinase gene (for negative selection of ES cell colonies). 2: wdr16 exon 2. 3: wdr16 exon 3. The lanes 2 - 5 of the agarose gel contain the DNA of four different bacterial colonies. Lane 1 contains the DNA ladder so that the sizes of the product bands can be accurately determined.

3 Discussion

3.1 Knockdown of wdr16 expression in EPCs

Lentiviral transfection of EPCs with lentiviral vectors encoding anti-wdr16 siRNAs and bearing GFP as a marker resulted in a successful knockdown of wdr16 expression. A very important step for the establishment of this experiment was the use of the wdr16 promoter, which is specifically recognized in kinocilia-bearing cells, to drive GFP reporter gene expression. It has been demonstrated here that the anti-wdr16 siRNA construct is very efficient in silencing wdr16, but that this siRNA expression in EPCs also causes a significant decrease in the abundance of the kinocilia marker Ak7. This decrease in ak7 expression reflected the selective damage to and loss of the kinocilia-bearing cells in the EPCs and may be attributed to either the expression of the siRNA or GFP under the control of a constitutively active promoter. The former may be toxic because it may lead to the degradation of partially complementary off-target mRNAs. It has been shown that siRNAs can reduce expression of mRNAs even when there are a few mismatches between the siRNA and the mRNA target sequence (Persengiev et al., 2004; Haley and Zamore, 2004). The stronger the expression of the siRNAs, the higher is the chance that this unwanted side effect occurs. Another negative effect of siRNA overexpression by a constitutive promoter could be the activation of the interferon response (Sledz et al., 2003; Jackson and Linsley, 2004). Overexpression of GFP in the EPCs on the other hand may interfere with the differentiation process of the ependymal cells. The first step for the establishment of RNAi in EPCs was to replace the EF1 promoter by the kinocilia-specific wdr16 promoter and thereby to prevent the expression of GFP until the onset of differentiation (starting at approx. DIV 6) of the kinociliated cells in the EPCs. In this way, the wdr16 expression could be suppressed without causing a significant loss of kinocilia-bearing cells from the cultures. Therefore the additional replacement of the H1 RNA polymerase-III (Pol III) promoter in front of the siRNA cassette with the wdr16 promoter was not necessary for effective silencing of wdr16 in EPCs. The efficacy of the RNAi

was validated at the protein level by Western blotting and immunocytochemistry and at the mRNA level by RT-PCR.

3.2 Effect of wdr16 silencing in EPCs

Even though the downregulation of wdr16 was significant, it was not possible to demonstrate a knockdown phenotype or noticeable differences compared to EPCs infected with the control-siRNA virus. EPCs infected with the RNAi viruses were analyzed for the rough morphology of the cells, apical-basal cell polarity, number and appearance of kinocilia, basal bodies and mitochondria, as well as for the intracellular distribution of β-actin and α-tubulin. Since RNAi does not totally abolish expression of the target gene (the downregulation of wdr16 varied between 50 and 80%), the remaining cellular Wdr16 protein could be sufficient to perform its unknown molecular function. This problem is characteristic for RNAi knockdowns and can explain the lack of a phenotype (e.g., Rasala et al., 2006).

Another possibility is that the differences induced by Wdr16 knockdown are very subtle and analytical methods other than morphological analysis and immunohistochemistry must be applied. For instance, wdr16 knockdown could result in a change of ciliary beat frequency or fluid flow directionality. Hypothetically, the influence of the wdr16 knockdown on the ciliary beat could have been analyzed by high-speed videography, but this was complicated by the difficulty to recognize under the phase contrast microscope the GFP-positive cells. Since the GFP signal was usually very weak, the cells had to be fixed with PFA and counterstained with an antibody against GFP, and this rendered any real-time analysis impossible. An in-depth analysis of directionality of the fluid flow over the cultured cells (e.g. using latex beads) was not performed, because in that respect judging from light microscopy the cultures infected with the anti-wdr16 virus did not behave differently from control cultures. Nonetheless, it would be important to analyze fluid flow directionality, because it could demonstrate that a lack of Wdr16 has a direct impact on kinocilia movement and that results like the hydrocephalus phenotype seen

after knockdown of Wdr16 in zebrafish is not only a result of altered water homeostasis or osmoregulation. It would be highly desirable to perform this detailed fluid flow analysis with ependymal primary cultures from knockout mice since the complete absence of Wdr16 protein should provide a higher chance to reveal such a phenotype.

3.3 Injection of the RNAi lentivirus into rat brain ventricles

The lentiviral vectors expressing anti-Wdr16-siRNA and the control-siRNA were injected into the cerebral ventricles of adult Sprague-Dawley rats by stereotactically-placed microinjections. Obviously the RNAi viruses had failed to infect the ependymal layer, because an expression of the reporter gene, the GFP gene, could not be detected on the frozen brain sections of the infected rats using anti-GFP immunohistochemistry. In general, *in vivo* infection of the ependyma should work because several successful attempts have been published. For instance, Watson and coworkers (2005) showed that injection of lentiviral vectors pseudotyped with vesicular stomatitis virus glycoprotein into the cerebral lateral ventricles resulted in targeted infection of the ependymal cells lining the ventricular system and the choroid plexus. The failure observed in the present study may be caused by the unsuccessful application of the virus, e.g. the virus may not have reached the ventricles after injection. This experiment was only performed once, albeit two rats were infected with the anti-Wdr16 virus and analyzed. There are other possible reasons for the failure of *in vivo* silencing of wdr16 in the ependyma lining the brain ventricles. Other studies doing similar experiments reported that there are three major determinants of the efficiency of siRNAs *in vivo*: the interfering sequence, the number of proviral copies integrated into the genome and the site of insertion of the provirus (Frka et al., 2009). It was demonstrated that even though an siRNA sequence can be very efficient in reducing the expression of a gene *in vitro*, the *in vivo* conditions may impose additional stringency on the expression and the survival of siRNA (Frka et al, 2009). This may be responsible for the fact that the anti-wdr16 siRNA used for this RNAi study is very effective in the infection of EPCs but ineffective in the infection of the ependyma *in vivo*. It must also be emphasized that for most experiments where siRNAs were successfully

introduced into ependymal cells, lentiviral vectors were injected at birth (Watson et al., 2005) or into very young animals (Dolcetta et al., 2006). It is known that a relationship exists between the differentiation state of the ependyma and its ciliated cells and lentiviral transfection efficiency. Even though the infection of the differentiated ependymal cells *in vivo* by lentiviral vectors can be achieved, transfection efficiencies are better when neonatal animals with less differentiated ependymal cells are used. Studies with other types of cells and tissues have confirmed that in some cases VSV-G pseudotyped HIV-1-derived vectors could not infect a fully differentiated kinociliated epithelium unless it was injured, e.g. the fully differentiated human airway epithelium and nasal epithelium of mice and rats. This entry block may be due to the absence or low numbers of VSV-G receptors on the apical membrane of the airway epithelium, as it has been identified for other viral vectors, or a post-entry block, concerning the endocytosis route and nuclear import of viral genomes (Copreni et al., 2004). However, it was not possible to infect neonatal rats with the RNAi viruses for this study in order to increase the chances of success. The stereotactic injections of the lentiviral vectors were conducted in collaboration and with kind support of the Section of Neuropharmacology (research group Prof. W. Schmidt, University of Tuebingen) which offered their expertise in performing the injections of adult rats; however, injections of newborn or juvenile rat were not possible. The problem to infect fully differentiated kinociliated epithelium is also reflected in the lentiviral transfection of ependymal primary cultures *in vitro*. In studies conducted by Kowtharapu and coworkers (2009) the infection of undifferentiated EPCs resulted in a significant increase (3.8 fold) in transfection efficiency compared to fully differentiated EPCs. The reduction of the transfection efficiency accompanying the differentiation of EPCs may be caused by the lack of specific viral receptors on the apical surface and the inaccessibility of the basalolateral surface of the kinociliated cells in their epithelial formation (Copreni et al., 2004).

3.4 Localization of Wdr16

Immunofluorescent stainings using a peptide antibody against rat Wdr16 generated in guinea pig showed that the protein is exclusively located in the cytosol of kinocilia-bearing cells (Hirschner et al., 2007). When applied to frozen sections of rat brain, the Wdr16 antibody specifically labels the cytoplasm of the ciliated ependymal cells. These results raise an important question: Does Wdr16 itself localize to the kinocilia or the basal bodies at their base or is it a purely cytoplasmic protein of kinocilia-bearing cells? There are some publications, mostly on experiments with protozoans, reporting that Wdr16 is found in cilia and basal bodies. The *Chlamydomonas* orthologue of Wdr16 (BUG14) was identified at the basal bodies of the green algae and its orthologue in trypanosomes appears to localize to the basal body and partially to the flagellum (Keller et al., 2005; Hodges et al., 2010). If these results are correct, it must be explained why the rat orthologue of Wdr16 does not localize to the kinocilia in ependymal primary cultures. One obvious reason for this difference could be that the function of Wdr16 changed in the course of evolution from protozoans to complex, multicellular organisms. As similar as their core structures and proteins (the 9+2 axoneme) may be, flagella and kinocilia differ greatly in some respect. For example, motile cilia are much shorter than flagella, are sessile and help moving fluids (like the CSF or mucus in the lung) past the immobile cells while the flagella are used for locomotion of sperm cells and protozoans.

Furthermore, kinocilia have acquired unique additional structures during evolution, e.g. they feature specific apical structures characterized by a narrowed distal portion and a ciliary crown, to single out just one (Kubo et al., 2008). And it should be kept in mind that in tissues of multicellular organisms innumerable signaling pathways exist to ensure proper coordination and communication between the cells, e.g. the planar cell polarity pathway (Wansleeben and Meijlink, 2011). All these differences provide various possibilities to explain why the function and subcellular location of Wdr16 could have changed during evolution. It can be hypothesized that Wdr16 developed from a classical flagellar protein located in the axoneme and basal body to a

cytosolic protein in multi-ciliated epithelial cells involved in sophisticated signalling or regulatory pathways. In contrast, another possible explanation could be that Wdr16 indeed localizes at the kinocilia and basal bodies of ependymal primary cultures and that the failure to detect Wdr16 at the cilia is due to technical difficulties. It is known that ciliary immunofluorescent stainings can be difficult. In a very similar case it was shown by Fernandez-Gonzalez and coworkers (2009) that adenylate kinase 7 (AK7) is a ciliary protein despite the fact that an anti-AK7 peptide antibody only detected the protein in the cytosol of rat ependymal primary cultures. An indication of this is that Keller and coworkers (2005) examined the location of human Wdr16 fused with GFP in HeLa cells and reported that it localizes to the centriole, the structure analogous to the basal body of cilia and flagella. However it must be noted that the attempt to reproduce this result with the rat orthologue of Wdr16 in HeLa cells failed in the experiments for the present doctoral thesis. Since Wdr16 is an evolutionaryly conserved protein it is unlikely that the human and rat orthologue of Wdr16 differ with regard to their subcellular location. It is more likely that either the experiments of Keller and coworkers (2005) or the experiments performed for the present thesis were imperfect, or suboptimal conditions were used. It is a well-known fact that different immunostaining protocols influence the outcome of immunolocalization protocols (Vekemans et al., 2004). A point in favor of the immunolocalization experiments of the present study is that both a C- and N-terminally GFP-tagged Wdr16 fusion protein were used whereas Keller and coworkers only examined the location of a C-terminally GFP-tagged Wdr16 protein.

3.5 Immunoprecipitation and the search for Wdr16 protein-protein interaction partners

One aim of this thesis was to identify and characterize novel Wdr16 protein interaction partners by Co-IP and mass spectroscopy. Previous attempts to identify binding partners by yeast-2-hybrid screening and tandem affinity purification had already failed (Daniela Scheible and Stephan Verleysdonk, personal communications). Initial unsuccessful Co-IP experiments had been performed as well with the available Wdr16 antibody attached covalently to

activated agarose beads (S. Verleysdonk, personal communication). This outcome was most probably due to the ineptitude of the anti-Wdr16 antibody used in these studies for Co-IP experiments. The follow-up experimental approach chosen for this PhD thesis therefore was to express Flag-tagged Wdr16 in EPCs and cell lines, and to repeat the Co-IP experiments with the anti-Flag antibody M2, which binds the Flag epitope tag in a calcium-independent manner and is very well established for Co-IP studies (Brizzard et al., 1994). Two lentiviruses expressing Flag-tagged Wdr16 under the control of the ubiquitously recognized EF1α promoter and under the control of the ciliated cell-specific wdr16 promoter, respectively, were produced. For unknown reasons, no synthesis of Flag-tagged Wdr16 could be observed following infection of EPCs with HIV/VSV-G/wdr16p-wdr16-Flag lentivirus. Consequently, a HEK293T cell line stably expressing Wdr16-Flag was generated with the EF1α lentivirus, and the Co-IP experiments had to be performed with pre-mixed lysates of the HEK293T-Wdr16-Flag cell line and EPCs. By these means, the Flag-tagged Wdr16 protein could be specifically precipitated as demonstrated by anti-Wdr16 Western blots. However, the blots and Coomassie or silver stainings showed no bands representing possible interaction partners in the Wdr16-Flag eluate compared to the negative control. That is why no mass spectrometry experiments could be performed. There are some possible technical reasons why the Flag Co-IP may have failed to identify new protein interaction partners. One reason could be a suboptimal composition of the Co-IP buffer. For a Co-IP, the lysis should be sufficiently mild so as to not interfere with the antibody-antigen binding, but harsh enough to efficiently extract proteins from the cells. Another critical parameter is the salt concentration. High ionic strength tends to reduce electrostatic repulsion between proteins and to aid protein-protein interactions. For the Flag Co-IPs performed in this study, different detergent conditions (from 0.5 % NP-40 to 1 % Triton X-100) and a physiological salt concentration were used. Of course, very important for the success of any Co-IP is the binding step which generates the ternary complex of antibody, resin and antigen. The order of addition of these three components can be critical. For this study, the M2 anti-Flag antibody was pre-bound covalently to a resin and the lysate was added to the immobilized antibody. If a Co-IP fails it can also be worthwhile to alternatively incubate the antibody with

the lysate and then to extract the antigen:antibody complex with a Protein A- or G-covered resin from the mixture. Furthermore, Co-IP can be performed in batch-mode using low amounts of antibody-coupled resin or at a larger scale using column chromatography. The latter is of course advantageous because it is possible to detect very low levels of the interacting protein. In this study the Co-IP could only be performed in batch format, because not enough Flag antibody agarose was available for the experiments.

The Co-IP eluates were checked by Western blotting for the possible interaction of Wdr16 with selected structural proteins (α-tubulin, β-actin, and γ-tubulin) but none of these interactions could be detected. Nonetheless it was natural to examine this, because α-tubulin is the main structural component of kinocilia and therefore represents the most significant part of the cilia proteome. The presence of β-actin in the Co-IP eluates was checked because Wdr16 bears a striking resemblance to Aip1, a 67-kDa WD repeat protein known to regulate the depolymerization of actin filaments (Voegtli et al., 2003). Ciliogenesis in multiciliated cells is preceded by the apical organization of an actin network that is necessary for basal body docking to the apical membrane (Pan et al., 2007). Finally, the interaction of Wdr16 with γ-tubulin was checked, because γ-tubulin is a key component of basal bodies and centrioles. It is critical for the initiation of ciliary microtubule assembly and forms a large ring-shaped complex with at least 6 other proteins (Jeng and Stearns, 1999).

3.6 Known protein interactions of Wdr16 and their relevance

There exists one publication (Silva et al., 2005) that reports the identification of Wdr16 interaction partners, i.e., the chaperone protein HSP70, BRCA2 and a subunit of the chaperonin-containing TCP-1 (CCT1) complex. They were identified by co-immunoprecipitation from transfected liver hepatocellular carcinoma HepG2 cell lysates of Flag-tagged Wdr16 with anti-Flag antibody. None of these interaction partners could be confirmed in the present study with a similar Co-IP experiment using the M2 anti-Flag antibody. It is doubtful whether these detected interaction partners (Silva et al., 2005) are really relevant for the molecular function of Wdr16, because Wdr16 expression is

confined to kinocilia-bearing cells and not observed in liver cells. HSP70 is an evolutionarily highly conserved molecular chaperone that assists in a large variety of protein folding processes and promotes the survival of stressed cells (Mayer and Bukau, 2005). BRCA2 is a protein associated with breast and ovarian cancer and a tumor suppressor gene with key functions in DNA repair, cell cycle progression and homologous recombination (Yoshida and Miki, 2004). The third of the presumptive interaction partners, the α-subunit of the chaperonin-containing T-complex, is known to be involved in the folding of actin and tubulin, it is also upregulated during spermatogenesis and it is a component of cilia and flagella in protozoa and mammals. TCP1α may be related to cilia biogenesis and axonemal protein dynamics as well (Stephans and Lemieux, 1999; Seixas et al., 2003). Since TCP1α could not be detected in EPCs (at least not with the commercial antibody available for the present study), the relevance of the interaction of TCP1α with Wdr16 in kinocilia-bearing cells could not be confirmed. The TCP1α complex has also been shown to interact with other members of the WD repeat protein family, in particular those with seven bladed propellers. (Gómez-Puertas et al., 2004; Valpuesta et al., 2002). Thus, it cannot be excluded that TCP1α has a tendency to interact unspecifically with the β propeller motif of WD-repeat proteins and that this effect is responsible for the Wdr16-TCP1α interaction observed using the HepG2 cell line (Silva et al., 2005). Another factor which could have led to Co-IP "artifacts" is the over-expression of the Flag-tagged Wdr16. It is known that excessively high expression levels of the "bait protein" can lead to protein misfolding and unnatural binding events (Walker and Rapley, 2008).

3.7 Baculoviral expression and purification of Wdr16

In the present study the use of a baculovirus vector system permitted the expression and purification of the Wdr16 protein after unsuccessful attempts to express Wdr16 in bacteria and yeast. Insect cells were successfully infected with a baculovirus expressing polyhistidine-tagged Wdr16 protein. The histidine-tags of tagged proteins have a high selective affinity for Ni^{2+} and a variety of other immobilized transition metal ions. Consequently, a protein containing a

histidine tag is selectively bound to a metal-ion charged matrix while other cellular proteins are washed out with the binding or wash buffers. The advantage of histidine tags is that they are small and therefore less prone than larger tags to be disruptive to the properties of the proteins which they are attached to. However, the purification of the fusion protein by IMAC using Ni-NTA matrices was not satisfactory. This may be due to the polyhistidine tag being hidden inside the fusion protein. This is particularly likely to occur when the affinity tag is located in the middle of the polypeptide. While in the case of Wdr16 the tag was N-terminal, due to the operation of a so-called “molecular velcro” mechanism in Wdr16, in which the N-terminal residues form the final β-strand of blade 14 in the second propeller (Voegtli et al., 2003), the tag may nevertheless have been obstructed. For this reason, the purification of 6xHis-Wdr16 was also performed under denaturing conditions. Nevertheless, this did not improve the purification results. Another possible reason for the failure to purify 6xHis-Wdr16 could be the *absence* of the His-tag. This could have been a result from degradation of the tag by endogenous proteases during the purification procedure. Protease inhibitors were added to the lysate prior to the purification procedure, but they may not have worked properly or they may have been used in too low a concentration. Only inhibitors effective against aspartic proteases (pepstatin), serine proteases (AEBSF) and against trypsin and related proteases (aprotinin) were used for the purification. There are still some other classes of proteases left (especially cysteine and threonine proteases) which could have caused protein degradation during the purification process. Unfortunately, the presence of the polyhistidine tag could not be directly verified because of the lack of an adequate anti-oligoHis antibody. Since the purification using the oligohistidine-tag was unsuccesful, a baculovirus expressing GST-tagged Wdr16 protein was produced and insect cell suspension cultures were successfully infected. The GST-tag binds to the glutathione ligand on a sepharose matrix and it often has the advantage of increasing the yield of expression and solubility of a recombinant protein. Indeed, the purification using GST-tagged Wdr16 was successful. A disadvantage of the purification using the GST-tag is that the removal of the GST-tag from the target protein is necessary due to its large size. This could be achieved through the use of “Presscission”

protease and it was possible to remove the GST-tag without protease contamination of the final preparation.

3.8 Circular dichroism and structural analysis

The purified Wdr16 protein was subjected to circular dichroism (CD) spectrometry in order to determine its folding state and to analyze its secondary structure. CD spectrometry measures differences in the absorption of left-handed polarized light versus right-handed polarized light which arise due to structural asymmetry. Two advantages of CD spectroscopy are that it requires only very small amounts of material (100 micrograms or less) and measurements can be done very quickly. α-helix, β-sheet, and random coil structures each give rise to a characteristic shape and magnitude of the CD spectrum. A widely used standard are the spectra for poly-L-lysine because it can adapt all three different conformations depending on pH and temperature which change the degree of ionization of the amino groups in the side chains (Ma and Asher, 2010). CD spectrometry can determine if a protein contains approximately 50% β-sheet, but it cannot determine which specific residues are involved in the β-sheets. The CD spectrum of Wdr16 confirmed its native folding and corresponded almost exactly to the spectrum of proteins exclusively composed of β-sheets. The CD spectrum of Wdr16 resembles the spectrum of poly-L-lysine in the β-sheet conformation which shows a negative band at 218 nm and a positive one at 196 nm. The result of the CD spectroscopy appears to confirm the tertiary structure prediction by threading, according to which the Wdr16 protein is exclusively composed of β-sheets and features two covalently linked seven-bladed β-propellers (Hirschner et al., 2007).

3.9 Generation of a wdr16 knockout mouse line

Despite substantial research effort, the molecular function of the kinocilia-bearing cell specific Wdr16 protein remains to be elucidated. For instance, silencing of wdr16 expression in kinocilia-bearing ependymal primary cultures

did not reveal a phenotype. Because WD-proteins are thought to be involved in protein-protein interactions and the assembly of larger protein complexes, the identification of its binding partner is likely to point to the physiological function of Wdr16. Since this has not yet been achieved, the generation of a mouse line bearing a deletion of the wdr16 gene shows the greatest promise for finding the precise molecular function of Wdr16. The main advantage of knockout mice is that the expression of the target gene is shut down one hundred percent and the target gene can be ablated in all tissues. This significantly increases the chance to reveal a phenotype. In addition, novel or unexpected actions of target genes often emerge because knockout models can be generated that are not limited to a specific tissue or system. The main disadvantage of knockout mice is that their generation is time-consuming and expensive compared to methods involving RNAi. This is the reason why knockout mice are often produced in specialized laboratories or service platforms. Moreover, it is sometimes desirable to obtain a tissue-specific knockout and in this case, the knockout mice must be cross-bred with a mouse line expressing Cre recombinase under a promoter of a gene the expression of which is characteristic for the tissue of interest. On the other hand, it is easy to achieve a tissue-specic knock-down, e.g. by using RNAi. For this, the interfering small RNAs must just be expressed under the control of a tissue- or cell type-specific promoter. In the case of wdr16, knockout mice would be beneficial because they are likely to definitely answer the question if the lack of wdr16 expression causes cilia-related defects such as hydrocephalus, abnormal spermatogenesis or respiratory pathology. Furthermore, the availability of ependymal primary cultures derived from wdr16 knockout mice would facilitate many pertinent investigations, e.g. on the regulation of ciliary beat and on subjects amenable to immunoelectron microscopy. It should also be emphasized that in the case of Wdr16 being an essential factor for embryonic development such a knock-out would result in embryonic or neonatal lethality of the mice, thus would prevent any further experiments, and therefore bar obtaining appropriate results. In this case, the deletion of the target gene must be possible at any time chosen. E.g., it would be necessary to cross-breed the genetically altered mice bearing the “floxed” wdr16 gene with a second mouse line in which the expression of the Cre

recombinase is under the control of a tissue-specific promoter which is transcribed during the appropriate developmental stage.

3.10 Possible molecular function of Wdr16

Based on the results of this PhD thesis and the preliminary experimental work done by Stephan Verleysdonk, Wolfgang Hirschner and Bhavani Khowtharapu in our research group it can be hypothesized that Wdr16 has a role in the subsequently discussed cellular contexts.

3.10.1 Water homoeostasis and osmoregulation

The fact that knockdown of wdr16 in zebrafish leads to hydrocephalus with apparently unaltered ciliary motility led to the hypothesis that Wdr16 may be responsible for directing ion channels, transporters and other molecules necessary for brain fluid homeostasis to their correct cellular location (Hirschner et al., 2007). While the ezrin localization data do not reveal any polarization deficit, it is nonetheless possible that the correct localization of aquaporins and ion channels is affected following wdr16 knockdown in EPCs. However, the respective antibodies (e.g. against aquaporin-4; Li et al., 2009) were not available for this PhD project.

3.10.2 Planar cell polarity (PCP) and orientation of cilia-driven fluid flow

The development of cilia-covered tissues like the ependyma (but also the respiratory epithelium and fallopian tube) critically depends on the coordination of the ciliary beating which guarantees an efficient directional fluid flow (Guirao et al., 2010). These workers have demonstrated that the orientation of kinocilia for directional beating is a two-step process wherein basal bodies first dock apically with random orientations and then reorient into a common direction. The reorientation into a common direction depends on the sensing of

hydrodynamic forces by the kinocilia themselves and the intracellular PCP pathway (Guirao et al., 2010). The PCP pathway is the signaling process by which cells in multicellular organism are polarized in the plane of the epithelial sheet, and which governs the dynamics of the actin network that again positions ciliary basal bodies (Wallingford, 2006). Wdr16 could be involved in the orientation of basal bodies and the establishment of directional cilia-driven fluid flow. The fact that until now the localization of Wdr16 at the basal body was only demonstrated in protozoans speaks against this hypothesis, since unicellular organisms do not need planar cell polarity or the coordination of ciliary beating between many ciliated cells. It cannot be excluded that Wdr16 may be a part of this process, e.g. as a kinocilia-specific PCP protein or as a protein that is involved in the sensing of the hydrodynamic forces. Pertinent in this context is that Jones et al. (2008) have demonstrated that another “classical” ciliary protein, Polaris/IFT88, is required for establishing epithelial PCP and basal body positioning.

3.10.3 Participation in cilia-generated signaling

Wang et al. (2006) have demonstrated in the green algae *Chlamydomonas* that IFT is not only required for assembling cilia and flagella but also for a cilium-generated signaling pathway. This cilia-dependent signal transduction pathway is also present in multiciliated cells and may pass on important information into the ependymal cells, e.g. about the osmolarity of the CSF or the direction of the cilia-driven fluid flow. One example where kinocilia are involved in cellular signaling processes and regulation of ion transport has been described by Banizs and coworkers (2005). They analyzed a mouse strain which bears a mutation of a crucial IFT gene, IFT88/polaris, and has severe developmental defects, e.g. cystic kidney disease and hydrocephalus. One of their main findings was that the malformed and dysfunctional ependymal kinocilia were not the principal reason for the hydrocephalus, because the hydrocephalus started prior to the development of kinocilia and the CSF flow was not obstructed in the early stages of the disease. They found out that these mice had increased intracellular cAMP levels in the ependyma and an elevated chloride

concentration in the CSF which contributes to excess CSF and the development of hydrocephalus. These data confirm that outward chloride transport and CSF production is regulated by intracellular cAMP and that this process depends on the normal function of the ependymal kinocilia. If Wdr16 would be involved in the cilia-dependent regulation of second messengers like cAMP or ion transport, this could explain why the knockdown of wdr16 in zebrafish results in hydrocephalus without impairment of the ciliary beat. Of course, this would also explain why there is no visible phenotype following knockdown of wdr16 in ependymal primary cultures.

3.10.4 Vesicular transport to the cilium

Cilia are dynamic structures that incorporate new protein both during their formation and in the steady state of their maintenance. The maintenance and function of cilia not only depends on the motor protein-powered IFT system. Another factor is the selective vesicular transport of ciliary proteins to the basal body in preparation of their further transport into the cilia. In addition, trafficking of vesicles to the cilium is necessary for the elongation of the ciliary membrane (Nachury et al., 2007). Vesicular transport to the cilium is a complicated process that involves many proteins, e. g. Rab GTPases and the Bardet-Biedl syndrome (BBS) proteins. BBS proteins are thought to underlie the human disease Bardet-Biedl syndrome, a rare ciliopathy with multisystem involvement. BBS proteins localize predominantly at the base of the cilia and act as adaptor molecules for the movement of selected target proteins from the cell into the cilium (Kim et al., 2004; Zaghloul and Katsanis, 2009). It is assumed that Wdr16, like most WD-repeat proteins, provides a platform for protein-protein interactions (Friesen et al., 2002), and it also may localize to the basal body. Accordingly, it would not be surprising if Wdr16 were involved in the vesicular transport to the cilium in multi-ciliated cells. For instance, the reduction in the amount of certain proteins following wdr16 knockdown could interfere with the normal ciliary function and could be the reason for the hydrocephalus in zebrafish. This hypothesis would also explain the presence of Wdr16 in the cytosol as well as the basal body and cilia of kinocilia-bearing cells.

3.11 Summary and outlook

1) Expression of wdr16 in kinocilia-bearing cells can be silenced by lentiviral transfection of EPCs with VSV-G pseudotyped lentiviral vectors expressing anti-wdr16-siRNAs.

2) The anti-wdr16-siRNA cassette could be expressed under the control of the constitutively active H1 promoter, whereas it was necessary to express the GFP reporter protein under the control of the ciliated cell-specific wdr16 promoter in order to prevent a significant loss of kinocilia-bearing cells.

3) Silencing of the wdr16 gene in EPCs does not result in an easily recognizable knockdown phenotype, and the ependymal cells infected with anti-wdr16 virus appear morphologically normal.

4) The overall number of kinocilia-bearing cells in EPC infected with the anti-wdr16 virus is only slightly reduced compared to EPC treated with the control-siRNA virus (approx. 5 %).

5) Detailed cellular analysis of apical-basal cell polarity, basal bodies, mitochondria and distribution of actin and tubulin did not reveal any phenotype of the kinocilia-bearing cells attributable to the transcription of the anti-wdr16-siRNA cassette.

6) The RNAi viruses failed to infect the ependymal layer *in vivo* following injection into the cerebral ventricles of adult rats.

7) A HEK293T cell line expressing Flag-Wdr16 was generated. Flag-tagged Wdr16 fusion protein could be immunoprecipitated from lysates of this cell line using anti-Flag M2 antibody coupled to agarose beads. Using this Co-IP approach it was not possible to identify novel Wdr16 interaction partners.

8) GFP fusion proteins and Flag-tagged variants of Wdr16 exclusively localized to the cytosol of transfected cultured cells in agreement with the results obtained by the available Wdr16 peptide antibody. The centriolar localization of exogenous Wdr16 in the HeLa cell line (reported by Keller et al., 2005) could not be confirmed.

9) Baculoviruses expressing polyhistidine- and GST-tagged Wdr16 were generated using a commercially available baculovirus expression vector system. These baculoviruses were used for the infection of insect cells in suspension culture, and GST-tagged Wdr16 protein could be purified by affinity chromatography. The tag could be removed proteolytically resulting in untagged folded Wdr16 protein.

10) The folding of the purified Wdr16 protein was analyzed by circular dichroism (CD) spectrometry. The obtained CD spectrum for Wdr16 confirms the bioinformatic prediction of secondary structure, according to which the Wdr16 protein is exclusively composed of β-sheets.

11) Large-scale purification in combination with x-ray crystallography would be useful for further investigations of the three-dimensional structure of Wdr16. Moreover, the purified GST-tagged protein could be employed for identifying protein interactions by using the GST-pulldown technique.

12) A targeting vector was cloned by “floxing” (loxP flanking) exons 2 and 3 of the wdr16 gene. This tool can be useful for the generation of a transgenic knockout mouse line. The ability of Cre recombinase to excise the intervening DNA sequence was confirmed following transformation of Cre-expressing bacteria by the targeting vector.

4 Materials and methods

4.1 Materials

4.1.1 Devices

Autoclave	Type 669, Aigner, München Type 5075 ELV, Systec, Wettenberg
Balances	Type 1403 and L2205, Sartorius, Göttingen
Cameras	Coolpix 995, Nikon, Düsseldorf; Canon EOS 350D, Canon, Krefeld
Cell incubators	Type B 5060 EC CO2, Function LINE, both from Heraeus, Hanau
Centrifuges	Varifuge K, Biofuge fresco, Multifuge 3 S-R, all three from Heraeus, Hanau
Containment hoods	Lamin Air HLB 2448 and TL 2448, Heraeus, Hanau; Technoflow 3F150-11GS, Integra Biosciences, Zizers (Switzerland)
Cryostat	Model CM1950, Leica, Wetzlar
Cryosystem	Chronos 80, Messer Austria, Gumpoldskirchen (Austria)
Drying oven	Type U-30, Memmert, Schwabach
Electroblotting chamber	Transblot SD, Bio-Rad, München
Electrophoresis chamber	Model B1 (110 mm x 90 mm), Owl separation systems, USA
Electroporation device	Gene Pulser Xcell, Bio-Rad, München
Heating block	Grant QBT, CLF Laborgeräte,

	Emersacker
Hybridisation oven	Model OV1, Biometra, Göttingen
Magnetic stirrer	IKAMAG RCT, Bachofer, Reutlingen
Microplate reader	Infinite M1000, Tecan, Männedorf
Microscopes	Model IM, IM 35, and Axiovision 2, all three from Zeiss, Oberkochen; Axiovert 25, Nikon, Jena
Microwave oven	Micro-Chef FM 3915 Q, Moulinex , Offenbach
Osmometer	Osmometer Automatic, Knauer, Eppelheim
PCR thermocycler	Primus 96 plus, MWG AG Biotech, Ebersberg
pH meter	PHM 92, Radiometer, Copenhagen, Denmark
Pipettors	Finn pipettors (5-40 µl, 40-200 µl, 200-1,000 µl), Labsystems, Finnland; Eppendorf pipettors (0.5-10 µl, 10-100 µl, 200-1,000 µl), Eppendorf, Hamburg; Multichannel pipettor Titerman, Eppendorf, Hamburg
Power supplies	Consort E 132, BioBlock Scientific, Illkirch, France; 2301 Macrodrive 1, LKB Bromma, Vienna, Austria; Power Supply Model 200, Bethesda Research Laboratories, Life Technologies, Inc., USA; Computer Controlled Electrophoresis Power Supply Model 3000 X, Bio Rad, Munich
Rotor for ultracentrifugation	Type 70 Ti, Beckman-Coulter , Krefeld

SDS-PAGE electrophoresis chamber	Mini-PROTEAN Tetra Cell, Bio-Rad, Munich
Shaker	Vortex Genie, Bender & Hobein, Munich
Shaking platform	Horizontal-Schüttelplattform KL2, Bühler, Tübingen
Sonifier	Branson B-30 with microtip, Heinemann, Schwäbisch Gmünd
Spectrophotometers	Uvikon 860 with Plotter 800, Kontron, Eching
Table top centrifuge	Centrifuge 5415 C, Eppendorf, Hamburg
Tissue homogeniser	Potter-Elvehjem homogeniser, Braun, Melsungen
Ultracentrifuge	Optima L-80, Beckman-Coulter, Krefeld
UV transilluminator	Benchtop transilluminator, UVP, Uvitec Cambridge, Cambridge, UK
Vacuum filter device	Sterile filtration apparatus, Millipore, Eschborn
Water bath	Julabo Standard, Julabo PC Thermostat, Labora, Mannheim; GFL-1083 shaking water bath, Helago laboratory equipment, Medingen
Water purification unit	USF Elga (0.22 µm-filter), Purelabs, USA
Welding apparatus for preparing mesh bags	Super Poly 281, Audion Elektron, Kleve
X-ray film developing machine	Röntgenfilm Entwicklungsmaschine SRX-101, Konica Europe, Hohenbrunn
X-ray film exposure cassette	Hypercassette, Amersham

	Buchler, Braunschweig

4.1.2 General material

Coverslips 12 mm (round), 18 mm x 18 mm (square)	Roth, Karlsruhe
Cryo tubes, 2 ml	Greiner, Frickenhausen
Culture dishes, 35 mm in diameter	Becton Dickinson Falcon, Heidelberg
Culture dishes, 90 mm in diameter	Nunc, Wiesbaden
Culture flasks, 75 cm^2 surface area (with vented cap)	Nunc, Wiesbaden
Filter paper (Whatman 3MM)	Whatman, Göttingen
Filtration units (sterile Millex units)	Millipore, Eschborn
Glass pipettes (1 ml, 5 ml, 10 ml)	Hirschmann, Eberstadt
Glassware	Schott, Mainz ; Brand, Wertheim
Hybridisation container	Fisher Scientific, Schwerte
Syringes, 20 ml, sterile	Braun, Melsungen
Microscope slides (26 mm x 76 mm x 1 mm)	Menzel via Roth, Karlsruhe
Microscope slides “Superfrost” (26 mm x 76 mm x 1 mm)	Menzel via Roth, Karlsruhe
Microtiter plates (Maxisorp Immuno plate F96)	Nunc, Wiesbaden
MµltiGuard ™ barrier tips	Sorenson Biosciences, Inc., via Roth, Karlsruhe
Nitrocellulose membrane (Trans-Blot, 0.45 µm)	Bio-Rad, Munich
Nylon cloth (132, 210 µm mesh size)	Sefar GmbH, Wasserburg/Inn

Nylon membrane, positively charged	QBIOgene, Heidelberg
PCR tubes (0.2 ml)	PeqLab, Erlangen
Petri dishes (AD94/H16mm)	Roth, Karlsruhe
Pipette tips	Braun, Melsungen
Plastic tubes, 14 ml	Greiner, Frickenhausen
Plastic tubes, 50 ml	Nunc, Wiesbaden
Plastic reaction tubes, 1.5 ml	Brand, Wertheim
Pursept®-A disinfectant solution	Merz via Fischer, Frankfurt
Safe Skin Satin Plus powder-free latex gloves	Kimberly Clark, Koblenz-Rheinhafen
Sterile filters (0.2 µm and 0.45 µm mesh)	Renner GmBH, Dannstadt
Sterile single-use serological pipets (10 ml)	Falcon via Multimed, Kirchheim u. Teck
X-ray film	Amersham Hyperfilm ECL, Amersham, Freiburg; Fuji X-Ray Medical Film Fujifilm Europe, Düsseldorf

4.1.3 Chemicals

Ammonium peroxodisulfate (APS)	Fluka, Steinheim Calbiochem, Darmstadt
Bradford assay dye reagent	Bio-Rad, München
Bromophenol blue	Fluka, Steinheim
Bovine serum albumin (BSA)	Sigma-Aldrich, Steinheim
Calcium chloride dihydrate	E. Merck, Darmstadt
Coomassie brilliant blue R 250	Sigma-Aldrich, Steinheim
D-glucose	Fluka, Steinheim
Dimethylsulfoxide (DMSO)	Sigma-Aldrich, Steinheim
Dithiothreitol (DTT)	Gibco BRL, Karlsruhe
Ethylenediaminetetraacetic acid	Roth, Karlsruhe

“Empigen” detergent, 30% solution (w/v)	Calbiochem, Darmstadt
Glycerol	Roth, Karlsruhe
Glycine	Roth, Karlsruhe
“Immu-mount”mounting medium	Thermo Shadon, Pittsburgh, USA, via Thermo Electron, Bremen
JetPEI™ transfection reagent	QBIOgene, Heidelberg
KCl	E. Merck, Darmstadt
Lipofectamine transfection reagent	Invitrogen, Karlsruhe
Mercaptoethanol	Roth, Karlsruhe
$MnCl_2$	Fluka, Steinheim
NaCl	Roth, Karlsruhe
$NaHCO_3$	Roth, Karlsruhe
p-Nitrophenylphosphate	Roche, Mannheim
PageRuler™ prestained protein ladder	MBI Fermentas
Paraformaldehyde	Fluka, Steinheim
RbCl	Sigma-Aldrich, Steinheim
Rotiphorese Gel 30	Roth, Karlsruhe
Sodium hypochlorite solution	Roth, Karlsruhe
Sodium dodecyl sulfate (SDS)	Fluka, Steinheim
Sucrose	Roth, Karlsruhe
N,N,N’,N’-Tetramethylethylenediamine (TEMED)	Sigma-Aldrich, Steinheim
Tris(hydroxymethyl)aminomethane (Tris)	Roth, Karlsruhe
Tween 20	Fluka, Steinheim

4.1.4 Kits

Enhanced chemiluminescence (ECL) detection reagent	Amersham, Freiburg

HotStarTaq Master Mix kit	Qiagen, Hilden
NucleoSpin® Extract II kit	Macherey-Nagel, Düren
NucleoSpin® Plasmid kit	Macherey-Nagel, Düren
NucleoSpin® Xtra Midi Plus kit	Macherey-Nagel, Düren
Omniscript Reverse Transcriptase kit	Qiagen, Hilden
RNeasy RNA isolation kit	Qiagen, Hilden
SMART^{TM} PCR cDNA synthesis kit	Clontech (now Takara Bio), Heidelberg
StrataClone PCR cloning kit	Stratagene, La Jolla (USA)
QIAEX II Gel extraction kit	Qiagen, Hilden
Zero Blunt TOPO PCR cloning kit	Invitrogen, Karlsruhe

4.1.5 Reagents for molecular biology

Agarose	PeqLab, Erlangen
Deoxyribonucleoside triphosphate (dNTP; 10 mM each)	PeqLab, Erlangen
GeneRuler 1 kb DNA ladder	MBI Fermentas, St. Leon-Rot
GeneRuler 100 bp DNA ladder plus	MBI Fermentas, St. Leon-Rot
Glutathione-Sepharose 4B	GE Healthcare, München
Ethidium bromide	Fluka, Steinheim
Oligo(dT_{15}) primer	Invitrogen, Karlsruhe
PCR primers	Invitrogen, Karlsruhe Biomers, Ulm
Phenol/chloroform/isoamylalcohol (25 :24 :1) (v/v/v)	Applichem, Darmstadt
T4 DNA ligation buffer (10x)	MBI Fermentas, St. Leon-Rot

4.1.6 Enzymes for molecular biology

BamHI	New England Biolabs, Frankfurt a.M.
Calf intestine alkaline phosphatase	MBI Fermentas, St. Leon-Rot

ClaI	New England Biolabs, Frankfurt a.M.
EcoRI	New England Biolabs, Frankfurt a.M.
EcoRV	New England Biolabs, Frankfurt a.M.
HindIII	New England Biolabs, Frankfurt a.M.
HotStart Taq DNA polymerase	Qiagen, Hilden
MfeI	New England Biolabs, Frankfurt a.M.
MluI	MBI Fermentas, St. Leon-Rot
Omniscript reverse transcriptase	Qiagen, Hilden
PacI	New England Biolabs, Frankfurt a.M.
PfuUltra™ Hotstart High-Fidelity DNA polymerase	Stratagene, Amsterdam
Phusion™ DNA polymerase	Finnzymes, Espoo (Finnland)
Polynucleotide kinase (from bacteriophage T4)	MBI Fermentas, St. Leon-Rot
PstI	New England Biolabs, Frankfurt a.M.
PvuII	New England Biolabs, Frankfurt a.M.
RNAse A (from bovine pancreas)	Qiagen, Hilden
SalI	MBI Fermentas, St. Leon-Rot
SmaI	New England Biolabs, Frankfurt a.M.
Taq DNA polymerase	Eppendorf, Hamburg
T4 DNA ligase	MBI Fermentas, St. Leon-Rot
XhoI	New England Biolabs, Frankfurt a.M.

4.1.7 Constituents and reagents for bacterial and mammalian cell cultures

Carbenicillin, disodium salt	Roth, Karlsruhe
Dulbecco's Modified Eagle's Medium (DMEM), powder, without pyruvate and $NaHCO_3$	Invitrogen, Karlsruhe
Fetal calf serum (FCS)	Biochrome, Berlin
Grace medium	Invitrogen, Karlsruhe
Hank's balanced salt solution (HBSS)	Invitrogen, Karlsruhe
Insulin	Sigma-Aldrich, Steinheim
Kanamycin	Applichem, Darmstadt
LB-agar	Fluka, Steinheim
LB, powder	Fluka, Steinheim
Minimal Essential Medium (MEM), powder	GibcoBRL, Karlsruhe
Penicillin G, potassium salt	Serva, Heidelberg
Pluronic F-68	Sigma-Aldrich, Steinheim
Superoptimal broth with catabolite repression (SOC)	Novagen, Schwalbach/Ts
Streptomycin sulfate	Serva, Heidelberg
Thrombin (human)	Kindly provided by Dr. Mirna Rapp, Aventis Behring, Marburg
Transferrin	Roche, Mannheim
Trypsin	ICN, Eschwege
Yeastolate ultrafiltrate	Invitrogen, Carlsbad (USA)

4.1.8 Primary antibodies

Monoclonal anti-acetylated-tubulin antibody	Sigma-Aldrich, Steinheim
Monoclonal anti-β-actin antibody	Sigma-Aldrich, Steinheim
Anti-Wdr16 antiserum	provided by Dr. Wolfgang

	Hirschner, IFIB, University of Tübingen (Hirschner et al., 2007)
Anti-AK7 serum	provided by Dr. Daniela Scheible, IFIB, University of Tübingen
Anti-GP-BB serum	provided by Dr. B. Pfeiffer-Guglielmi, IFIB, University of Tübingen (Pfeiffer-Guglielmi et al., 2003)
Anti-Ezrin (C-19) , polyclonal	Santa Cruz Biotechnology, Santa Cruz (USA)
Anti-γ-tubulin (GTU-88), monoclonal	Sigma-Aldrich, Steinheim
Anti- β-actin (AC-15), monoclonal	Sigma-Aldrich, Steinheim

4.1.9 Secondary antibodies

Donkey anti-guinea pig IgG Cy3 conjugate	Jackson, via Dianova, Hamburg
Donkey anti-guinea pig IgG peroxidase conjugate	Jackson, via Dianova, Hamburg
Goat anti-mouse IgG Alexa Fluor 568 conjugate	Molecular Probes, via Invitrogen, Karlsruhe
Goat anti-mouse IgG peroxidase conjugate	Jackson, via Dianova, Hamburg
Streptavidin-alkaline phosphatase conjugate	Jackson, via Dianova, Hamburg
Donkey anti-rabbit IgG, peroxidase conjugate	Jackson, via Dianova, Hamburg
Goat anti-rabbit IgG, alkaline phosphatase conjugate	Jackson, via Dianova, Hamburg

4.1.10 Bacterial strains

DH5α	Invitrogen, Karlsruhe
NovaBlue	Novagen, Darmstadt

4.1.11 Animal cell lines

293T human embryonic kidney cells	Provided by Dr. Roland Vogel, Université Pierre et Marie Curie, Paris
HeLa cells	Provided by Dr. Richard Schäfer, Zentrum für Klinische Transfusions-medizin, University of Tübingen
Sf9 insect cells	Invitrogen, Carlsbad (USA)

4.1.12 Animals

Wistar rats	Purchased from Charles River, Kisslegg; bred in the animal facility of the institute
BL 6 mice	Purchased from Charles River, Kisslegg

4.1.13 Plasmids

4.1.13.1 Plasmid for the generation of a gene targeting vector

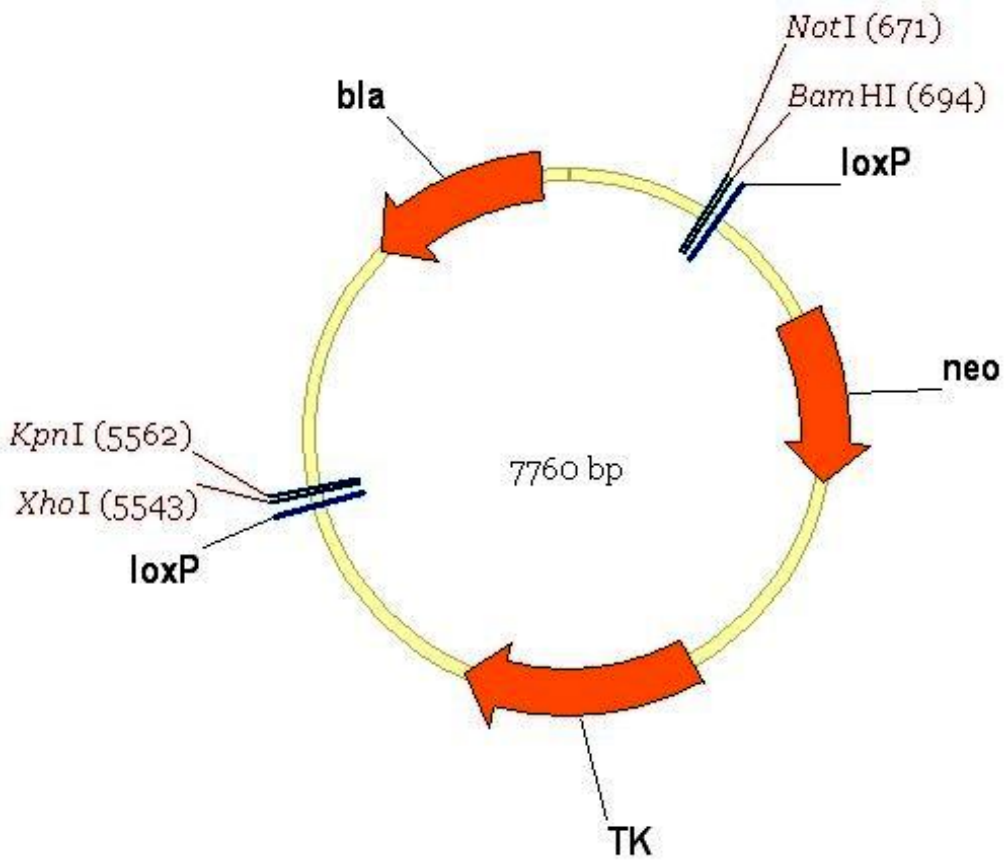

Fig. 24. Vector map of the plasmid pBs-loxP-neoTK-loxP. A kind gift from Prof. R. Feil (IFIB, University of Tuebingen).

4.1.13.2 Lentiviral vectors

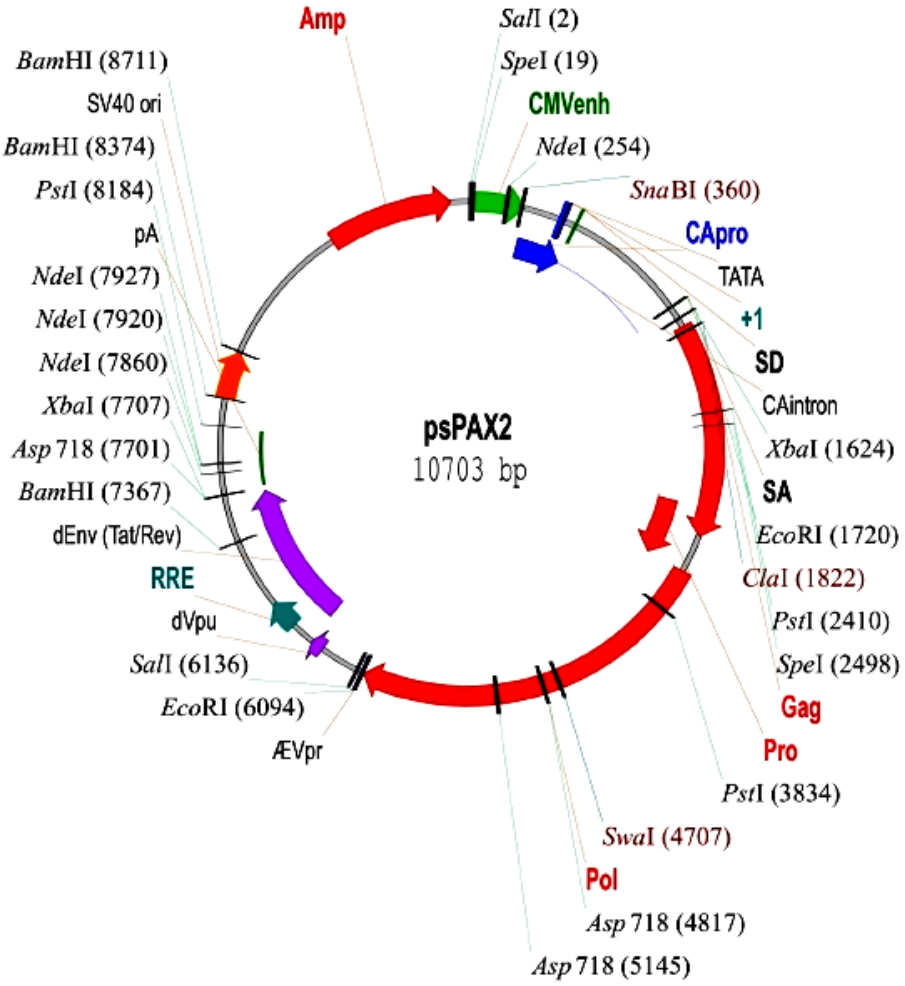

Fig. 25. Vector map of the plasmid psPAX2. Purchased from Prof. Didier Trono, EPFL, Lausanne (Wiznerowicz and Trono, 2005).

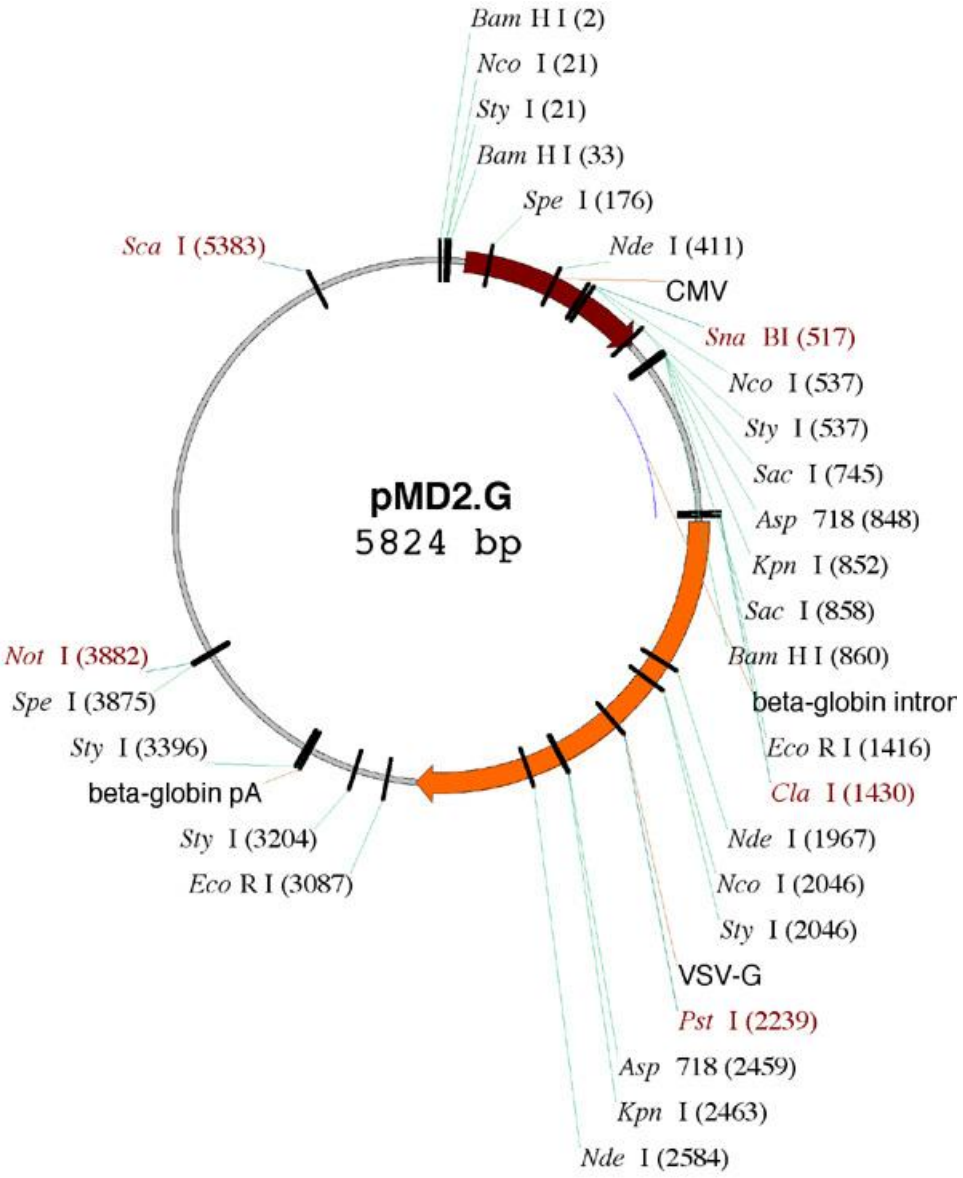

Fig. 26. Vector map of the plasmid pMD2.G. Purchased from Prof. Didier Trono, EPFL, Lausanne (Wiznerowicz and Trono, 2005).

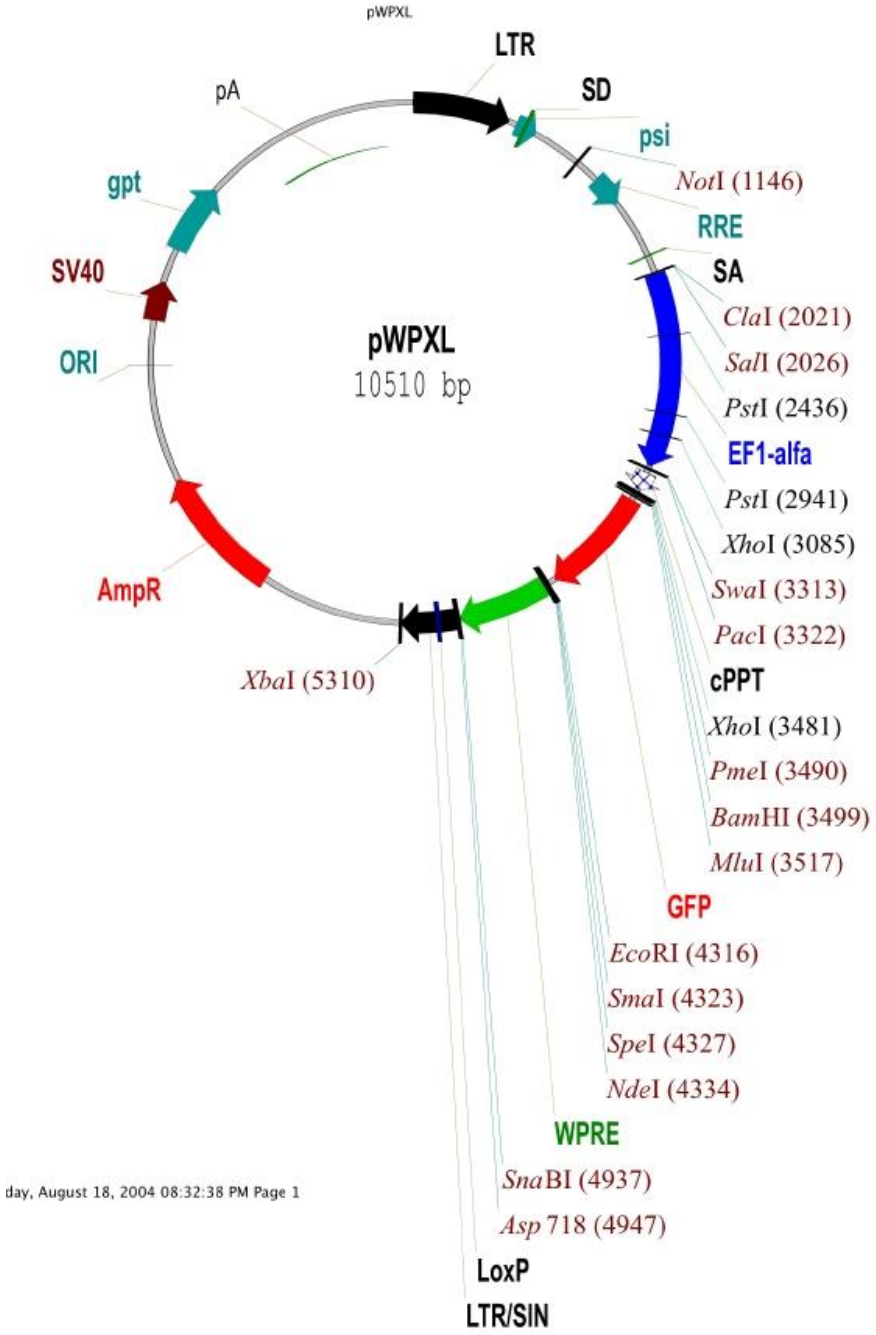

Fig. 27. Vector map of the plasmid pWPXL. Purchased from Prof. Didier Trono, EPFL, Lausanne (Wiznerowicz and Trono, 2005).

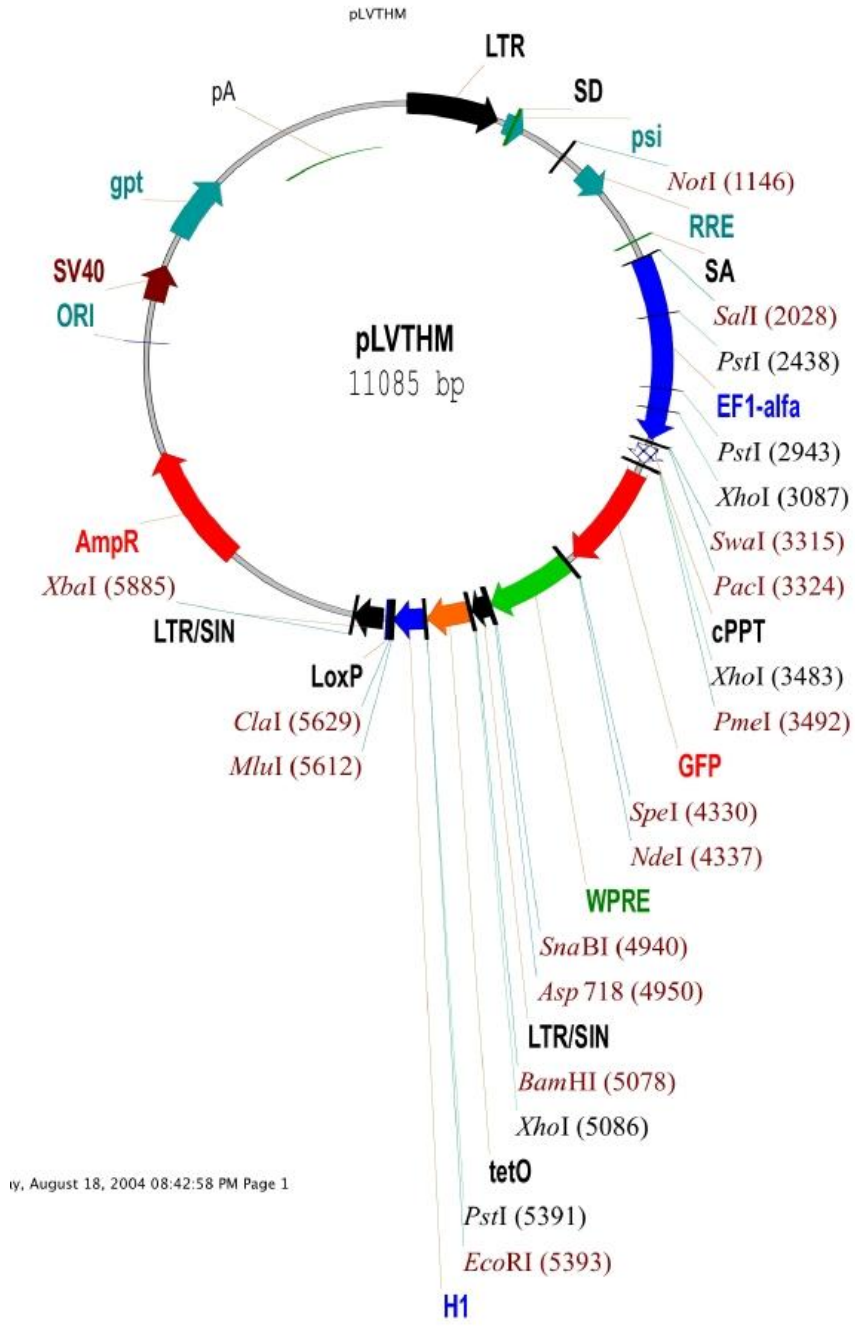

Fig. 28. Vector map of the plasmid pLVTHM. Purchased from Prof. Didier Trono, EPFL, Lausanne (Wiznerowicz and Trono, 2005).

4.1.13.3 Baculoviral expression vectors

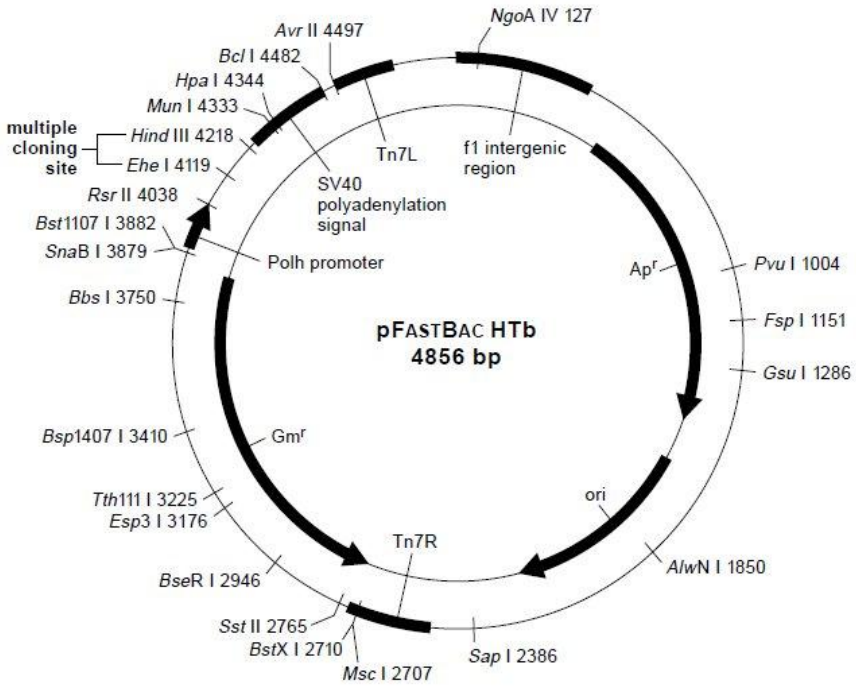

Fig. 29. Vector map of the plasmid pFastBac-HTB (Invitrogen, Carlsbad, USA).

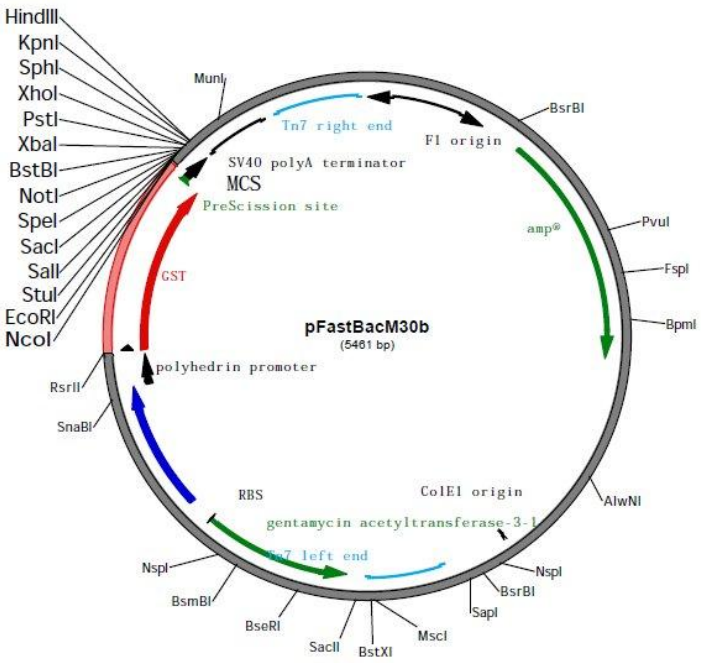

Fig. 30. Vector map of the plasmid pFastBac-M30b. Kindly provided by Dr. Arie Geerlof (Helmholtz-Zentrum, München).

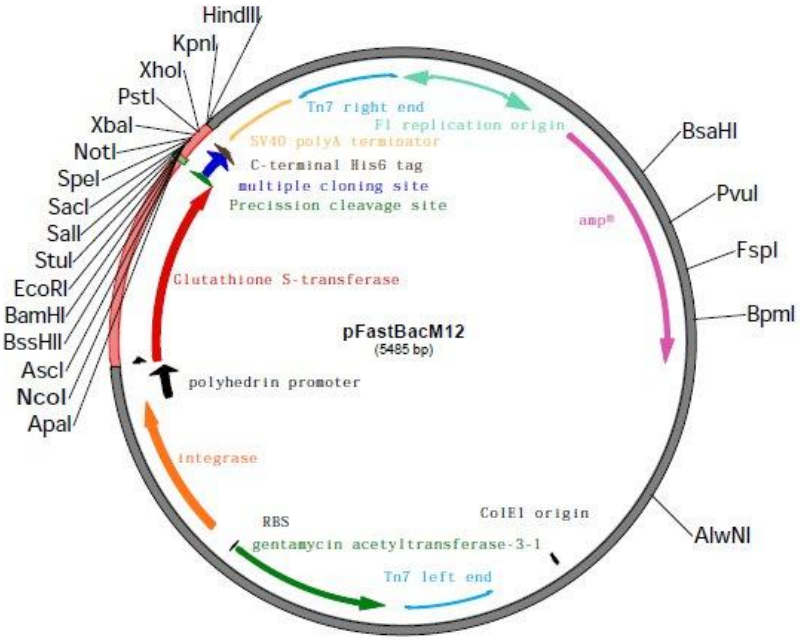

Fig. 31. Vector map of the plasmid pFastBac-M12b. Kindly provided by Dr. Arie Geerlof (Helmholtz-Zentrum, München).

4.2 Methods

4.2.1 Preparation of medium for bacterial liquid cultures

LB (20 g) was dissolved in 1 liter of ddH_2O with a magnetic stirrer. Afterwards, the solution was autoclaved at 121°C for 20 min. After cooling down to RT, 1 ml of a 1,000-fold concentrated stock solution of antibiotic was added to LB. The LB was stored at 4°C in the dark for up to 1 month. Working concentrations of antibiotics: carbenicillin (50 mg/ml), kanamycin (50 µg/ml).

4.2.2 Preparation of agar plates

LB agar powder (30 g) was dissolved in ddH_2O using a magnetic stirrer, and the solution was autoclaved at 121°C for 20 min. After the liquid had cooled down to approximately 50-60°C, 1 ml of 1,000-fold antibiotic stock solution was added. Afterwards the liquid was distributed among Petri dishes under a sterile containment hood. After the agar had solidified, the plates were stored at 4°C until use.

4.2.3 Bacterial liquid cultures

A single bacterial colony from a fresh streakout was transferred to the antibiotic-containing LB with a sterile pipette tip. For a “mini” scale plasmid preparation, 5 ml of LB in sterile polypropylene tubes were used, and for a “maxi” scale plasmid preparation, 400 ml of LB in an Erlenmeyer flask were used. The liquid bacterial cultures were incubated on a shaking platform overnight (ca. 16 h) at 37°C.

4.2.4 Preparation of bacterial glycerol stocks

For preparing bacterial glycerol stocks, 0.5 ml of a bacterial overnight culture and 0.5 ml of glycerol were mixed in cryovials and stored at -80°C.

4.2.5 Transformation of competent bacteria

One vial containing 50 µl of competent cells (Novagen or self-made Dh5α competent bacteria) was thawed on ice and mixed gently. Two µl of the ligated plasmid DNA or 1-2 ng of plasmid for re-transformation were added and the contents of the reaction vessel were mixed gently. The tube was subsequently incubated on ice for 5 min. Then, it was heated to 43°C for exactly 40 s in a water bath and afterwards placed on ice for 2 min. Immediately afterwards, 250 µl of SOC (RT) were added. The mixture was transferred to a 15 ml polypropylene tube and incubated at 37°C in a rotary shaker (250 rpm) for 45 min prior to plating on antibiotic-containing LB agar plates.

4.2.6 Digestion of DNA with restriction endonucleases

For DNA cloning, 5 to 10 µg of purified plasmid DNA or PCR product were digested with 10 units of the desired restriction enzyme in the appropriate buffers for at least 6 h. (total reaction volume: 50 µl). If a plasmid or PCR product had to be digested with two different restriction enzymes, a sequential digestion was performed. After digestion with the first restriction endonuclease, the enzyme was heat-inactivated and afterwards the DNA was purified using the Nucleospin Extract II kit according to the manufacturer's instructions. The purified DNA was then subjected to the digestion with the second restriction enzyme. For the analysis of plasmid DNA by restriction digestion, only 0.5 µg of DNA were used and the DNA was digested with two restriction enzymes simultaneously (double digestion).

4.2.7 Dephosphorylation of DNA

For the dephosphorylation of DNA 5'-termini, calf intestine alkaline phosphatase (CIAP) was used. Five microliters of 10x CIAP reaction buffer or compatible restriction enzyme buffer were added to 10 - 40 µl of DNA solution. The reaction mixture was brought to a volume of 50 µl with deionized water and 1 unit of CIAP was added. The dephosphorylation reaction was allowed to proceed at 37°C for 30 min. Thereafter, it was stopped by keeping the solution at 85°C for 15 min.

4.2.8 Agarose gel electrophoresis of DNA

Agarose powder was dissolved in 100 ml of TAE buffer (made up from 50-fold concentrated TAE buffer; 2 M Tris, 0.1 M EDTA, adjusted to pH 8.5 with glacial acetic acid) by heating the mixture in a microwave oven. Afterwards, the solution was allowed to cool down to approx. 50°C (measured using a mercury-in-glass thermometer), and then it was poured into the sealed gel tray of the electrophoresis chamber, into which the comb had been inserted to generate sample pockets. After solidifying, the gel was submerged in TAE buffer, and the DNA samples were loaded into the sample pockets as mixtures with 6-fold DNA loading buffer. The “1 kb plus DNA ladder” from Fermentas was used as a size standard. Electrophoresis was conducted at 60 V (for preparative DNA purification) or 120 V (for analytical purposes. After electrophoresis, the DNA bands were visualized by incubation of the gels in 0.005% (w/v) ethidium bromide in TAE buffer for 20 min and washed with deionized water. Finally, the gels were inspected on a UV transilluminator and their photographs taken with a Nikon digital camera.

4.2.9 Extraction of DNA from agarose

Five microliters of the DNA solution were loaded into the lane of an agarose gel next to the lane with the DNA standard. The rest of the DNA solution (45 µl)

was loaded into the next two adjacent (preparative) lanes. Since each cloning was started with at least 5 µg of vector or insert DNA, the concentration of the DNA solution was at least 100 ng/µl. After electrophoresis, the size marker and first sample (5 µl) lanes were cut off with a scalpel and stained with ethidium bromide solution. The position of the target band in the analytical lane was marked by excision under UV illumination. Next, the analytical lane was again aligned exactly to the preparative lane and the markings were used to cut out the invisible target band from the preparative lane. The piece of agarose gel containing the target band was weighed and the DNA was isolated using the Nucleospin Extract II kit according to the manufacturer's instructions.

4.2.10 Phenol-chloroform extraction of DNA with subsequent ethanol precipitation

First, the DNA solution was mixed vigorously with 1 volume phenol / chloroform / isoamyl alcohol (25: 24: 1, v/v/v), on a "Vortex" mixer and centrifuged (13,000 rpm, RT, 5 min) in a tabletop centrifuge. Then the upper, aqueous phase was transferred to a new reaction tube and mixed with 3 volumes of pure ethanol. The DNA was allowed to precipitate at -20°C for 2 h. After centrifugation (13,000 rpm, 4°C, 10 min), the pellet was washed with 80% ethanol, air-dried and dissolved in 44 µl ddH_2O.

4.2.11 Purification of plasmid DNA and PCR products

The NucleoSpin Extract II kit from Macherey-Nagel was used for the direct purification of plasmid DNA and PCR products. The samples were mixed with 2 volumes of buffer NT and transferred to a purification column with collection tube. After centrifugation (13,000 rpm, RT, 1 min), the flow-through was discarded and the column membrane was washed once with 600 µl of buffer NT3. After two centrifugation steps (13,000 rpm, RT, 1 min), the column was placed into a fresh microcentrifuge tube and 15-20 µl of elution buffer NE were added to the dry silica membrane. After 1 min incubation and subsequent

centrifugation (13,000 rpm, RT, 1 min), the concentration of the extracted DNA was measured photometrically.

4.2.12 Ligation of DNA fragments

For the ligation of PCR products and other DNA fragments, 25 ng of vector DNA and a 5-fold molecular excess of insert DNA was used. The amount of insert DNA was calculated using the equation:

Amount insert = 25 ng vector × length insert (bp) / length vector (bp).

The vector and insert DNA were supplemented with 1 µl 10-fold concentrated ligation buffer and 1 µl T4-ligase (5 U/µl). The reaction mixture was then filled up to a total volume of 10 µl with ddH_2O. The ligation reaction mixture was incubated overnight at 16°C. On the next day, the enzyme was inactivated by heating at 65°C for 10 min.

4.2.13 "Mini"-scale preparation of plasmid DNA

The Nucleospin Plasmid kit (Macherey & Nagel) was used for the small-scale isolation of plasmid DNA from bacteria. The manufacturer's instructions given in the protocol "Isolation of high-copy plasmid DNA from E. coli" were followed. In the evening, 5 ml LB cultures were inoculated each with a single *E.coli* colony using sterile pipet tips and incubated overnight at 37°C on a shaking platform. The next morning, the saturated cultures were centrifuged in a benchtop microcentrifuge at 11,000 x g for 30 s and the supernatant was discarded. The bacterial pellet was resuspended in 250 µl of buffer containing RNAse (buffer A1) on a Vortex mixer. The exact formulation of all buffers used for this procedure was not disclosed by the manufacturer. Next, 250 µl of lysis buffer (A2) was added and the bacterial suspension was mixed gently by inverting the tube five times. The mixture was incubated at RT for 5 min until the lysate appeared clear. The cell lysis was finished by adding 300 µl of neutralization buffer (buffer A3) and gentle mixing by inverting the tube five times. For the

clarification of the lysate, the mixture was centrifuged (11,000 x g, RT, 5 min). A Nucleospin plasmid column was placed in a collection tube and the supernatant of the clarification step (max. 750 µl) was pipetted onto the column. Next, the column was centrifuged at 11,000 x g for 1 min. Afterwards the column was washed with 500 µl pre-heated (50°C) buffer AW and 750 µl ethanolic wash buffer A4. For both washing steps the columns were centrifuged at 11,000 x g for 1 min. Following centrifugation, the column was placed back into the empty collection tube and centrifuged again at 11,000 x g for 1 min in order to dry the silica membrane. For the elution of DNA, the Nucleospin column was placed into a fresh 1.5 ml microcentrifuge tube and 50 µl of elution buffer AE were added. The column was incubated at RT for 1 min. Finally the microcentrifuge tube with the column was placed into the benchtop centrifuge and spun at 11,000 x g for 1 min. The DNA solution was stored at -20°C in a freezer.

4.2.14 "Maxi"-scale preparation of plasmid DNA

The Nucleobond Xtra Maxi kit (Macherey & Nagel) was used for the large-scale isolation of plasmid DNA from bacteria according to the manufacturer's instructions.

4.2.15 Measurement of nucleic acid concentration and purity

The concentration of DNA or RNA in solution was determined photometrically. For this, the absorbance (OD) was measured at the wavelength of 260 nm. An OD_{260} value of 1 corresponds to a concentration of 50 µg/ml for double-stranded DNA and of 40 µg/ml for RNA. The samples were diluted in such a way that the absorbance fell into the range from 0.1 to 1, assuring proportionality between nucleic acid concentration and absorbance. To estimate the purity of samples, the OD_{260}/OD_{280} ratio was calculated (Warburg and Christian, 1942). A protein-free DNA solution normally displays a ratio from 1.8 to 2.0.

4.2.16 Cloning of a wdr16 knockout targeting vector

4.2.16.1 Cloning of a loxP site in the vector pBS-loxP-neoTK-loxP

The plasmid pBs-loxP-neoTK-loxP was used for the construction of the wdr16 knockout targeting vector. This plasmid (a gift from Prof. R. Feil) contains a selection cassette with a neomycin resistance gene and the Herpes simplex virus thymidine kinase gene enclosed by two loxP sites.

First, an additional loxP site was inserted into the plasmid. This loxP site was manufactured by annealing two DNA oligonucleotides to the plasmid. They were designed to contain the recognition sequences for BamHI and NotI, respectively, and their nucleotide sequences were:

loxP_sticky_forw: 5'-TAAGTTGGGTAACGCCAGGGT-3'

loxP_sticky_rev: 5'-TTGGCTGGACGTAAACTCCTCTTC-3'

The oligonucleotides were synthesized commercially by Eurofins MWG and dissolved in water to give a concentration of 100 µM. Volumes of 5 µl of the solutions of each complementary oligonucleotide were mixed with 40 µl of annealing buffer (10 mM Tris, pH 7.5; 50 mM NaCl, 1 mM EDTA), respectively, in a 1.5 ml microfuge tube. The tube was placed in a standard heating block at 95°C for 1 min and was then allowed to cool to RT on the benchtop for approximately 1 h. The annealing of the oligonucleotides resulted in a loxP site with BamHI-compatible 5'-sticky ends and NotI compatible 3'-sticky ends. A mass of 5 µg of the vector pBsloxPneoTKloxP was digested overnight with 10 units of BamHI in the appropriate buffer. After thermal inactivation of the endonuclease by heating at 80°C for 20 min, the vector DNA was purified with the Nucleospin Extract II Kit according to the manufacturer's protocol for "PCR clean-up". The purified DNA was eluted in 50 µl of 5 mM Tris/HCl (pH 8.5). The vector was digested one more time with 10 units of NotI in 5 µl Fermentas buffer O overnight. Afterwards, the nuclease was heat-inactivated by incubation at 65°C for 20 min, and the vector DNA was purified using the Nucleospin Extract II Kit. Since the DNA piece that had been cut out from the vector was smaller than 50 bp, no gel extraction was necessary. The vector was not

dephosphorylated, because the annealed oligonucleotides had been synthesized without 5’ phosphate groups. The double-stranded loxP site with cohesive ends was joined to the vector using T4 DNA ligase. To this end, a mass of 50 ng of vector DNA, ca. 40 ng of double-stranded loxP insert, 2 µl of 10x T4 ligase buffer and 1 Weiss unit of T4 DNA ligase were mixed in a 1.5 ml reaction tube. The mixture was filled up to 20 µl with double-distilled water and the ligation was performed at 18°C overnight. Then the T4 ligase was inactivated by incubation at 65°C for 10 min. The entire inactivated ligation reaction mixture was used for the transformation of competent E.coli bacteria (NovaBlue, Novagen). One vial containing 50 µl of competent cells was thawed on ice and mixed gently. Then 2 µl of ligation reaction mixture was added and the content of the tube was gently mixed by flicking the test tube with the finger several times. The tube was subsequently incubated on ice for 5 min, heated for exactly 40 s in a water bath kept at 42 - 43°C and finally placed on ice for 2 min. Then, 250 µl of SOC (RT) were added. The mixture was shaken at 250 rpm and 37°C for 45 min in a rotary incubator prior to spreading it on carbenicillin-containing LB agar plates. The plates were incubated overnight and, on the next day, bacterial colonies were used for inoculation of individual 5 ml LB cultures containing carbenicillin antibiotic. The cultures were incubated at 37°C overnight and the plasmid DNA was isolated using the Nucleospin Plasmid Kit according to the manufacturer’s standard protocol. The plasmids were screened by restriction analysis with SacI and HindIII restriction enzymes, and the accuracy of the cloning was confirmed by DNA sequencing.

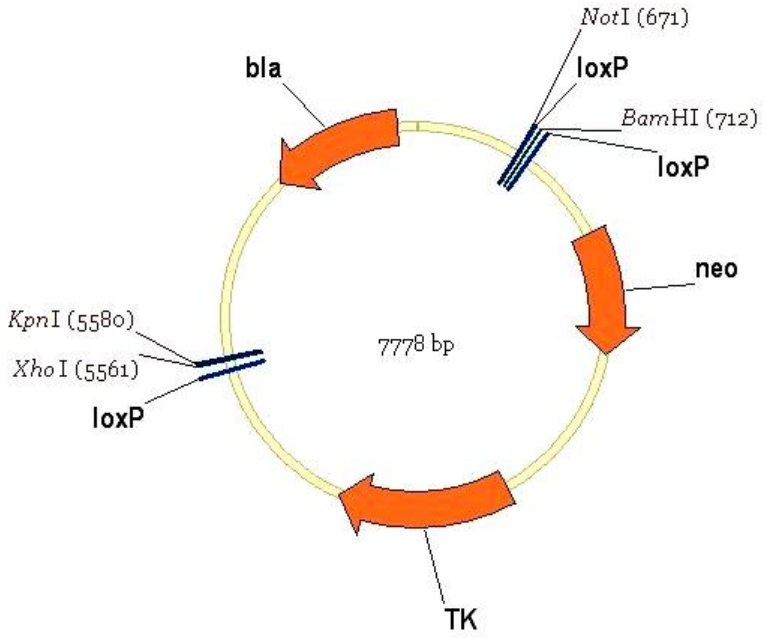

Fig. 32. Vector map of the plasmid pBS-loxP-loxP-neoTK-loxP. Abbreviations: beta-lactamase (bla): gene that confers resistance to beta-lactam antibiotics (e.g. penicillins). Neomycin phosphotransferace gene (neo): gene that codes for an enzyme which inactivates by phosphorylation a range of aminoglycoside antibiotics such as neomycin or geneticin (G418). LoxP: locus of X-over P1; 34 bp sequence on the bacteriophage P1 genome where the double-stranded DNA is cut by the Cre recombinase during Cre/loxP recombination. Herpes simplex virus thymidine kinase gene (TK): acts as a negative selection marker after addition of a nucleoside analog (ganciclovir) to the cell culture medium.

4.2.16.2 Cloning of the vector pBS-loxP-SA-loxP-neoTK-loxP

The “short arm” of the wdr16 knockout targeting construct flanked by two NotI restriction sites was amplified by PCR from C57BL/6 mouse embryonic stem cell DNA using Phusion Hot Start DNA polymerase and the following specific primers:

Shortarm_up: 5’-GCTTGCCTACAGCTGGATCAG-3’

Shortarm_dn: 5’-TCTTTGGGGTAATTTAGCTAC-3’

The PCR product was checked by agarose gel electrophoresis. The blunt-end PCR product was subcloned in the vector pCR-Blunt II-TOPO using the Zero Blunt TOPO^{TM} PCR Cloning Kit (Invitrogen) according to the manufacturer’s instructions. Five micrograms of the vector containing the 5’-end arm (shortarm)

was digested with 10 units of NotI restriction enzyme overnight. Next, the restriction enzyme was inactivated by heating at 65°C for 20 min. Subsequently, the DNA solution was loaded in two lanes of an agarose gel prepared with low melting-point agarose. After electrophoresis, the band corresponding to the "short arm" of the wdr16 knockout targeting vector was cut out from the gel with a scalpel, and the DNA was isolated using the QUIAEX^{TM} II gel extraction kit. Five micrograms of the vector pBS-loxP-loxP-neoTK-loxP (Fig. 32) was digested overnight with 10 units of NotI, the vector DNA was desphosphylated with 1 unit of calf intestine alkaline phosphatase (37°C, 30min) and then purified using the Nucleospin Extract II kit. Vector DNA and "short arm" insert were ligated using T4 DNA ligase. For this purpose, 50 ng vector DNA, 50 ng insert DNA, 2 µl of T4 DNA ligase buffer and 1 Weiss unit of T4 DNA ligase were mixed in a microfuge tube, and the reaction vessel was filled up to 20 µl with deionized water. The ligation was completed after incubation at exactly 18°C using a PCR thermocycler. The ligation reaction mixture was inactivated by heating at 65°C for 15 min, and 2 µl were used for the transformation of competent cells. The plates containing carbenicillin antibiotic were incubated overnight and, on the next day, bacterial colonies were used for inoculation of 5 ml aliquots of LB containing carbenicillin. The cultures were incubated at 37°C overnight, and the plasmid DNA was isolated using the Nucleospin Plasmid Kit according to the manufacturer's standard protocol. The plasmids were screened by restriction analysis and the identity of the desired product was confirmed by DNA sequencing.

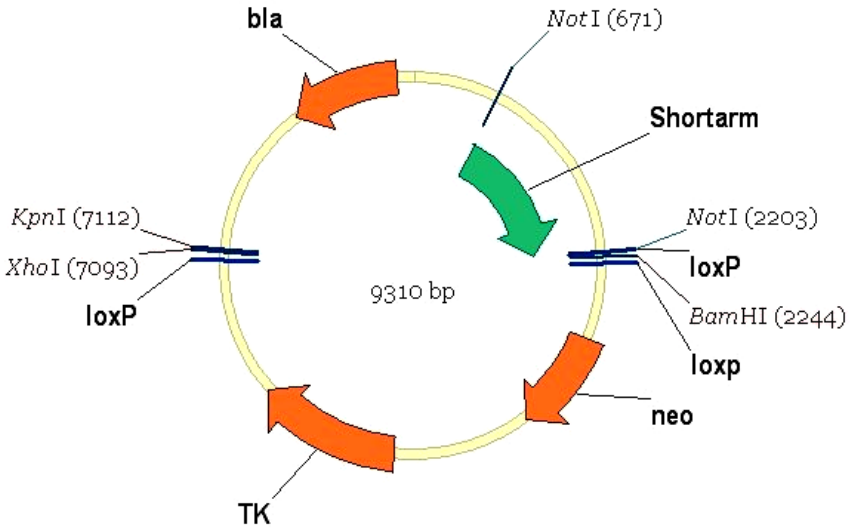

Fig. 33. Vector map of the plasmid pBS-loxP-SA-loxP-neoTK-loxP.

4.2.16.3 Cloning of the deletion cassette into the vector pBS-loxP-SA-loxP-neoTK-loxP

The “deletion cassette” with exons 2 and 3 of the wdr16 knockout targeting construct (Fig. 21) flanked by two BglII restriction sites was amplified by PCR from C57BL/6 mouse embryonic stem cell DNA using Phusion Hot Start DNA polymerase and specific primers. The cohesive ends of the BglII and BamHI restriction sites are compatible. BamHI was not used because the “deletion cassette” has a BamHI restriction site. The PCR primers employed were:

Deletion_cassette_up: 5’-CAGGCAATAAATACTAATGAC-3’

Deletion_cassette_dn: 5’-TCAGCTCCCTCTTCTTAACTG-3’

The blunt end PCR product was checked by agarose gel electrophoresis and cloned in the vector pCR-Blunt II-TOPO using the Zero Blunt TOPO^{TM} PCR Cloning Kit according to the manufacturer’s instructions. The vector pCR-BluntII-TOPO-Deletion_cassette (5 µg) was digested with 10 units of BglII restriction enzyme overnight. Afterwards, the DNA solution was loaded in two lanes of an agarose gel prepared with low melting-point agarose. The band corresponding to the “deletion cassette” of the wdr16 knockout targeting vector

was cut out with a scalpel, and the DNA was isolated using the QUIAEX^{TM} II gel extraction kit. Five micrograms of the vector pBS-loxP-SA-loxP-neoTK-loxP (Fig. 33) was digested overnight with 10 units of BamHI, the vector DNA was desphosphorylated with 1 unit of CIAP at 37°C for 30 min and then purified using the Nucleospin Extract II kit. Vector DNA and “deletion cassette” insert were ligated using T4 DNA ligase. For this purpose, 50 ng vector DNA, 41 ng insert DNA, 2 µl of T4 DNA ligase buffer and 1 Weiss unit of T4 DNA ligase were mixed in a microfuge tube, and the reaction mixture was filled up to 20 µl with deionized water. The ligation was completed after incubation in a thermocycler at 18°C for 12-24 h. The ligase was heat-inactivated at 65°C for 15 min, and 2 µl of the mixture were used for the transformation of competent cells. The plates containing carbenicillin antibiotic were incubated overnight, and, on the next day, bacterial colonies were used for inoculation of 5 ml LB containing carbenicillin. The cultures were incubated at 37°C overnight, and the plasmid DNA was extracted from the bacteria using the Nucleospin Plasmid Kit according to the manufacturer’s standard protocol. The plasmids were screened by restriction analysis and the accuracy of the cloning was confirmed by DNA sequencing (Fig. 34).

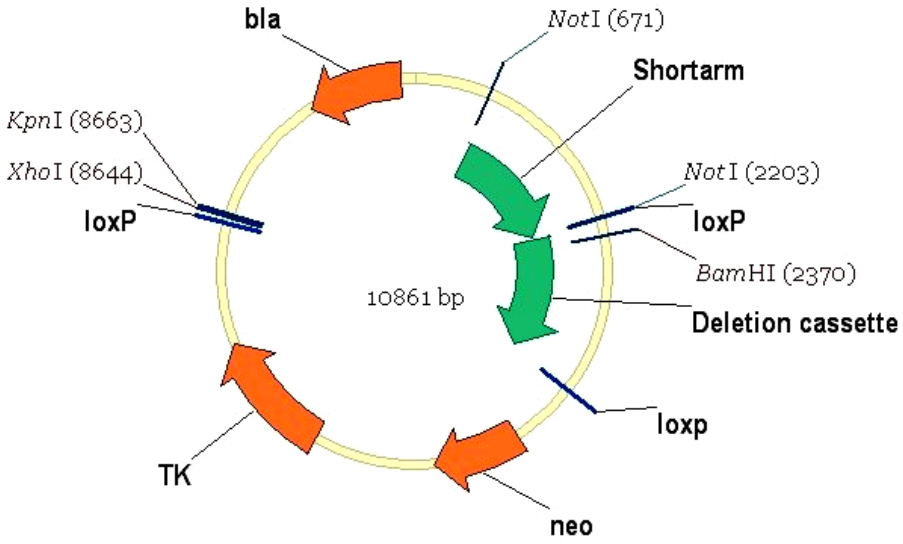

Fig. 34. Vector map of the plasmid pBS-loxP-SA-DC-loxP-neoTK-loxP.

4.2.16.4 Cloning of the the vector pBS-loxP-SA-DC-loxP-neoTK-loxP-LA

The “long arm” of the wdr16 knockout targeting construct, flanked by a 5’-prime XhoI and a 3’-prime KpnI restriction site, was amplified by PCR from C57BL/6 mouse embryonic stem cell DNA using Phusion Hot Start proofreading DNA polymerase and the following specific primers:

Long_arm_up: 5’-GTAATGTTTGACAGAGAGGAGCT-3’

Long_arm_dn: 5’-ATGCCAAGTTTGAGGCCAACT-3’

The blunt end “long arm” PCR product was checked by agarose gel electrophoresis and subcloned in the vector pCR-Blunt II-TOPO using the Zero Blunt TOPO^{TM} PCR Cloning Kit according to the manufacturer’s instructions. The vector pCR-BluntII-TOPO-Longarm (5 µg) was digested with 10 units of KpnI overnight. The enzyme was heat-inactivated at 80°C for 20 min. Thereafter, the DNA was purified using the Nucleospin Extract II kit according to the manufacturer’s instructions. The purified DNA was eluted in 50 µl of 5 mM Tris/HCl (pH 8.5). The vector was digested once more with 10 units of XhoI restriction enzyme overnight after addition of 5 µl of Fermentas buffer R to the tube. Afterwards, the DNA solution was loaded in two lanes of an agarose gel

prepared with low melting-point agarose. The band corresponding to the “long arm” of the wdr16 knockout targeting vector was cut out with a scalpel, and the DNA was isolated using the QUIAEX^{TM} II gel extraction kit. Five micrograms of the vector pBS-loxP-SA-DC-loxP-neoTK-loxP was digested with 10 units of Kpn1 overnight, and then purified with the Nucleospin Extract II kit after heat inactivation of the enzyme at 65°C at 20 min. The purified vector was digested overnight with 10 units of XhoI, 5’-desphosphylated with 1 unit of calf intestine alkaline phosphatase at 37°C for 30 min and then repurified using the Nucleospin Extract II kit. Vector DNA and “long arm” DNA fragment were ligated with T4 DNA ligase. For this purpose, 50 ng vector DNA, 180 ng insert DNA, 2 µl of T4 DNA ligase buffer and 1 Weiss unit of T4 DNA ligase were mixed in a microfuge tube, and the reaction mixture was filled up to 20 µl with deionized water. The ligation was completed after incubation at 18°C for 12-24 h. The ligase was inactivated by heating at 65°C for 15 min, and 2 µl of the reaction mixture were used for the transformation of competent *E.coli* cells. The bacteria were spread on agar plates containing carbenicillin antibiotic and incubated at 37°C overnight. On the next day, bacterial colonies from these plates were used for inoculation of 5 ml LB containing carbenicillin. The cultures were incubated at 37°C overnight, and the plasmid DNA was isolated using the Nucleospin Plasmid Kit according to the manufacturer’s standard protocol. The plasmids were screened by restriction analysis, and the accuracy of the cloning was confirmed by DNA sequencing.

4.2.17 Cultures of the human embryonic kidney cell line HEK293T

4.2.17.1 Recovery of cryopreserved cultures

HEK293T cells were obtained as a gift from Dr. Roland Vogel and supplied as a cryostock at passage 5. The culture was started by rapidly thawing the cryostock at 37°C in a pre-warmed water bath. After thawing, the cell suspension was transferred to an 80 cm^2 cell culture flask containing 25 ml of growth medium (DMEM, 10% FCS, 100 U penicillin, 100 µg streptomycin). Five

hours after seeding, when the cells were attached to the culture dish, the medium was aspirated, and fresh growth medium was added.

4.2.17.2 Maintenance and passaging of the HEK293T cells in culture

The HEK293T cells were cultured in cell culture dishes 10 cm in diameter. DMEM supplemented with 10% FCS, 100 U penicillin and 100 µg streptomycin was used as the growth medium. The cells were cultured at 37°C in an atmosphere of 90% air and 10% CO_2. When the cells became 90% confluent, the culture medium was removed and the cell monolayer was washed twice with 5 ml prewarmed DMEM without FCS or, alternatively, with autoclaved PBS. Afterwards, the washing solution was discarded and replaced by 1 ml of a 0.05% solution of trypsin in PBS. The culture dish was incubated in the cell incubator for ca. 5 min until most cells started to detach. The cells that were still attached to the culture dish were dislodged using a sterile plastic cell scraper. The detached cells were resuspended in 10 ml of growth medium in a fresh 15 ml conical tube. Subsequently, the cells were centrifuged (500 x g, 5 min, RT), the supernatant was discarded and the cell pellet was resuspended in 5 ml growth medium. To start a new passage, 1 ml of this cell suspension was added to a fresh culture dish 10 cm in diameter containing 9 ml of DMEM / 10% FCS.

4.2.17.3 Cryopreservation of HEK293T cells

For the cryopreservation of HEK293T cells, nearly confluent cultures in dishes 10 cm in diameter were trypsinised, the cells collected by centrifugation (see maintenance of HEK293T cells) and resuspended in 2 ml of freezing medium (90% DMEM / 10% FCS / 10% dimethyl sulfoxide). Aliquot parts of 1 ml of the cell suspension were transferred to cryovials and frozen at -80°C in an ultra-deep freezer over one hour. For long-term storage, the cryostocks were transferred to a cell bank and stored over liquid nitrogen.

4.2.18 Production of HIV-1-derived lentiviral vectors in HEK293T cells

Day 1: Seeding of cells

The day before calcium phosphate-mediated transfection, HEK293T cells were seeded into cell culture dishes of 10 cm in diameter at a density of 3 x 10^6 cells per plate.

Day 2: Transfection

The HEK293T cells were transfected by the calcium phosphate method (Jordan et al., 1996). Twenty micrograms of transfer vector (pWPXL (Fig.27) or pLVTHM (Fig.28) carrying the gene of interest or siRNA), 15 µg of packaging plasmid (psPAX2, Fig. 25) and 6 µg of envelope plasmid (pMD2.G, Fig.26) were mixed in a sterile Eppendorf tube. To this DNA solution, 50 µl of 2.5 M $CaCl_2$ solution was added. The solution was brought to a volume of 0.5 ml with autoclaved ddH_2O and mixed thoroughly. Double-concentrated HBS (0.5 ml; containing 1.5 mM Na_2HPO_4) was transferred to another Eppendorf tube, and the $CaCl_2$ / DNA mixture was added to HBS in the course of approximately 2 min to allow the formation of the calcium phosphate-DNA precipitate. Incubation at RT for 15 min was followed by dropwise addition of the precipitate to the cells under gentle shaking of the plate. The plate was placed in a cell incubator for 7 h, and then the cells were washed briefly with either DMEM or autoclaved PBS, before 6 ml of fresh MEMc supplemented with 25 mM glucose were added to the plate. The plate was further incubated at 37°C in a humidified atmosphere of 90% air and 10% CO_2.

Days 3, 4 and 5: Collection of virus

The virus-containing supernatant was harvested every 24 h for three consecutive days. The supernatant was transferred into a sterile conical tube, centrifuged (3,000 rpm, 5 min, RT), filtered through a 0.45 µm mesh filter and stored at 4°C. The virus-containing, filtered supernatants collected over all three days were pooled and stored frozen at -80°C until further use. Alternatively, the virus was concentrated by ultracentrifugation (see below).

4.2.19 Concentration of lentiviral particles by ultracentrifugation

The unconcentrated, filtered virus supernatant was transferred into sterile Beckman centrifuge tubes (25 mm x 89 mm) and centrifuged (100,000 g, 2 h, 4°C) in an ultracentrifuge (Beckman-Coulter, Optima L-80) using the Type 70 Ti rotor. After the centrifugation, the supernatant was discarded and the virus pellet was resuspended in 1 ml of MEM_C or sterile PBS. Aliquots of 50 µl were prepared and stored frozen at -80°C.

4.2.20 Ependymal primary cultures

The EPC were prepared from brains of newborn Wistar rats according to the method of Weibel et al. (1986) as modified by Prothmann et al. (2001).

Media and solutions:

Puck's D1 solution: 137 mM NaCl, 5.4 mM KCl, 0.22 mM KH_2PO_4, 0.17 mM Na_2HPO_4; pH 7.4

Puck's D1 / Gluc / Suc solution:
5 mM D-glucose, 58.4 mM sucrose, in Puck`s D1 solution

MEM_{Wash} :
9.65 g MEM powder and 2.2 g $NaHCO_3$, dissolved in 1 l ddH_2O. The medium was gassed with CO_2 until the colour became orange.

MEM_C :
MEM_{wash} medium supplemented with 0.5 g/l BSA, 5 mg/l insulin, 10 mg/l transferrin

MEM_{CT} : MEM_C supplemented with 500 U/l thrombin

Table 1. Media formulation of MEM (Invitrogen, Karlsruhe; Eagle, 1959)

Components	Concentration	
	mg/L	mM
L-Arginine Hydrochloride	126.64	0.6
L-Cystine 2HCl	31	0.099
L-Glutamine	292	2
L-Histidine Hydrochloride-H_2O	42	0.2
L-Isoleucine	52	0.397
L-Leucine	52	0.397
L-Lysine Hydrochloride	72.5	0.396
L-Methionine	15	0.101
L-Phenylalanine	32	0.194
L-Threonine	48	0.403
L-Tryptophan	10	0.049
L-Tyrosine Disodium Salt	52	0.231
L-Valine	46	0.393
Choline Chloride	1	0.00714
D-Calcium Pantothenate	1	0.0021
Folic Acid	1	0.00227
Niacinamide	1	0.0082
Pyridoxal Hydrochloride	1	0.0049
Riboflavin	0.1	0.000266
Thiamine Hydrochloride	1	0.00297
i-Inositol	2	0.0111
Calcium Chloride ($CaCl_2$) (anhyd.)	200	1.8
Magnesium Sulfate ($MgSO_4$) (anhyd.)	97.67	0.814
Potassium Chloride (KCl)	400	5.33
Sodium Chloride (NaCl)	6,800	117.24
Sodium Phosphate Monobasic (NaH_2PO4-H_2O)	140	1.01
D-Glucose (Dextrose)	1,000	5.56
Phenol Red	10	0.0266

Coating of culture dishes with fibronectin

Fibronectin was isolated according to Prothmann et al. (2001). Cell culture dishes 35 mm in diameter (with or without round 18 mm coverslips) were incubated at 37°C with 1 ml of sterile-filtered fibronectin solution (> 200 µg/ml)

each for at least 3 h. Subsequently, the fibronectin solution was collected, and each culture dish was washed with 2 ml MEM_{wash}. The coated culture dishes were stored in the cell incubator at 37°C until the cells were seeded (2 h at most).

Preparation of rodent brains

Newborn rats or mice were decapitated with a pair of scissors. The brains were squeezed through the foramen magnum by application of pressure to the skull roof and transferred to a sterile Petri dish containing 10 ml ice-cold Puck's saline D1 solution (with glucose and sucrose; see above)

Dissociation of brains

Nylon gauze bags (approx. 2 cm wide) were made from nylon cloth (132 µm and 210 µm mesh size) with a welding apparatus. The nylon bags were autoclaved before they were used in the preparation of the cultures. The brains were packed into a 210 µm mesh size nylon gauze bag and dissociated by massaging them through the mesh with sterile bent forceps. The suspension was collected in a Petri dish filled with 10 ml ice cold Puck's saline D1 solution (with glucose and sucrose), where it was triturated to apparent homogeneity with a 10 ml glass pipette. Removal of the remaining large aggregates was further achieved by passing the cell suspension through a 132 µm mesh size gauze bag, and the cell suspension was collected in a 50 ml plastic tube. After 5 min of centrifugation in a Heraeus/Christ Varifuge K at 1500 rpm and 4°C, the supernatant was sucked off, and the pellet was resuspended in 10 ml of MEM_c. The suspension was passed through a 132 µm mesh size gauze bag into an appropriate volume of MEM_C to yield the seeding suspension. For each dissociated brain, 30 ml of MEM_C were used as culture medium as described in Weibel et al. (1986).

Seeding of dissociated brain cells

MEM_{wash} was removed from fibronectin-coated dishes and replaced by either 2 ml of cell suspension when dishes in 35 mm diameter were used, or by 0.5 ml of cell suspension for each well of a 24-well plate. Seeded cells were cultivated at 37°C in an atmosphere of 95% air and 5% CO_2. After 2 days, MEM_c was

replaced by MEM_{ct} (containing thrombin). The culture medium was renewed every 2 days. The state of the cultures was regularly monitored under a phase contrast microscope.

4.2.21 Immunostaining of cultured cells

For immunostaining of both EPCs and cell lines, the cells were grown on coverslips. After removal of the culture medium, the cells were first washed with pre-warmed PBS and afterwards fixed with 4% (w/v) PFA in PBS at RT for 15 min. The remaining PFA was inactivated by washing with 0.1% (w/v) glycine in PBS for 5 min. The coverslips were then washed again three times with PBS. Next, the cells were permeabilized with 1 % (w/v) Triton X-100 in PBS for 5 min and washed again three times with PBS. The first antibody was diluted in PBS (see Table 2 for dilutions) and incubated at RT in a humid chamber for 45 min. The coverslips were then washed five times with PBS. The commercially acquired secondary antibody was diluted 1:1,000 in PBS. The incubation time at RT was 30 min. Thereafter the coverslips were washed five times with PBS. Finally, the nuclei of the cells were stained with DAPI solution (10 µg/ml) in PBS for 5 min. Then the coverslips were mounted cells down on microscope slides using “Immu-Mount” mounting medium.

Table 2. Antibody dilutions for immunostainings of cells and tissues
mAB, monoclonal antibody

Antibody against	type	Species antibody was derived from	First antibody, dilution	Secondary antibody, dilution
Wdr16	serum	guinea pig	1:1,800	1:300
Ak7	serum	rabbit	1:200	1:500
GP-BB	serum	rabbit	1:200	1:500
Ezrin	mAb	rabbit	1:50	1:500
α-Tubulin	mAb	mouse	1:100	1:500
Acetylated α-tubulin	mAb	mouse	1:1,000	1:1,000
γ-Tubulin	mAb	mouse	1:2,000	1:300
AFP	mAb	mouse	1:100	1:300

4.2.22 Immunostaining of rat brain cryosections

Blocking solution: 2.5% (w/v) BSA, 0.1% (w/v) Triton X-100 in PBS

The area of interest on each slide was circled with a hydrophobic pen and the cryosections were incubated with blocking solution at RT for 1h. The first antibody was diluted in blocking solution (see Table 2) and incubated with the tissue in a humid atmosphere for 2 h. The cryosections were then washed five times with 0.1% (w/v) Triton X-100 in PBS. Afterwards, the secondary antibody, diluted in blocking solution, was added. Incubation time at RT was 1 h. Subsequently, the slides were washed five times with 0.1% (w/v) Triton X-

100/PBS, and the cellular nuclei were stained with DAPI solution (10 µg/ml) in PBS for 5 min. The slides were mounted using “Immu-Mount” mounting medium and stored at -20°C.

4.2.23 Computational deconvolution analysis in fluorescent microscope images

Computational deconvolution analysis was used for the reduction of out-of-focus fluorescence in fluorescent microspcope images. Deconvolution can improve the localization of proteins in specimens that are thicker than the focal plane without applying confocal microscopy. The deconvolution analysis was conducted using the Axiovision software (Carl Zeiss AG, Germany). Instead of only one single picture, the software automatically aquires a z-stack of images with a defined spacing. The distance used for all deconvoluted micrographs in this doctoral thesis was 0.5 µm.

4.2.24 Injection of anti-wdr16 lentivirus into the rat brain ventricles

Ten microliters suspension of anti-wdr16 virus, control-siRNA virus or vehicle were injected into both lateral ventricles of Sprague-Dawley rats. The stereotactically placed microinjections were performed by Ferdinand Kluge, a member of the Section of Neuropharmacology of the University of Tübingen (research group Prof. W. Schmidt) according to their standard procedures. Both concentrated and unconcentrated virus preparations (in MEM_c) were used. After 6 weeks, the rats were anaesthetized using sodium pentobarbital (50 mg/kg) and the still alive rats were perfused with 4% paraformaldehyde solution according to standard procedures. The brains were removed from the dead rats, treated with highly concentrated sucrose solution for cryoprotection and frozen thin sections (10 - 15 µm) were produced using a Leica cryostat.

4.2.25 Cloning of the vector pWPXL-wdr16p-MCS-Flag

A multiple cloning site (MCS) and DNA coding for a Flag tag were inserted into the transfer plasmid pWPXL. First, two DNA primers called MCSFlag_sticky_forw and MCSFlag_sticky_rev were annealed.

MCSFlag_sticky_forw: 5'- ACGCGTTCGGCTTCAACCGCA-3'

MCSFlag_sticky_rev: 5'-CGATTGCACAATGCGATCA-3'

The oligodeoxynucleotides were dissolved at the same molar concentration (100 µM). Five microliters of each complementary oligonucleotide was mixed with 40 µl of annealing buffer (10 mM Tris, pH 7.5; 50 mM NaCl, 1 mM EDTA) in a 1.5 ml microfuge tube. The tube was placed in a water bath at 95°C for 1 min and was then allowed to cool to RT on the work bench for ca. 1 h. A multiple cloning site containing DNA coding for a Flag tag with a MluI-compatible sticky 5'- and a SpeI-compatible 3'-end resulted from the annealed deoxynucleotides. The vector pWPXL-wdr16p-EGFP (5 µg) was digested overnight with 10 units of MluI in buffer R (Fermentas). After thermal inactivation of the enzyme at 65°C for 20 min, the vector DNA was purified with the Nucleospin Extract II Kit according to the manufacturer's protocol for "PCR clean-up". First, the binding conditions were adjusted by mixing the DNA solution with two volumes of buffer NTI. A PCR clean-up column was placed in a 2 ml collection tube and the sample was loaded on the column. After centrifugation (30 s / 11,000 g), the flow-through was discarded and 700 µl of ethanolic buffer NT3 was loaded on the column for the subsequent washing step. Following centrifugation (30 s / 11,000 g), the column was dried by centrifugation (30 s / 11,000 g) and 50 µl of elution buffer (5 mM Tris/HCl, pH 8.5) was loaded on the column. After incubation for 1 min, the column was centrifuged (30 s / 11,000 g) and the eluate was collected in a fresh microcentrifuge tube. The vector was digested once more overnight, this time with 10 units of SpeI. Afterwards, the DNA solution was loaded into two lanes of an agarose gel prepared with low melting-point agarose. The band corresponding to the pWPXL vector backbone was cut out with a scalpel, and the DNA was isolated using the QUIAEX^{TM} II gel extraction kit. The double-stranded MCS-Flag oligonucleotide with cohesive ends was joined to the vector using T4 DNA ligase. Fifty nanograms of vector

DNA, ca. 40 ng of insert, 2 µl of 10x T4 ligase buffer and 1 Weiss unit of T4 DNA ligase were mixed in a microfuge tube. The mixture was filled up to 20 µl with deionized water before the ligation took place at 18°C overnight. The T4 ligase was heat-inactivated at 65°C for 10 min. The unpurified and inactivated mixture was used for the transformation of competent E.coli bacteria (Novagen). One vial containing 50 µl of competent cells was thawed on ice and mixed gently. Two milliliters of ligation reaction mixture were added and stirred gently to mix. The tube was incubated on ice for 5 min. The tube was heated in a water bath to 43 °C for 40 s and afterwards placed on ice for 2 min. Thereafter, 250 µl of SOC (RT) was added. The mixture was incubated at 37°C in a rotary shaker set to 250 rpm for 45 min and then plated on carbenicillin-containing LB agar plates. The plates were incubated at 37°C overnight, and, on the next day, bacterial colonies were used for the inoculation of individual 5 ml LB portions containing carbenicillin antibiotic at a final concentration of 100 mg/ml. The cultures were incubated overnight at 37°C, and the plasmid DNA was isolated using the Nucleospin Plasmid Kit (Macherey & Nagel) according to the manufacturer's standard protocol. The plasmids were screened by restriction endonuclease double digestion with MluI and SpeI in two-fold concentrated Tango^{TM} buffer.

4.2.26 Cloning of the plasmid pWPXL-wdr16p-Wdr16-Flag

The wdr16 cDNA flanked by SpII and RsrII restriction sites was amplified from the plasmid pFastbac-HTB-wdr16 obtained from Prof. Robert Feil using the primers Wdr16_forw and Wdr16_rev.

Wdr16_forw: 5'-ACTAGTATTGCATTCATAGAT-3'

Wdr16_rev: 5'- GAATCGATACATGGCCAGGC -3'

The PCR was performed using Phusion polymerase according to the manufacturer's instructions. The PCR product was then purified using the Nucleospin Extract II kit according to the manufacturer's instructions. Afterwards, 5 µg of the purified PCR product was digested with 10 units of SpII in the appropriate buffer. Following thermal inactivation of the enzyme, the PCR

product was again purified using the Nucleospin Extract II kit. The PCR product was now digested with 10 units of RsrII. After the second digestion, RsrII was heat inactivated at 65°C for 20 min and the PCR product purified again using the Nucleospin Extract II kit. The vector pWPXL-wdr16p-Wdr16-EGFP was also subjected to sequential digestion with SpII and RsrII. After the second digestion and heat-inactivation of the endonucleases, the plasmid DNA was dephosphorylated with CIAP. CIAP was subsequently also inactivated by heating at 85°C for 15 min and the DNA solution was subjected to preparative agarose gel electrophoresis. The band corresponding to the linearized pWPXL vector backbone still containing the wdr16 promoter was cut out and the DNA isolated from the agarose gel using the Nucleospin Extract II kit according to the manufacturer's instructions. Next, 25 ng of the vector DNA was ligated with a 5-fold molecular excess of the PCR product insert at the SpII and RsrII sites by T4 ligase in the respective buffer. The ligation mixture was incubated in a PCR machine at 16°C overnight. After heat-inactivation of the ligase, 2 µl of the reaction mixture was used to transform competent bacteria in a volume of 50 µl by heat shock treatment. The bacteria were spread on carbenicillin-containing agar plates and incubated at 37°C overnight.

4.2.27 Transfection of HEK293T and HeLa cells

Cell lines were transfected using the jetPEI^{TM} polyethylenimine-based transfection reagent. For each well of a 6-well-plate, 3 µg of plasmid DNA was added to 100 µl of 150 mM NaCl solution. The solution was mixed gently and spun down briefly. Six microliters of jetPEI were then diluted to 100 µl by the addition of 150 mM NaCl solution. Afterwards, the jetPEI solution was added to the DNA solution all at once. Next, the solutions were immediately mixed by using a Vortex mixer and the mixture was spun down briefly to collect all liquid at the bottom of the tube. The DNA/jetPEI mixture was then incubated at RT for 15 to 30 min. Following incubation, the 200 µl of jetPEI/DNA mixture were added drop-wise to the serum-containing medium in each well, and the mixture was made homogeneous by gentle swirling. After a normal transfection period

of 48 h, the transgene expression was assessed by Western blotting or fluorescence microscopy.

4.2.28 Generation of a HEK293T cell line stably expressing Wdr16-Flag

HEK293T cells (approximately 1 x10^5 cells) were seeded in a cell culture dish (35 mm in diameter). One day later, the cell culture medium was replaced with a mixture of 1 ml viral supernatant (HIV/VSV-G/ EF1p-Wdr16-Flag) and 1 ml of fresh growth medium. Two days post infection, the cells were trypsinized and diluted to a final concentration of approximately five cells per ml. Afterwards, 200 µl aliquots of the cell suspension were distributed over a 96-well plate. After 1 day, the 96-well plate was observed using a phase contrast microscope and 10 wells containing only one single attached cell were labeled using a marker pen. After 5 days, the labeled wells were trypsinized again and one half of the cell suspension of each cell clone was distributed to one well of a fresh cell culture dish and a cell culture plate containing a coverslip at the bottom. After 3 days, the coverslips were analysed for the expression of Flag-tagged Wdr16 by immunostaining and fluorescence microscopy. The cells of the HEK293T clones expressing Wdr16-Flag were further propagated and the cell culture dishes containing non-expressing cells were discarded.

4.2.29 Immunoprecipitation of Wdr16

Five dishes (100 mm in diameter) with 80-90 % confluent HEK293T cells (Graham et al., 1977) or HEK293T cells expressing Wdr16-Flag were washed twice with 5 ml pre-warmed (37°C) PBS. Afterwards, the cells were collected in 2-5 ml ice-cold PBS with a cell scraper and spun down in a 15 ml conical tube (4°C, 2,200 rpm, 5 min). After centrifugation, the cell pellet was resuspended in 5 ml of fresh ice-cold PBS before the suspension was re-centrifuged. The supernatant was discarded and the cells were stored in a -80°C freezer until usage. Shortly before starting the experiment, the pellets were thawed on ice. The cells were resuspended in 1 ml (RT) lysis buffer with protease inhibitors

(0.1 mM aprotinin, 0.1 mM AEBSF and 1 µg/ml pepstatin). Lysates of EPC were prepared in exactly the same manner, except that 20 dishes (35 mm in diameter) were used on DIV 12, and 0.5 ml of lysis buffer was used. Subsequently, the cell lysates were centrifuged at 13,000 g (4°C) for 15 min, and the supernatant was transferred into fresh pre-chilled 1.5 ml reaction tubes. The protein concentration (Bradford, 1976; BSA as the standard) of the lysates of the normal HEK293T cells and the HEK293T cells expressing Flag-Wdr16 was approximately 13-15 µg/µl. The protein concentration of the EPC lysate was 9-11 µg/µl. The lysates were immediately used for the IP of Wdr16, rather than frozen or stored for longer periods of time. The IP was performed using a mixed lysate of HEK293T cells expressing Flag-Wdr16 and EPC and simultaneously using a mixed lysate of normal HEK293T and EPC (negative control). For both, EPC cell lysate containing a total amount of 4.5 mg protein was added to the respective HEK293T cell lysate containing 4.5 mg of protein, and the volume was adjusted to 1 ml with cold lysis buffer. Finally, sodium azide at a final concentration of 0.02 % (w/v) was added to each sample (1 ml total volume) to prevent microbial growth before the reaction tubes were closed. The samples were mixed by an over-head shaker in the coldroom (4°C) overnight. From now on all steps were performed in the coldroom at 4°C and with a pre-chilled centrifuge rotor. For each sample 30 µl of M2 Flag agarose slurry was used. The agarose was washed three times with 0.5 ml lysis buffer and then centrifuged at 8,000 x g for 1 min. The supernatant was removed and, afterwards, the lysates were added to the washed agarose and the microfuge tubes were placed in an over-head shaker at ca. 10 rpm overnight. On the next day, after centrifugation at 8,000 x g for 1 min, the agarose beads were washed three times with 0.6 ml lysis buffer. The washing buffer was discarded afterwards. For the evaluation of the results, the agarose beads were resuspended in 5-fold concentrated Laemmli sample buffer [300 mM Tris-HCl pH 6.8, 10% (w/v) SDS, 50% (v/v) glycerol, 25% (w/v) mercaptoethanol, 0.05% (w/v) bromophenol blue]. Finally, the samples were applied to a SDS-PAGE gel, transferred to a nitrocellulose membrane and then subjected to immunoblotting in comparison to Wdr16 and other proteins of interest.

4.2.30 Protein assay

Protein was assayed according to Bradford (1976) using the Bio-Rad dye reagent. The reagent was diluted in water (1 in 6) and mixed with 10 µl of the sample (prediluted in ddH_2O, if necessary) to yield a final volume of 1 ml, and incubated at RT for 15 min. Afterwards, 300 µl of the reaction mixture were transferred to a well of a 96-well plate and the absorbance was measured at a wavelength of 595 nm in a microplate reader. The protein concentrations were calculated from a standard curve prepared by using BSA as a standard.

4.2.31 Discontinuous SDS-PAGE

SDS-PAGE was carried out as described by Laemmli (1970), with the modifications by Garfin (1990).

Solutions:

Rotiphorese Gel 30 [(29.2% (w/v) acrylamide, 0.8% (w/v) bisacrylamide)]

10% (w/v) SDS solution

10% (w/v) APS solution

Tetramethylethylenediamine (TEMED)

1.5 M Tris/HCl, pH 8.8 (running gel buffer)

1.5 M Tris/HCl, pH 6.8 (stacking gel buffer)

25 mM Tris, 192 mM glycine, 0.1% (w/v) SDS (electrode buffer)

0.16 M Tris/HCl, 4% (w/v) SDS, 20% (w/v) glycerol, 0.38 M mercaptoethanol, 0.008% (w/v) bromophenol blue; pH 6.8 (5x sample buffer)

The gel size was 8 cm x 10 cm x 1 mm. The gels were prepared from ingredients according to Table 3.

Table 3. Preparation of polyacrylamide gels for SDS-PAGE

Concentrations of acrylamide:	**8%**	**10%**	**12%**	**5%**
	separation gel			**stacking gel**
1. H_2O [ml]	4.6	4.0	3.3	3.4
2.Rotiphorese Gel 30 [ml]	2.7	3.3	4.0	0.83
3. 1.5 M Tris [ml]	2.5 pH 8.8	2.5 pH 8.8	2.5 pH 8.8	0.63 pH 6.8
4. 10% SDS [ml]	0.1	0.1	0.1	0.05
5. 10% APS [ml]	0.1	0.1	0.1	0.05
6. TEMED [µl]	6	4	4	5

The protein samples were mixed with 5-fold concentrated SDS-PAGE sample buffer and the reaction volume was brought to 20 µl with dd$H_2$0 to yield a final concentration of 1-fold sample buffer. The samples were then heated to 95°C for 3 min. After a brief centrifugation, the supernatants of the samples were applied to the gel. Electrophoresis was carried out under constant current (20 mA per gel) in a Mini-PROTEAN Tetra Cell (Bio-Rad) system for vertical gel electrophoresis. When the bromophenol blue front had reached the end of the

running gel, the electrophoresis was stopped. The gels were either stained with Coomassie Brilliant Blue R 250 or used for Western blotting.

4.2.32 Western blotting with chemiluminescence detection

The proteins were separated by discontinuous SDS-PAGE. The protein bands were transferred from the gel to a nitrocellulose membrane using the Transblot SD Semi-Dry Electrophoretic Transfer Cell (Biorad). First, a sheet of extra thick filter paper soaked in transfer buffer was placed onto the platinum anode. Next, the pre-wetted nitrocellulose membrane was placed on top of the filter paper. A pipet was rolled over the surface of the membrane to expel all air bubbles. Afterwards, the gel was equilibrated with transfer buffer (48 mM Tris, 39 mM glycine, 20% methanol; pH 9.2) and was then placed on top and in the center of the transfer membrane. Finally another sheet of pre-soaked filter paper was put on top of the gel. After closing the transfer unit, the power supply was turned on. The proteins were transferred at 15 - 25 V for 30 - 60 min. For the detection of the bands, the membrane was incubated (1 h) with blocking solution (20 mM Tris-HCl, 150 mM NaCl, 0.02% (v/v) Tween 20; pH 7.4; see Table 4 for the amount of milk powder added) at RT in order to block unspecific protein binding sites. The membrane was then washed 3 times with washing buffer (20 mM Tris-HCl, 150 mM NaCl, 0.02% (v/v) Tween 20; pH 7.4). The first antibody was diluted in washing buffer according to Table 4. The membrane was incubated at 4°C with the solution of the first antibody overnight. The membrane was washed three times for 5 min with washing buffer, before the solution of the secondary antibody was applied. Different secondary antibodies conjugated to peroxidase were used and diluted in washing buffer 1:50,000. The incubation time was 1 h. The membrane was washed again three times for 5 min in washing buffer and rinsed briefly with PBS, before the ECL detection solution (proprietary luminol and peroxide solutions, ThermoScientific) was added dropwise to the membrane. After 1 min, the solution was removed and the membrane wrapped in transparent plastic foil. An X-ray film was exposed to this arrangement in an exposure cassette for 5 to 30 min. The film was developed in an X-ray film developing machine.

Table 4. Antibody dilutions for Western blotting

Antibody against	Type	Species antibody was derived from	Dilution of first antibody	Addition of milk powder
Wdr16	serum	guinea pig	1:10,000	none
Ak7	serum	rabbit	1:5,000	2% (w/v)
GP-BB	serum	rabbit	1:10,000	none
Ezrin	mAb	rabbit	1:10,000	2% (w/v)
α-Tubulin	mAb	mouse	1:10,000	none
β-Actin	mAb	mouse	1:5,000	none
γ-Tubulin	mAb	mouse	1:10,000	none
TCP1α	mAb	rat	1:5,000	5% (w/v)

4.2.33 Coomassie Blue staining of polyacrylamide gels

Solutions:

Staining solution: 50% methanol, 40% H_2O, 10% glacial acetic acid, 1% (w/v) Coomassie Brilliant Blue R 250 (in water)

Destaining solution: Methanol: H_2O: glacial acetic acid (3: 6: 1)

Polyacrylamide gels were incubated with staining solution at RT for 30 min. Thereafter, the gels were briefly rinsed with water and transferred to the destaining solution on a shaking platform. When the blue background had disappeared and single protein bands had become visible, the destaining

solution was discarded and the gel was washed with ddH2O. Protein bands were documented with a digital camera.

4.2.34 Cloning of the wdr16 cDNA into the vector pFastbac-HTB

The donor plasmid pFastbac-HTB has an N-terminal 6xHis affinity-tag and its length is 4856 bp. Behind the affinity tag, the plasmid features a spacer region with 21 bp and a Tev protease cleavage site.

The full-length cDNA of rat wdr16 flanked by restriction sites for BamHI and SalI was amplified by PCR from the plasmid pWPXL-N-TAP-wdr16 using Phusion Hot Start DNA polymerase and the specific primers

Forw_FastbacHTB: 5‘-TACCGTACGATGGAAGAACAAATTTTACCC-3‘

Rev_FastbacHTB: 5‘-CGGCGGACCGGGAGCAAATGGGTATTTCCA-3‘.

The blunt-end PCR product was digested in BamHI buffer from Fermentas with 10 units BamHI at 37°C overnight. The next day, the BamHI restriction enzyme was heat-inactivated at 80°C for 20 min, and the PCR product was purified with the Nucleospin Extract II kit according to the manufacturer’s protocol for “PCR clean-up”. Afterwards, the PCR product was digested in Fermentas buffer O with 10 units of SalI restriction enzyme. After heat-inactivation of the SalI restriction enzyme at 65°C for 20 min, the PCR product was purified again with the Nucleospin Extract II kit. Then it was used for ligation. The vector pFastbac-HTB (Invitrogen) was digested with BamHI and SalI just like the wdr16 PCR product, except that, before the final purification, the vector was desphosphorylated by incubation with 1 unit of CIAP in CIAP-buffer from Fermentas at 37°C for 30 min. Vector DNA and the wdr16 PCR product were ligated in the appropriate T4 ligation buffer from Fermentas using T4 DNA ligase. In a microfuge tube, 50 ng vector DNA, 80 ng insert DNA, 2 µl of T4 DNA ligase buffer and 1 Weiss unit of T4 DNA ligase were mixed, and the reaction was filled up to 20 µl with deionized water. The ligation reaction mixture was incubated in a PCR machine at 18°C overnight. The ligase enzyme was heat-inactivated (65°C, 15 min), and 2 µl of the solution were used for the

transformation of competent cells. The plates containing carbenicillin antibiotic were incubated overnight and, on the next day, bacterial colonies were used for inoculation of small LB cultures (5 ml each, with carbenicillin). The cultures were incubated at 37°C overnight, and the plasmid DNA was isolated using the Nucleospin plasmid kit (Macherey & Nagel) according to the manufacturer's standard protocol. The plasmids were screened by restriction analysis and the accuracy of the cloning was confirmed by DNA sequencing.

4.2.35 Cloning of the wdr16 cDNA into the vector pFastbac-M30b

The vector pFastbac-M30 was digested consecutively with restriction enzymes BamHI and SalI in twofold concentrated Tango^{TM} buffer, dephosphorylated with CIAP in CIAP buffer from Fermentas and purified using the Nucleospin Extract II kit according to the manufacturer's instructions. To obtain a full-length rat wdr16 cDNA insert, the vector pFastbac-HTB-wdr16 was digested consecutively with BamHI and SalI. After thermal inactivation of the nucleases (65°C, 20 min), the DNA solution was mixed with 10 µl DNA loading dye, and loaded on two lanes of an agarose gel prepared with low melting-point agarose. After the gel run, the band corresponding to the wdr16 cDNA was cut out with a scalpel, and the DNA was isolated using the QUIAEX^{TM} II gel extraction kit. Vector DNA and the wdr16 insert were ligated using T4 DNA ligase. In a microfuge tube, 50 ng vector DNA, 80 ng insert DNA, 2 µl of T4 DNA ligase buffer and 1 Weiss unit of T4 DNA ligase were mixed and the reaction mixture was filled up to 20 µl with deionized water. The ligation was complete after overnight incubation at 18°C. The enzyme was heat inactivated at 65°C for 15 min, and 2 µl of the reaction mixture were used for the transformation of competent cells. The agar plates, containing carbenicillin antibiotic and the spread transformation mixture, were incubated overnight and, on the next day, bacterial colonies were used for inoculation of small LB medium cultures (5 ml each, with carbenicillin antibiotic). The cultures were incubated at 37°C overnight, and the plasmid DNA was isolated using the Nucleospin plasmid kit (Macherey & Nagel) according to the manufacturer's standard protocol. The

plasmids were screened for correctness by restriction analysis and the DNA of positive clones was stored at –20°C.

4.2.36 Cloning of the wdr16 cDNA into the vector pFastbac-M12b

The vector pFastbac-M30 was digested consecutively with BamHI and SalI restriction enzymes in twofold concentrated Fermentas buffer for double digestion (Tango^{TM} buffer), dephosphorylated with CIAP in CIAP buffer from Fermentas and isolated using the Nucleospin Extract II kit according to the manufacturer's instructions. To obtain a full-length rat wdr16 cDNA insert, the vector pFastbac-HTB-wdr16 was digested consecutively with BamHI and SalI. After thermal inactivation of the enzymes at 65°C for 20 min, the DNA solution was mixed with 10 µl DNA loading dye and loaded into two large wells of an agarose gel prepared with low melting-point agarose (2 x 30 µl). After the gel run, the band corresponding to the wdr16 cDNA was cut out with a scalpel, and the DNA was isolated using the QUIAEX^{TM} II gel extraction kit. Vector DNA and the wdr16 insert were ligated using T4 DNA ligase. In a microfuge tube, 50 ng vector DNA, 80 ng insert DNA, 2 µl of T4 DNA ligase buffer and 1 Weiss unit of T4 DNA ligase were mixed, and the reaction mixture was filled up to 20 µl with deionized water. The ligation was complete after incubation at 18°C overnight. The ligase enzyme was inactivated by heating at 65°C for 15 min. Subsequently, 2 µl of the reaction mixture were used for the transformation of competent cells. The agar plates, containing carbenicillin antibiotic and the spread cells, were incubated overnight and, on the next day, bacterial colonies were used for inoculation of 5 ml LB containing carbenicillin. The cultures were grown at 37°C overnight, and the plasmid DNA was isolated using the Nucleospin plasmid kit (Macherey & Nagel) according to the manufacturer's standard protocol. The plasmids were screened for correctness by restriction analysis and stored at –20°C.

4.2.37 Preparation of electro-competent DH10Bac cells

A single bacterial colony of DH10Bac™ cells was placed in a polypropylene tube containing 5 ml of LB without antibiotics. The culture was incubated overnight on a shaking platform with 250 rpm at 37°C. On the next day, the bacterial culture was stored in the refrigerator at 4°C. In the evening, 50 ml of LB without antibiotics were inoculated with 0.5 ml of the first bacterial culture. The second 50 ml culture was then incubated overnight on a rotary shaker at 180 rpm and 37°C. On the next day, each of 4 batches of 500 ml LB without antibiotics was inoculated with 10 ml of the second bacterial culture. The cultures were incubated on a rotary shaker platform at 180 rpm and 37°C until the cultures reached an OD_{650} of 0.5 – 0.7. The cells were then harvested by centrifugation (5,000 g, 10 min, 4°C, Beckman centrifuge J2-HS; Rotor: JA-10). Afterwards, the individual cell pellets were washed twice with 1 l ice-cold autoclaved water purified by means of a Millipore filtration unit in a multi-step process: pretreatment with bacteriostatic activated carbon, reverse osmosis, electro-deionization and UV irradiation and (3 times) with ice-cold 10% aqueous glycerol. The bacteria were finally resuspended in 4 ml 10% (v/v) glycerol/water, aliquoted (100 µl portions) and shock-frozen in liquid N_2. The cells were stored at -80°C.

4.2.38 Electroporation of DH10Bac™ cells and transposition

LB agar plates were prepared with the following antibiotics and supplements: 50 µg/ml kanamycin, 7 µg/ml gentamicin, 10 µg/ml tetracycline, 100 µg/ml X-gal and 40 µg/ml IPTG. The suspension of electrocompetent DH10Bac™ cells (100 µl) was thawed on ice and the suspension was dispensed into 5 ml round-bottom polypropylene tubes. Electrocompetent cells can be transformed using electroporation. In this process of electroporation electrical field pulses create pores which allow genetic material to permeate the bacterial membrane. About 10 nanograms of recombinant plasmid (in 5 µl), e.g. pFastbac-HTB-wdr16, were added to the tube and the content was gently mixed. The electroporation cuvette (BioRad; 0.2 cm electrode distance) and the polypropylene tube were incubated on ice for 5 min. The DNA/bacteria-mixture was then transferred to

the electroporation cuvette. The bacteria were electroporated at 2.5 kV, 25 µF capacity and 200 Ω using a Gene Pulser Xcell device (Bio-Rad). Immediately after electroporation, 0.9 ml SOC without antibiotics was added to the cells, and the cells were transferred to a sterile 15 ml tube. For 4 h the mixture was placed in a shaking incubator at 37°C with rotary agitation (225 rpm). Of the bacterial suspension, 1 ml was divided equally and spread on ten agar plates. The agar plates were then incubated at 37°C for 48 h.

4.2.39 Isolation of recombinant "bacmid" DNA and PCR screening

The white colonies containing the recombinant "bacmid" were selected for the isolation of "bacmid" DNA. A "bacmid" is a shuttle vector that can be propagated in both bacteria and insect cells. The bacterial colonies were restreaked on fresh agar plates containing kanamycin, gentamycin, tetracycline, X-gal and IPTG in order to verify the phenotype. A single colony confirmed as having a "white" phenotype was used to inoculate a liquid culture containing the above-mentioned antibiotics but no IPTG or x-gal. The "bacmid" DNA was isolated from the bacterial pellet (see chapter 4.2.13) using the PC 100 kit and AX 100 columns (Macherey & Nagel) according to the manufacturer's instructions for plasmid MIDI preparation, except that 12 ml instead of 4 ml of the three buffers were used for alkaline lysis.

4.2.40 Culture of the Spodoptera frugiperda insect cell line Sf9

The Sf9 cells were cultured in complete Grace medium (Table 5) supplemented with lactalbumin hydrolysate, autolyzed yeast extract (liquid yeastolate ultrafiltrate; Invitrogen), 100 U penicillin, 100 µg streptomycin and 10% FCS. To reduce shear forces, 0.1 % Pluronic F-68 detergent was added to the suspension cultures. The cells were cultured at 27°C without CO_2. The pH was in the range of 6.1 – 6.4 (at RT) and the osmolarity was approx. 350 mOsmol/kg. The Sf9 cells were cultivated in sterile cell culture flasks (25 cm^2 - 175 cm^2; Corning or Greiner Bio One) or Erlenmeyer flasks of different sizes for

the suspension cultures. All cell culture work was performed under a laminar flow hood.

Table 5. Media formulation of Grace's insect medium (Invitrogen, Karlsruhe; Grace, 1962; Xu et al., 2006; Walther et al., 2005).

Components	**Concentration**	
	mg/L	**mM**
Glycine	650	8.67
L-Alanine	225	2.53
L-Arginine Hydrochloride	700	3.32
L-Asparagine	350	2.65
L-Aspartic Acid	350	2.63
L-Cystine	22	0.0917
L-Glutamic Acid	600	4.08
L-Glutamine	600	4.11
L-Histidine	2500	16.13
L-Isoleucine	50	0.382
L-Leucine	75	0.573
L-Lysine Hydrochloride	625	3.42
L-Phenylalanine	150	0.909
L-Proline	350	3.04
L-Serine	550	5.24
L-Threonine	175	1.47
L-Tryptophan	100	0.49
L-Tyrosine	50	0.276
L-Valine	100	0.855
beta-Alanine	200	2.25
Biotin	0.01	0.000041
Choline Chloride	0.2	0.00143
D-Calcium Pantothenate	0.02	0.0000419
Folic Acid	0.02	0.0000454
Nicotinic Acid (Niacin)	0.02	0.000163
Para-Aminobenzoic Acid	0.02	0.000146
Pyridoxine Hydrochloride	0.02	0.0000971
Riboflavin	0.02	0.0000532
Thiamine Hydrochloride	0.02	0.0000593
i-Inositol	0.02	0.000111
Calcium Chloride (CaCl2) (anhyd.)	750	6.76
Magnesium Chloride (MgCl2-6H2O)	2,280	11.23

Magnesium Sulfate (MgSO4-7H2O)	2,780	11.3
Potassium Chloride (KCl)	4,100	54.67
Sodium Bicarbonate (NaHCO3)	350	4.17
Sodium Phosphate Monobasic	1,013	7.34
Alpha-Ketoglutaric Acid	370	2.53
D-Fructose	400	2.22
D-Glucose (Dextrose)	700	3.89
Fumaric Acid	55	0.474
Malic Acid	670	5
Succinic Acid	60	0.508
Sucrose	26,680	78.01

4.2.41 Thawing of Sf9 cells

A cryostock with 1 x 10^6 or 2 x 10^7 was removed from the cell bank and thawed in a water bath at 37°C. The exterior of the cryovial was wiped or sprayed with 70 % ethanol. The content (1 - 2 ml) of the cryostock was transferred to a sterile 50 ml tube containing ca. 20 ml complete Grace medium (RT) using adjustable pipettes with sterile plastic tips and centrifuged at 500 g for 5 min. Afterwards, the cell pellet was resuspended in fresh Grace medium. The cells were either diluted to 0.5 x 10^6 cells /ml for suspension culture or seeded in cell culture flasks (1 x 10^6 in a 80 cm^2 flask, 5x 10^6 in a 175 cm^2 flask) for monolayer culture.

4.2.42 Monolayer culture of Sf9 cells

The medium containing floating or dead cells of a monolayer culture was aspirated and discarded. Each 75 cm^2 flask was supplied with 12 ml of complete Grace medium. The cells were detached from the cell culture surface by pipetting the medium directly onto the monolayer or by beating against the sides of flask. No enzymatic dissociation of cells is necessary. Adequate cell detachment was verified by observing the monolayer under an inverse microscope. For counting of viable cells, 45 µl of the cell suspension was mixed with 5 µl trypan blue. An aliquot of this mixture was transferred to a Neubauer

cell counting chamber and the viable non-blue cells were counted under the inverted phase contrast microscope. The remainder of the cell suspension was used to inoculate fresh monolayer cultures. The cultures were incubated at 28°C with loose caps to allow gas exchange. On day 4 post-seeding, or when the cultures were 90% confluent, the spent medium was aspirated and discarded and the monolayer was subcultured again as described above.

4.2.43 Suspension culture of Sf9 cells

Some insect cells are not matrix-dependent and can be cultured in suspension. This facilitates the culture of large amounts of cells for the expression of recombinant proteins. Certain insect cell lines may require adaptation to suspension culture by serially passaging (10-20 times) them in suspension culture until they reach high cell densities (> 10^7 cells/ml). However, the cells used for the present study had already been subjected to this procedure. The cells were diluted to 0.5 x 10^6 cells/ml in complete Grace medium containing 0.1% Pluronic-F68. The cell suspension was added to a sterile 75 cm^2 cell culture flask with vented cap and placed on an orbital shaker at 100 rpm and 28°C. The culture was incubated until it reached a density of 2-3 x 10^6 cells/ml (mid-log phase). To subculture the shaker culture, the cells were diluted again to 0.5 x 10^6 cells/ml. Once every three weeks, the suspension culture was gently centrifuged at 100 x g for 5 min, the supernatant was discarded, and the pellet resuspended in fresh medium.

4.2.44 Cryopreservation of Sf9 insect cell cultures

The desired quantity of cells in suspension was grown in suspension culture. The cells were harvested in the exponential (mid-log) growth phase and the number of viable cells and the required volume of cryopreservation medium determined using a Neubauer cell counting chamber. The final cell density was set to be 1 -2 x 10^7 cells / ml. The cryopreservation medium consisted of 92.5% of fresh complete Grace medium/7.5% dimethyl sulfoxide, pre-chilled to 4°C

until use. The cells were centrifuged down (100 x g, RT, 5 min) and resuspended with the calculated amount of chilled cryopreservation medium. Aliquots of cell suspension were dispensed into cryovials and exposed to a temperature of -20°C for 30 – 60 min, followed by exposure to -80°C for 1 h. Afterwards, the cryovials were stored in a cell bank over liquid nitrogen.

4.2.45 Transfection of Sf9 cells with recombinant "bacmid" DNA

Baculoviruses have a double-stranded circular DNA genome. This facilitates the production of recombinant baculoviruses by transfection of insect cell cultures. Two wells of a 6-well plate were seeded with 9x 10^5 of Sf9 cells in 2 ml of complete Grace medium without FCS. The cells were incubated at 27°C for at least one hour to allow sufficient attachment of the cells to the surface of the culture vessel. Ten microliters of "bacmid" solution and 10 µl of autoclaved, double-distilled water (negative control) were added to 100 µl of complete Grace medium (Walther et al., 2005; Xu et al., 2006) without FCS and antibiotics. Six microliters of lipofectamine transfection reagent (Invitrogen) were mixed with 100 µl of complete Grace medium without antibiotics and FCS. The "bacmid" and lipofectamine solutions were mixed and incubated at RT for 45 min. The medium was aspirated from the two wells, and the cells were washed once with complete Grace medium without antibiotics and FCS. Eight hundred microliters of Grace medium without antibiotics and FCS were mixed with the transfection samples. The medium was aspirated from the wells and the 1 ml transfection sample added to the cells. The cells were incubated at 27°C for 5 h. Afterwards the cells were washed with complete Grace medium and 2 ml of cell suspension were added to the wells. The 6-well plate was incubated at 27°C for 5 - 7 d without CO_2 until the virus infection was visible (lack of growth, disintegration and increased diameter of cells) except in the wells "transfected" with autoclaved water (negative control). The baculovirus containing supernatant was transferred to a fresh 15 ml conical tube. Dead cells and cellular debris were separated from the virus preparation by centrifugation (500 x g, RT, 5 min) and the virus preparation (P1) was stored at 4°C in the dark.

4.2.46 Amplification of the baculovirus

The virus preparation P1 was used to inoculate uninfected Sf9 cells at a multiplicity of infection below 0.1 pfu/cell. All virus preparations P1 (His-Wdr16, GST-Wdr16 and His-Wdr16-GST had a titer of ca. 1 x 10^6 pfu/ml. Ca. 2 x 10^7 Sf9 cells were seeded in a 175 cm^2 flask. The cells were incubated for ca. 1 h. When the cells had become attached the culture was inoculated with 100 µl of P1 virus preparation. The cells were incubated up to 7 d until almost all insect cells showed the characteristic signs of baculoviral infection and had become detached from the bottom of the cell culture flask. The resulting viral preparations A1 had virus titers of ca. 3-5 x 10^7 pfu/ml.

4.2.47 Baculoviral infection of Sf9 suspension cultures

A suspension culture of Sf9 cells (300 ml, 2 x 10^6 cells/ml) was inoculated with ca. 30 ml of viral preparation A1 (multiplicity of infection of ca. 2 pfu/cell). The culture was incubated without agitation at 27°C for 30 min. Afterwards the culture was placed on an orbital shaker at 27°C and 100 rpm for 48 h. Subsequently, the cells were harvested by centrifugation (1,000 x g, RT, 5 min). The supernatant was discarded since infection of cultures with MOI > 1 leads to the accumulation of non-infectious, defective virus.

4.2.48 Purification of GST-tagged Wdr16 protein

Preparation of infected insect cells:

Two days post infection (48 h p.i.), the suspension culture of Sf9 cells (300 ml) was transferred from the Erlenmeyer flask to 6 Falcon tubes (50 ml each) and then harvested by centrifugation at 2,500 rpm for 5 min (RT). The cells were washed twice with cold PBS and the pellet was stored at -80°C until use. The cells were resuspended in 2-5 ml of ice cold PBS with protease inhibitors (0.1 mM aprotinin, 0.1 mM AEBSF and 1 µg/ml pepstatin). After sonification the cell

lysate was cleared by centrifugation (10,000 x g, 4°C, 20 min). The cleared cell lysate was transferred to a new pre-chilled 15 ml conical tube.

Preparation of matrix:

The bottle with the glutathione-Sepharose 4B was mixed gently to resuspend the matrix. With a pipet 266 µl of the resuspended 75% slurry was transferred to a fresh Eppendorf tube resulting in a bed volume of 200 µl. One milliliter of bed volume will bind approximately 5 mg of glutathione-S-transferase. The matrix was sedimented by centrifugation at 500 x g for 5 min and the supernatant was carefully removed to avoid the loss of glutathione-Sepharose. The matrix was washed twice with 2-10 ml of cold PBS. Afterwards, it was resuspended in 200 µl of cold PBS which resulted in a 50% slurry.

Batch purification of GST-tagged Wdr16

The cell lysate containing the GST-Wdr16 protein was transferred to the pre-chilled (4°C) 15 ml Falcon polypropylene tube containing the glutathione-Sepharose 4B and the reaction vessel was closed. The mixture was incubated overnight with gentle agitation. Prior to this, sodium azide was added at a final concentration of 0.01% (w/v) to prevent the growth of microorganisms. On the next day, the suspension was centrifuged at 500 x g for 5 min to sediment the matrix. The matrix was washed three times with ice-cold PBS. To the sedimented matrix 100 µl of elution buffer (PBS or 50 mM Tris/HCl, pH 8.0) with 20 mM reduced glutathione was added. After short mixing, the suspension was incubated at RT for 10 min. Afterwards, the suspension was centrifuged again at 500 x g for 5 min and the supernatant containing the Wdr16 protein was saved in a fresh centrifuge tube.

5 References

Alaiwi W.A., Lo S.T., Nauli S.M. (2009) Primary cilia: highly sophisticated biological sensors. *Sensors* **9**, 7003-7020.

Assies J., Schellekens A.P., Touber J.L. (1978) Protein hormones in CSF: evidence for retrograde transport of prolactin from the pituitary to the brain in man. *Clin Endocrinol (Oxf)* **6**, 487-491.

Badano J.L., Mitsuma N., Beales P.L., Katsanis N. (2006) The ciliopathies: an emerging class of human genetic disorders. *Annu Rev Genomics Hum Genet* ***7***, 125-148.

Banizs B., Pike M.M., Millican C.L., Ferguson W.B., Komlosi P., Sheetz J., Bell P.D., Schwiebert E.M., Yoder B.K. (2005) Dysfunctional cilia lead to altered ependyma and choroid plexus function, and result in the formation of hydrocephalus. *Development* **123**, 5329-5339.

Bernstein E., Caudy A.A., Hammond S.M., Hannon G.J. (2001) Role for a bidentate ribonuclease in the initiation step of RNA interference. *Nature* **409**, 363–366.

Berryman M., Franck Z., Bretscher A. (1993) Ezrin is concentrated in the apical microvilli of a wide variety of epithelial cells whereas moesin is found primarily in endothelial cells. *J Cell Sci* **105**, 1025-1043.

Bornhorst J.A., Falke J.J. (2000) Purification of proteins using polyhistidine affinity tags. *Methods Enzymol* **326**, 245-254.

Bowman A.B., Goldstein L.S.B. (2001) Dynein and Kinesin. In: Encyclopedia of Life Science. *John Wiley & Sons (Hoboken, USA)*

Bradford M.M. (1976) A rapid and sensitive method for the quantitation of microgram quantities of protein utilizing the principle of protein-dye binding. *Anal Biochem* **72**, 248-254.

Brizzard B.L., Chubet R.G., Vizard D.L. (1994) Immunoaffinity purification of FLAG epitope-tagged bacterial alkaline phosphatase using a novel monoclonal antibody and peptide elution. *Biotechniques* **16**, 730-735.

Bronson R.T., Lane P.W. (1990) Hydrocephalus with hop gait (hyh): a new mutation on chromosome 7 in the mouse. *Brain Res Dev Brain Res* **54**, 131-136.

Buchschacher G.L. (2003) Lentiviral vector systems for gene transfer. *Kluywer Academic / Plenum Publishers (New York, USA).*

Cao X., Ding X., Guo Z., Zhou R., Wang F., Long F., Wu F., Bi F., Wang Q., Fan D., Forte J.G., Teng M., Yao X. (2005) PALS1 specifies the localization of ezrin to the apical membrane of gastric parietal cells. *J Biol Chem* **280**, 13584-13592.

Carlén M., Meletis K., Göritz C., Darsalia V., Evergren E., Tanigaki K., Amendola M., Barnabé-Heider F., Yeung M.S., Naldini L., Honjo T., Kokaia Z., Shupliakov O., Cassidy R.M., Lindvall O., Frisén J. (2009) Forebrain ependymal cells are Notch-dependent and generate neuroblasts and astrocytes after stroke. *Nat Neurosci* **12**, 259-267.

Chae T. H., Kim S., Marz K. E., Hanson P. I., Walsh C. A. (2004) The hyh mutation uncovers roles for alpha-Snap in apical protein localization and control of neural cell fate. *Nat Genet* **36**, 264-270.

Chermann J.C., Barré-Sinoussi F. (1987) Role of the human immunodeficiency virus in the physiopathology of AIDS. *Antibiot Chemother* **38**, 13-20.

Copreni E., Penzo M., Carrabino S., Conese M. (2004) Lentivirus-mediated gene transfer to the respiratory epithelium: a promising approach to gene therapy of cystic fibrosis. *Gene Ther* **11**, 67-75.

Cordingley M.G., Callahan P.L., Sardana V.V., Garsky V.M., Colonno R.J. (1990) Substrate requirements of human rhinovirus 3C protease for peptide cleavage in vitro. *J Biol Chem* **265**, 9062-9065.

Darling A.J., Boose J.A., Spaltro J. (1998) Virus assay methods: accuracy and validation. *Biologicals* **26**, 105-110.

Davson H., Welch K., Segal M.B. (1987) The physiology and pathophysiology of the cerebrospinal fluid. *Churchill Livingston (Edinburgh, UK).*

Devroe E., Silver P.A. (2004) Therapeutic potential of retroviral RNAi vectors. *Expert Opin Biol Ther* **4**, 319-327.

Dolcetta D., Perani L., Givogri M., Galbiati F., Amadio S., Del Carro U., Finocchiaro G., Fanzani A., Marchesini S., Naldini L., Roncarolo M.G., Bongarzone E. (2006) Design and optimization of lentiviral vectors for transfer of GALC expression in Twitcher brain*. J Gene Med* **8**, 962-971.

Eagle H. (1959) Amino acid metabolism in mammalian cell cultures. *Science* **130**, 3373-3432.

Elbashir S.M., Harborth J., Lendeckel W., Yalcin A., Weber K., Tuschl T. (2001) Duplexes of 21-nucleotide RNAs mediate RNA interference in cultured mammalian cells. *Nature* **411** (6836), 494-498.

Fändrich M., Dobson C.M. (2002) The behaviour of polyamino acids reveals an inverse side chain effect in amyloid structure formation. *EMBO J* **21**, 5682-5690.

Fernandez-Gonzalez A., Kourembanas S., Wyatt T.A., Mitsialis S.A. (2009) Mutation of murine adenylate kinase 7 underlies a primary ciliary dyskinesia phenotype. *Am J Respir Cell Mol Biol* **40**, 305-313.

Fire A., Xu S., Montgomery M.K., Kostas S.A., Driver S.E., Mello C.C. (1998) Potent and specific genetic interference by double-stranded RNA in Caenorhabditis elegans. *Nature* **391** (6669), 806-811.

Fishman M.A. (1992) Brain biopsy in herpes simplex encephalitis. *Acta Paediatr Jpn* **34**, 344-349.

Flament-Durand J., Brion J.P. (1985) Tanycytes: morphology and functions: a review. *Int Rev Cytol* **96**, 121-155.

Fleming D.O., Hunt D.L. (2000) Biological safety: principles and practices. *ASM Press (Washington, USA).*

Friesen W.J., Wyce A., Paushkin S., Abel L., Rappsilber J., Mann M., Dreyfuss G. (2002) A novel WD repeat protein component of the methylosome binds Sm proteins. *J Biol Chem* **277**, 8243-8247.

Frka K., Facchinello N., Del Vecchio C., Carpi A., Curtarello M., Venerando R., Angelin A., Parolin C., Bernardi P., Bonaldo P., Volpin D., Braghetta P., Bressan G.M. (2009) Lentiviral-mediated RNAi in vivo silencing of Col6a1, a gene with complex tissue specific expression pattern. *J Biotechnol* **141**, 8-17.

Garfin D.E. (1990) Isoelectric focusing. *Methods Enzymol* **182**, 459-477.

Goldman M. J., Lee P.S., Yang J.S. and Wilson J.M. (1997) Lentiviral vectors for gene therapy of cystic fibrosis. *Hum Gene Ther* **8**, 2261-2268.

Gómez-Puertas P., Martín-Benito J., Carrascosa J. L., Willison K.R., Valpuesta J.M. (2004) The substrate recognition mechanisms in chaperonins. *J Mol Recognit* **17**, 85-94.

Grace T.D. (1962) Establishment of four strains of cells from insect tissues grown in vitro. *Nature* **195**, 788-789.

Graham F.L., Smiley J., Russell W.C., Nairn R. (1977) Characteristics of a human cell line transformed by DNA from human adenovirus type 5. J Gen Virol **36**, 59-74.

Guirao B., Meunier A., Mortaud S., Aguilar A., Corsi J. M., Strehl L., Hirota Y., Desoeuvre A., Boutin C., Han Y. G., Mirzadeh Z., Cremer H., Montcouquiol M., Sawamoto K., Spassky N. (2010) Coupling between hydrodynamic forces and planar cell polarity orients mammalian motile cilia. *Nat Cell Biol* **12**, 341-350.

Hagen G.A., Elliott W.J. (1973) Transport of thyroid hormones in serum and cerebrospinal fluid. *J Clin Endocrinol Metab.* **37**, 415-422.

Haley B., Zamore P.D. (2004) Kinetic analysis of the RNAi enzyme complex. *Nat Struct Mol Biol* **11**, 599-606.

Hammond S.M., Bernstein E., Beach D., Hannon G.J. (2000) An RNA-directed nuclease mediates post-transcriptional gene silencing in Drosophila cells. *Nature* **404**, 293–296.

Hirschner W., Pogoda H.M., Kramer C., Thiess U., Hamprecht B., Wiesmüller K.H., Lautner M., Verleysdonk S. (2007) Biosynthesis of Wdr16, a marker protein for kinocilia-bearing cells, starts at the time of kinocilia formation in rat, and wdr16 gene knockdown causes hydrocephalus in zebrafish. *J Neurochem* **101**, 274-288.

Hodges M.E., Scheumann N., Wickstead B., Langdale J.A., Gull K. (2010) Reconstructing the evolutionary history of the centriole from protein components. *J Cell Sci* **123**, 1407-1413.

Ibañez-Tallon I., Pagenstecher A., Fliegauf M., Olbrich H., Kispert A., Ketelsen U.P., North A., Heintz N., Omran H. (2004) . Dysfunction of axonemal dynein heavy chain Mdnah5 inhibits ependymal flow and reveals a novel mechanism for hydrocephalus formation. *Hum Mol Genet* **13**, 2133-2141.

Inceoglu A.B., Kamita S.G., Hammock B.D. (2006) Genetically modified baculoviruses: a historical overview and future outlook. *Adv Virus Res* **68**, 323-360.

Jackson A.L., Linsley P.S. (2004) Noise amidst the silence: off-target effects of siRNAs? *Trends Genet* **20**, 521-524.

Jeng R. and Stearns T. (1999) Gamma-tubulin complexes: size does matter. *Trends Cell Biol* **9**, 339-342.

Johansson C.B., Momma S., Clarke D.L., Risling M., Lendahl U, Frisen J. (1999) Identification of a neural stem cell in the adult mammalian central nervous system. *Cell* **96**, 25-34.

Jones C., Roper V. C., Foucher I., Qian D., Banizs B., Petit C., Yoder B. K., Chen P. (2008) Ciliary proteins link basal body polarization to planar cell polarity regulation. *Nat Genet* **40**, 69-77.

Jordan M., Schallhorn A., Wurm F.M. (1996) Transfecting mammalian cells: optimization of critical parameters affecting calcium-phosphate precipitate formation. *Nucleic Acids Res* **24**, 596-601.

Keller L.C., Romijn E.P., Zamora I., Yates J.R. 3rd, Marshall W.F. (2005) Proteomic analysis of isolated chlamydomonas centrioles reveals orthologs of ciliary-disease genes. *Curr Biol* **15**, 1090-1098.

Keller L.C., Geimer S., Romijn E., Yates J.R. 3rd, Zamora I., Marshall W.F. (2009) Molecular architecture of the centriole proteome: the conserved WD40 domain protein POC1 is required for centriole duplication and length control. *Mol Biol Cell* **20**, 1150-1166.

Kile B.T., Panopoulos A.D., Stirzaker R.A., Hacking D.F., Tahtamouni L.H., Willson T.A., Mielke L.A., Henley K.J., Zhang J.G., Wicks I.P., Stevenson W.S., Nurden P., Watowich S.S., Justice M.J. (2007) Mutations in the cofilin partner Aip1/Wdr1 cause autoinflammatory disease and macrothrombocytopenia. *Blood* **110**, 2371-2380.

Kim J.C., Badano J.L., Sibold S., Esmail M.A., Hill J., Hoskins B.E., Leitch C.C., Venner K., Ansley S.J., Ross A.J., Leroux M.R., Katsanis N., Beales P.L. (2004) The Bardet-Biedl protein BBS4 targets cargo to the pericentriolar region and is required for microtubule anchoring and cell cycle progression. *Nat Genet* **36**, 462-470.

Kohn M.I., Tanna N.K., Herman G.T., Resnick S.M., Mozley P.D., Gur R.E., Alavi A., Zimmerman R.A., Gur R.C. (1991) Analysis of brain and cerebrospinal fluid volumes with MR imaging. Part I. Methods, reliability, and validation. *Radiology* **178**, 115-122

Kost T.A., Condreay J.P., Jarvis D.L. (2005) Baculovirus as versatile vectors for protein expression in insect and mammalian cells. *Nat Biotechnol* **23**, 567-575.

Kowtharapu B.S., Vincent F.C., Bubis A., Verleysdonk S. (2009) Lentiviral transfection of ependymal primary cultures facilitates the characterization of kinocilia-specific promoters. *Neurochem Res* **34**, 1380-1392.

Kubo A., Yuba-Kubo A., Tsukita S., Tsukita S., Amagai M. (2008) Sentan: a novel specific component of the apical structure of vertebrate motile cilia. *Mol Biol Cell* **19**, 5338-5346.

Laemmli U.K. (1970) Cleavage of structural proteins during the assembly of the head of the bacteriophage T4. *Nature* **227**, 680-685.

Letunic I., Doerks T., Bork P. (2009) SMART 6: recent updates and new developments. *Nucl Acids Res* **37**, D229-D232.

Li D., Roberts R. (2001) WD-repeat proteins: structure characteristics, biological function, and their involvement in human diseases. *Cell Mol Life Sci* **58**, 2085-2097.

Li X., Kong H., Wu W., Xiao M., Sun X., Hu G. (2009) Aquaporin-4 maintains ependymal integrity in adult mice. *Neuroscience* **162**, 67-77.

Lodish H., Berk A., Zipursky S.L., Matsudaira P., Baltimore D., Darnell J. (2000) Molecular Cell Biology. 4th edition. *W. H. Freeman (New York, USA)*.

Luckow V.A., Summers M.D. (1988) Signals important for high-level expression of foreign genes in Autographa californica nuclear polyhedrosis virus expression vectors. *Virology* **167**, 56-71.

Luckow V.A., Lee S.C., Barry G.F., Olins P.O. (1993) Efficient generation of infectious recombinant baculoviruses by site-specific transposon-mediated insertion of foreign genes into a baculovirus genome propagated in Escherichia coli. *J Virol* **67**, 4566-4579.

Ma L., Asher S. (2010) Resonance Raman study of the pH dependence of poly-L-lysine conformations. XXII International Conference on Raman spectroscopy. *AIP Conference Proceedings* **1267**, 617-618.

Maiti M., Lee H.C., Liu Y. (2007) QIP, a putative exonuclease, interacts with the Neurospora Argonaute protein and facilitates conversion of duplex siRNA into single strands. *Genes Dev* **21**, 590-600.

Matranga C., Tomari Y., Shin C., Bartel D.P., and Zamore, P.D. (2005) Passenger-strand cleavage facilitates assembly of siRNA into Ago2-containing RNAi enzyme complexes. *Cell* **123**, 607–620.

Mayer M. P., Bukau B. (2005) Hsp70 chaperones: cellular functions and molecular mechanism. *Cell Mol Life Sci* **62**, 670-684.

Milara J., Armengot M., Mata M., Morcillo E.J., Cortijo J. (2010) Role of adenylate kinase type 7 expression on cilia motility: possible link in primary ciliary dyskinesia. *Am J Rhinol Allergy* **24**, 181-185.

Miller L. (1997) The baculoviruses. *Plenum Press (New York, USA)*.

Mitchell D.R. (2006) The evolution of eukaryotic cilia and flagella as motile and sensory organelles. *Adv Exp Med Biol* **607**, 130-140.

Nachury M.V., Loktev A.V., Zhang Q., Westlake C. J., Peränen J., Merdes A., Slusarski D. C., Scheller R. H., Bazan J. F., Sheffield V. C., Jackson P. K. (2007) A core complex of BBS proteins cooperates with the GTPase Rab8 to promote ciliary membrane biogenesis. *Cell* **129**, 1201-1213.

Narayan O., Clements J.E. (1989) Biology and pathogenesis of lentiviruses. *J Gen Virol* **70** , 1617-1639.

Nicholson C. (1999) Signals that go with the flow. *Trends Neurosci* **22**, 143-145.

Nilsson C., Lindvall-Axelsson M., Owman C. (1992) Neuroendocrine regulatory mechanisms in the choroid plexus-cerebrospinal fluid system. *Brain Res Brain Res Rev* **2**, 109-138.

Nojima D., Linck R.W., Egelman E.H. (1995) At least one of the protofilaments in flagellar microtubules is not composed of tubulin. *Curr Biol* **5**, 158-167.

O'Reilly D.R., Miller L.K., Luckow V.A. (1994) Baculovirus expression vectors: a laboratory manual. *Oxford University Press (Oxford, UK).*

Ostrowski L.E., Blackburn K., Radde K.M., Moyer M.B., Schlatzer D.M., Moseley A., Boucher R.C. (2002) A proteomic analysis of human cilia: identification of novel components. *Mol Cell Proteomics* **1**, 451-465.

Pagon R.A., Bird T.D., Dolan C.R., Stephens K., Adam M.P. (2003) Bardet-Biedl Syndrome. GeneReviews^{TM} [Internet] (Seattle, USA) [updated 2011 Sept. 29th].

Pan J., You Y., Huang T., Brody S.L. (2007) RhoA-mediated apical actin enrichment is required for ciliogenesis and promoted by Foxj1. *J Cell Sci* **120**, 1868-1876.

Persengiev S.P., Zhu X., Green M.R. (2004) Nonspecific, concentration-dependent stimulation and repression of mammalian gene expression by small interfering RNAs (siRNAs). *RNA* **10**, 12-18.

Petrov T., Howarth A.G., Krukoff T.L., Stevenson B.R. (1994) Distribution of the tight junction-associated protein ZO-1 in circumventricular organs of the CNS. *Brain Res Mol Brain Res* **21**, 235-246.

Pfeiffer-Guglielmi B., Fleckenstein B., Jung G., Hamprecht B. (2003) Immunocytochemical localization of glycogen phosphorylase isozymes in rat nervous tissues by using isozyme-specific antibodies *J Neurochem* **85**, 73-81.

Praetorius H.A., Spring K.R. (2003) The renal cell primary cilium functions as a flow sensor. *Curr Opin Nephrol Hypertens* **12**, 517-520.

Prothmann C., Wellard J., Berger J., Hamprecht B., Verleysdonk S. (2001) Primary cultures as a model for studying ependymal functions: glycogen metabolism in ependymal cells. *Brain Res* **920**, 74-83.

Provost P., Dishart D., Doucet J., Frendewey D., Samuelsson B., Radmark O. (2002) Ribonuclease activity and RNA binding of recombinant human Dicer. *EMBO J* **21**, 5864–5874.

Rasala B.A., Orjalo A.V., Shen Z., Briggs S., Forbes D.J. (2006) ELYS is a dual nucleoporin/kinetochore protein required for nuclear pore assembly and proper cell division. *Proc Natl Acad Sci USA* **103**, 17801-17806.

Reichler I.M., Hoerauf A., Guscetti F., Gardelle O., Stoffel M.H., Jentsch B., Walt H., Arnold S. (2001) Primary ciliary dyskinesia with situs inversus totalis, hydrocephalus internus and cardiac malformations in a dog. *J Small Anim Pract* **42**, 345-348.

Rodríguez E.M., Blázquez J.L., Pastor F.E., Peláez B., Peña P., Peruzzo B., Amat P. (2005) Hypothalamic tanycytes: a key component of brain-endocrine interaction. *Int Rev Cytol* **247**, 189-164.

Satir P., Christensen S.T. (2008) Structure and function of mammalian cilia. Histochem. Cell Biol **129**, 687–693.

Sauer B., Henderson N. (1988) Site-specific DNA recombination in mammalian cells by the Cre recombinase of bacteriophage P1. *Proc Natl Acad Sci USA* **85**, 5166-5170.

Sawamoto K., Wichterle H., Gonzalez-Perez O., Cholfin J.A., Yamada M., Spassky N., Murcia N.S., Garcia-Verdugo J.M., Marin O., Rubenstein J.L., Tessier-Lavigne M., Okano H., Alvarez-Buylla A. (2006) New neurons follow the flow of cerebrospinal fluid in the adult brain. *Science* **311**, 629-632.

Scheible D., Kowtharapu B.S., Hamprecht B., Verleysdonk S. (2007) Adenylate kinase 7 is a differentiation marker of kinocilia-bearing cells. *BMC Neuroscience* **8**, (Suppl 1):P7.

Schultz J., Milpetz F., Bork P., Ponting C.P. (1998) SMART, a simple modular architecture research tool: identification of signaling domains. *Proc Natl Acad Sci U S A* **95**, 5857-5864.

Seehusen D.A., Reeves M.M., Fomin D.A. (2003) Cerebrospinal fluid analysis. *Am Fam Physician* **68**, 1103-1108.

Seixas C., Casalou C., Melo L. V., Nolasco S., Brogueira P., Soares H. (2003) Subunits of the chaperonin CCT are associated with Tetrahymena microtubule structures and are involved in cilia biogenesis. *Exp Cell Res* **290**, 303-321.

Shields, T.W., LoCicero J., Reed C.E., Feins R.H. (2009) General Thoracic Surgery 7th edition. *Lippincott Williams & Wilkins (Philadelphia, USA).*

Siegel A., Sapru H.N. (2006) Essential neuroscience; page 67. *Lippincott Williams & Wilkins (Philadelphia, USA).*

Silva F. P., Hamamoto R., Nakamura Y., Furukawa Y. (2005) WDRPUH, a novel WD-repeat-containing protein, is highly expressed in human hepatocellular carcinoma and involved in cell proliferation. *Neoplasia* **7**, 348-355.

Sledz C.A., Holko M., de Veer M.J., Silverman R.H., Williams B.R. (2003) Activation of the interferon system by short-interfering RNAs. *Nat Cell Biol* **5**, 834-839.

Sleigh M.A. (1989) Protozoa and Other Protists. *Cambridge University Press (Cambridge, UK).*

Spassky N., Merkle F.T., Flames N., Tramontin A.D., García-Verdugo J.M., Alvarez-Buylla A. (2005) Adult ependymal cells are postmitotic and are derived from radial glial cells during embrogenesis. *J Neurosci* **25**, 10-18.

Stephans R.E., Lemieux N.A. (1999) Molecular chaperones in cilia and flagella: implications for protein turnover. *Cell Motil Cytoskeleton* **44**, 274-283.

Stewart S.A., Dykxhoorn D.M., Palliser D., Mizuno H., Yu E.Y., An D.S., Sabatini D.M., Chen I.S., Hahn W.C., Sharp P.A., Weinberg R.A., Novina C.D. (2003) Lentivirus-delivered stable gene silencing by RNAi in primary cells. *RNA* **9**, 493-501.

Thomas K.R., Capecchi M.R. (1990) Targeted disruption of the murine int-1 proto-oncogene resulting in severe abnormalities in midbrain and cerebellar development. *Nature* **346**, 847-850.

Tritschler F., Murín R., Birk B., Berger J., Rapp M., Hamprecht B., Verleysdonk S. (2007) Thrombin causes the enrichment of rat brain primary cultures with ependymal cells via protease-activated receptor 1. *Neurochem Res* **32**, 1028-1035.

Valpuesta J. M., Martín-Benito J., Gómez-Puertas P., Carrascosa J. L., Willison K.R. (2002) Structure and function of a protein folding machine: the eukaryotic cytosolic chaperonin CCT. *FEBS Lett* **529**, 11-16.

VandenDriessche T., Thorrez L., Naldini L., Follenzi A., Moons L., Berneman Z., Collen D., Chuah M.K. (2002) Lentiviral vectors containing the human immunodeficiency virus type-1 central polypurine tract can efficiently transduce nondividing hepatocytes and antigen-presenting cells in vivo. *Blood* **100**, 813-822.

Vekemans K., Rosseel L., Wisse E., Braet F. (2004) Immuno-localization of Fas and FasL in rat hepatic endothelial cells: influence of different fixation protocols. *Micron* **35**, 303-306.

Verleysdonk S. (2006) The ependyma: Biochemical and molecular characterization. *Habilitation thesis*, University of Tuebingen.

Verleysdonk S., Kistner S., Pfeiffer-Guglielmi B., Wellard J., Lupescu A., Laske J., Lang F., Rapp M., Hamprecht B. (2005) Glycogen metabolism in rat ependymal primary cultures: regulation by serotonin. *Brain Res* **1060**, 89-99.

Virchow R. (1858) Über das granulierte Ansehen der Wandungen der Gehirnventrikel. *Allg Z Psychiatrie* **3**, 242-250.

Voegtli W. C., Madrona A. Y., Wilson D. K. (2003) The structure of Aip1p, a WD repeat protein that regulates cofilin-mediated actin depolymerization. *J Biol Chem* **278**, 34373-34379.

Walinski H. (2004) Studying gene function: creating knockout mice. *The Science Creative Quarterly*. August 2004 issue. (Internet: http://www.scq.ubc.ca/studying-gene-function-creating-knockout-mice/)

Walker J.M., Rapley R. (2008) Molecular Biomethods Handbook (Second edition) *Humana Press* (*Totowa*, USA), pp. 464-467

Wallingford J. B. (2006) Planar cell polarity, ciliogenesis and neural tube defects. *Hum Mol Genet* **15**, 227-234.

Walther R.F., Atlas E., Carrigan A., Rouleau Y., Edgecombe A., Visentin L., Lamprecht C., Addicks G.C., Haché R.J., Lefebvre Y.A. (2005) A serine/threonine-rich motif is one of three nuclear localization signals that determine unidirectional transport of the mineralocorticoid receptor to the nucleus. *J Biol Chem* **280**, 17549-17561.

Wang Q., Pan J., Snell W.J. (2006) Intraflagellar transport particles participate directly in cilium-generated signaling in Chlamydomonas. *Cell* **125**, 549-562.

Wansleeben C., Meijlink F. (2011) The planar cell polarity pathway in vertebrate development. *Dev Dyn* **240**, 616-626.

Warburg O., Christian W. (1942) Isolation and crystallization of enolase. *Biochem Z* **310**, 384-421.

Waters A. M., Beales P. L. (2011) Bardet-Biedl Syndrome. GeneReviews [Internet]. *Seattle (WA): University of Washington, Seattle.*

Watson D.J., Passini M.A., Wolfe J.H. (2005) Transduction of the choroid plexus and ependyma in neonatal mouse brain by vesicular stomatitis virus glycoprotein-pseudotyped lentivirus and adeno-associated virus type 5 vectors. *Hum Gene Ther* **16**, 49-56.

Weibel M., Pettmann B., Artault J.C., Sensenbrenner M., Labourdette G. (1986) Primary culture of rat ependymal cells in serum-free defined medium. *Brain Res* **390**, 199-209.

Wiznerowicz M., Trono D. (2003) Conditional suppression of cellular genes: lentivirus vector-mediated drug-inducible RNA interference. *J Virol* **77**, 8957-8961.

Wiznerowicz M., Trono D. (2005) Harnessing HIV for therapy, basic research and biotechnology. *Trends Biotechnol* **23**, 42-47.

Xu L., Harada H., Yokohama-Tamaki T., Matsumoto S., Tanaka J., Taniguchi A. (2006) Reuptake of extracellular amelogenin by dental epithelial cells results in increased levels of amelogenin mRNA through enhanced mRNA stabilization. *J Biol Chem* **281**, 2257-2262.

Yamadori T., Nara K. (1979) The directions of ciliary beat on the wall of the lateral ventricle and the currents of the cerebrospinal fluid in the brain ventricles. *Scan Electron Microsc* **3**, 335-340.

Yoder B. (2008) Ciliary function in mammalian development. Preface. *Curr Top Dev Biol* **85,** xv-xix.

Yoshida K., Miki J. (2004) Role of BRCA1 and BRCA2 as regulators of DNA repair, transcription, and cell cycle in response to DNA damage. *Cancer Sci.* **95**, 866-871.

Zaghlou N.A., Katsanis N. (2009) Mechanistic insights into Bardet-Biedl syndrome, a model ciliopathy. *J Clin Invest* **119**, 428-437.

Zamore P.D., Tuschl T., Sharp P.A., Bartel D.P. (2000) RNAi: double-stranded RNA directs the ATP-dependent cleavage of mRNA at 21 to 23 nucleotide intervals. *Cell* **101** 25–33.

Zufferey R., Dull T., Mandel R.J., Bukovsky A., Quiroz D., Naldini L., Trono D. (1998) Self-inactivating lentivirus vector for safe and efficient in vivo gene delivery. *J Virol* **72**, 9873-9880.

Zufferey R., Donello J.E., Trono D., Hope T.J. (1999) Woodchuck hepatitis virus posttranscriptional regulatory element enhances expression of transgenes delivered by retroviral vectors. *J Virol* **73**, 2886-2892.